ELECTRODEPOSITION OF QUANTUM CONFINED THIN FILMS AND NANOSTRUCTURES BY ELECTROCHEMICAL ATOMIC LAYER EPITAXY (EC-ALE).

by

RAMAN VAIDYANATHAN

(Under the Direction of Professor John L. Stickney)

ABSTRACT

Semiconductors show quantization effects when their physical dimensions are less than the Bohr radius for an exciton in the material. Controlling the physical size of materials can be used to tune the material properties. The length scale at which these effects begin to occur range from 3 to 70 nm for typical semiconductors (groups IV, III-V, II-VI). In my research group, we have developed an analog of atomic layer epitaxy, the electrochemical atomic layer epitaxy (EC-ALE). In electrochemistry, surface limited reactions are generally refe**r**red to as under potential deposition. An atomic layer of one element can frequently be electrodeposited on a second at a potential under that needed to deposit the element on itself, and this process is referred to as under potential deposition (UPD). EC-ALE is the use of UPD for the surface limited reactions in an ALE cycle. This provides atomic level control in stoichiometry, thickness and facilitates 2-D growth of the material. This makes EC-ALE a good candidate to form thin films, superlattices, and nanowires, where the compound deposited is modulated on the nanometer scale. In the following chapters, I have reported my research in the electrodeposition of III-V compound semiconductor InAs, In_2Se_3, Cu_2Se, PbSe, PbTe and PbSe / PbTe superlattice thin films by EC-ALE. Strong quantum confinement effects were observed in InAs, PbSe, and PbTe thin films formed by EC-ALE. PbSe / PbTe strain layered superlattice thin films with 2^{nd} order Bragg diffraction peaks and different periodicities is reported and the first attempt to form semiconductor nanowires by ECALE, using the template electrodeposition is also reported.

INDEX WORDS: Under Potential Deposition, EC-ALE, X-ray Diffraction, III-V, IV-VI, Semiconductors, Electrodeposition, Superlattice, Nanowires and Quantum Confinement

ELECTRODEPOSITION OF QUANTUM CONFINED THIN FILMS AND NANOSTRUCTURES BY ELECTROCHEMICAL ATOMIC LAYER EPITAXY (EC-ALE).

by

RAMAN VAIDYANATHAN

B. Tech Chemical and Electrochemical Engineering, Central Electrochemical Research Institute, India, 1998

A Dissertation Submitted to the Graduate Faculty of The University of Georgia in Partial Fulfillment of the Requirements for the Degree

DOCTOR OF PHILOSOPHY

ATHENS, GEORGIA

2003

ELECTRODEPOSITION OF QUANTUM CONFINED THIN FILMS AND NANOSTRUCTURES BY ELECTROCHEMICAL ATOMIC LAYER EPITAXY (EC-ALE).

by

RAMAN VAIDYANATHAN

Major Professor:	John L. Stickney
Committee:	Jonathan I. Amster James L. Anderson James A. de Haseth Uwe Happek

Electronic Version Approved:

Maureen Grasso
Dean of the Graduate School
The University of Georgia
August 2003

DEDICATION

I would like to thank my parents, my brother and sister, who have been supportive and encouraging to me through out my career. My fiancée Ofelya has been the backbone of encouragement and emotional support to me through out my PhD. I dedicate my PhD thesis to my fiancée and my parents.

ACKNOWLEDGEMENTS

The most rewarding experience in my life has been working for Professor John Stickney. He is my mentor, well-wisher and friend during the 5 years of my doctoral study in the United States. I acknowledge his support and friendship, which has guided me to my doctoral degree. I also acknowledge the support of my group members, who were always there for me during my stay at The University Of Georgia. I also acknowledge Professor Uwe Happek and his students at the Physics department, who were very cooperative and helpful in promoting excellent collaborative research. I would like to acknowledge the following people (present and past group members) who have been very helpful and supportive of me.

Dr. John L. Stickney, Dr. Uwe Happek, Dr. Travis L. Wade, Dr. Thomas A. Sorenson, Dr. Lindell C. Ward, Dr. Billy H. Flowers Jr., Dr. Chris Varazo, Mkhulu K. Mathe, Madivannan Muthuvel, Nattapong Srisook, Dr. Marcus Lay and Stephen M. Cox.

TABLE OF CONTENTS

Page

Chapter One

Introduction and Literature Review

The dimensions of semiconductor devices continue to decrease in size and nanoscale control in the deposition of semiconductors is required. Atomic layer control of the deposition of semiconductors was developed by Suntola et.al [1,2]. ALE is based on the formation compounds a monolayer at a time, using surface limited reactions. Surface limited reactions are used to control the growth rate and morphology. ALE offers greater control over deposit structure than methods based on controlling reactant fluxes for all elements simultaneously.

Control of growth at the nanometer level is a major frontier of material science. Unique properties can be achieved by manipulating the unit cell. By construction of superlattices [3-11], nanowires [12-36] and nanoclusters [36-43], and by forming nanocrystalline materials [42,44-54], the fundamental electronic structure, optical properties, of a semiconductor, its bandgap, can be engineered. That is, the wavelengths emitted or absorbed by a compound can be adjusted over a broad range of wavelengths. By direct analogy with the quantum mechanical model of a particle in a box, we know that the smaller the box containing an electron, the further apart its energy levels. This translates directly for some semiconductor structures, the smaller the thickness of the layers or the dimensions of a particle, the larger the resulting bandgap. This effect is generally known as quantum confinement [12,55-61]. Superlattices are examples of nano-structured materials [11,62], where the unit cell of the material is artificially manipulated in one dimension. By alternately depositing thin films of two materials, a material is created with a new unit cell, defined by the superlattice period, the thickness of one layer each of the component compounds. For e.g, an 80 period superlattice of 4PbSe / 4PbTe is made by alternating 1 period (4 layers of PbSe, 4 layers of PbTe) up to 80 periods. Changing the number of layers within

a period of the superlattice will change its optical properties and diffraction peaks. The periodicity H of a superlattice can be determined from the difference between the angle of satellite peak $\Delta(2\theta)$ and Bragg diffraction peak [63]

$$H = 57.3\,\lambda / \Delta(2\theta)\,\mathrm{Cos}\theta$$

Recent developments in the frontiers of materials science are regarding the formation of quantum dots, quantum wires and superlattices. Quantum confinement effects are exhibited by semiconductors [9], ceramic and magnetic materials [11]. In the case of a semiconductor, when a photon is injected onto the material, an electron and a hole are generated. This electron-hole pair revolves in the lattice with a particular radius and this is called the Bohr radius of the semiconductor (a_0). Typical Bohr radii value for some of the semiconductors is shown in table 1.1. When the dimension (x, y, and z) of the semiconductor material is less than that of the Bohr radius, the electron-hole pair is confined in the lattice. Thin films ($z < a_0$) exhibit 1-D quantum confinement; nanowires ($x=y < a_0$, z – several microns) exhibit 2-D quantum confinement etc. Some of the semiconductors that have large Bohr radius values are InAs, InSb, PbSe, PbTe, PbS and HgS. IV-VI compound semiconductors like PbSe, PbTe and PbS, have small and equal electron and hole masses ($m_h = m_e$) compared to III-V or II-VI compound semiconductors, which enables large confinement energies to be split equally between the carriers and they exhibit better confinement effects compared to InSb, InAs or HgS [12,55,61,64-67]. Hence, the IV-VI compound semiconductors in particular will exhibit strong

quantum confinement, i.e, the band gap of the quantum confined material will be larger compared to the bulk value of the lead chalcogenides (0.2 – 0.3 eV).

The primary methodologies for forming thin film materials, quantum dots and superlattices with atomic level control are molecular beam epitaxy (MBE) [67-70], vapor phase epitaxy (VPE) [71,72], and a number of derivative vacuum based techniques [67,73]. These methods depend on controlling the flux of reactants and the temperature of the substrate and reactants. The growth temperature in MBE and VPE is an important variable and deposits formed even at moderate temperatures (200-500 °C), result in interdiffusion of the component elements. Where the intent was to form a superlattice, the interfaces blur [74], resulting in a material that is more of an alloy. Frequently, the integrity of a junction determines the quality of the device.

Single bath or Co-deposition

One of the standard methods for compound electrodeposition is co-deposition, where a set reduction potential or current density is applied to a single solution containing precursors for all the elements in a compound [13,16,75-105]. Literature in the co-deposition of II-VI, and III-V semiconductors is large, and a recent review by Stickney [106-108] is an excellent source of references on both co-deposition and electrochemical atomic layer epitaxy. Post deposition annealing or the use of precursors in co-deposition was generally required to adjust stoichiometry, crystallinity, and the phase formation.

Template based electrochemical synthesis of semiconductor nano-structures has been investigated in several research laboratories. Those studies generally involved electrodeposition into commercial template membranes [12,109-113]. The first example appears to be that of Sailor and Martin, where a nanoelectrode array based on an

anodized aluminum membrane was used to form an array of nano diode wires, based on the compounds CdSe and CdTe [13]. A unique compound electrodeposition methodology, sequential monolayer electrodeposition (SMED), was used. SMED is based on a cyclic potential program and a single solution. The potential program was designed to improve stoichiometry in the deposits by stripping excess Se each cycle [114].

Co-deposition of superlattices made up of semiconductors [11,101,115-117], ceramic [11,118] and magnetic materials [10,11,14,118-125] have been pursed in various laboratories. In particular, semiconductor superlattices electrodeposited by co-deposition suffers from limitation of control over stoichiometry and alloy formation during deposition process.

Electrochemical atomic layer epitaxy

Electrodeposition is generally performed near room temperature, avoiding problems with interdiffusion and mismatched thermal expansion coefficients. In my research group, we have developed an analog of atomic layer epitaxy, the electrochemical atomic layer epitaxy (EC-ALE) [126,127]. In electrochemistry, surface limited reactions are generally refe**r**red to as under potential deposition [128-131]. An atomic layer of one element can frequently be electrodeposited on a second at a potential under that needed to deposit the element on itself, and this process is referred to as under potential deposition (UPD). EC-ALE is the use of UPD for the surface limited reactions in an ALE cycle. This provides atomic level control in stoichiometry, thickness and facilitates 2-D growth of the material. This makes EC-ALE a good candidate to form thin films, superlattices, and nanowires, where the compound deposited is modulated on the nanometer scale.

The following experimental methodologies and instrumentation were used in the electrodeposition and characterization of compound semiconductor thin films by EC-

ALE: cyclic voltammetry in the flow cell, automated flow deposition system, ellipsometry, atomic force microscopy, X-ray diffraction and infrared reflection absorption measurements.

Cyclic voltammograms were performed in the flow cell to identify the deposition potentials of each element. Films were typically deposited on gold substrates as follows: The cell is filled by a pump from a reservoir containing an electrolyte solution of the element of interest (Pb). A surface limited amount of the element is deposited at -0.300 V. The cell is then rinsed with a blank electrolyte solution and filled with another electrolyte solution of the next element (Se). A stoichiometric amount of this element is then deposited on the previous element at -0.300 V and the cycle repeated. In the case of PbTe, an atomic layer of Te is deposited at -0.4 V and Pb is deposited at -0.3 V. The layers of PbSe and PbTe are alternated to form a superlattice. The films were characterized using electron probe microscope analysis (EPMA), atomic force microscopy (AFM) and X-ray diffraction. The optical properties of the films were studied via infrared absorption measurements.

Hardware

Figure 1.1 is a schematic diagram of a basic electrochemical flow deposition systems used for electrodepositing thin-films using EC-ALE, showing the solution reservoirs, pumps, valves, electrochemical cell, potentiostat, and computer. A number of electrochemical cell designs have been tried. A larger thin-layer electrochemical flow-cell is now used [8,132], with a deposition area of about 2.5 cm^2, and a cell volume of 0.1 mL, resulting in a hundredth the volume/cycle. The cell includes an Au coated indium tin oxide (ITO) auxiliary electrode, as the opposite wall of the cell from the working

electrode, allowing observation of the deposit during growth, as well as providing an optimal current distribution.

Villegas et al. used a wall-jet configuration, with very good results, in the formation of CdTe deposits on Au [133]. The quality of their deposits appear equivalent to those recently produced by this group, with the thin-layer flow-cell. A wall-jet configuration has also been used by Foresti et al., in their studies of thin-film growth using EC-ALE on Ag electrodes [134,135].

The pumps used in the flow system in Figure 1.1 are standard peristaltic pumps (Cole Parmer). The main requirement for the pumps is that they are clean. If smoother pumping is required, pulse dampening, or syringe pumps could be used. Foresti et al. have used pressurized bottles, without pumps, to deliver solution [134,136]. In Figure 1.1, there is one pump for each line, to push solution through the cell. Villegas et al. used a single pump on the outlet to suck each solution into the cell, in an elegant simplification [137]. There are a number of vendors that sell solenoid actuated Teflon valves, which are easily interfaced to a computer. Care must be taken to choose a design where the internal volume at the valve outlet can be flushed easily between steps, however [138]. Rotary selection valves have been used as well, but given the number of rotations needed for a 200 cycle deposit, various failure modes reveled themselves.

As the deposition of most of the relevant atomic layers involves reduction at relatively low potentials, oxygen has proven to be a major problem. It has been shown repeatedly that oxygen not rigorously excluded results in thinner deposits, if they are formed at all. For this reason, extensive sparging of the solution reservoirs is critical. Sparging alone is generally not sufficient to prevent problems with oxygen, as most tubing has some

oxygen permeability. To better avoid this problem, the solution delivery tubes were threaded through larger ID tubes and into the Plexiglas box (Figure 1.1) that houses the pumps and valves. The sparging N_2 was made to flow out of the solution reservoirs, through the large ID tubes (around the outside of the solution delivery tubes) and into the box, greatly decreasing oxygen exposure. The measured oxygen content of the N_2 leaving the Plexiglas box was 10 - 30 ppm, as measured with a glove box oxygen analyzer (Illinois Instruments, model 2550).

Substrates

The majority of deposits formed in this group have been on Au electrodes, as they are robust, easy to clean, have a well characterized electrochemical behavior, and reasonable quality films can be formed by a number of methodologies. However, Au it is not well lattice-matched to most of the compounds being formed by EC-ALE.

Some deposits have been formed on Au single crystals. However, single crystals are too expensive to use in forming larger deposits, and have to be recycled. A number of disposable substrates have been investigated, so that the deposits can be kept around. The first deposits were made on cold rolled gold foil, which proved too expensive, and polycrystalline after etching. Au vapor deposited on Si(100) at room temperature was used extensively, as the films were more reproducible and resembled Au mirrors. On the nanometer scale, however, the films consisted of 40 nm hemispheres. Au vapor deposited on mica at 300-400^{o} is known to form large (111) terraces [139-144]. Several attempts to use these films in the flow-cell resulted in delamination, due to the constant rinsing.

Presently, Au on glass is being used to form most of the deposits in the flow-cells. These substrates are microscope slides, etched in HF, coated with 3 nm of Ti, and then 600 nm

of Au, at about 400° [145-147]. The deposits do not, in general, show as many large terraces as Au on mica, however they are orders of magnitude better then Au on Si. To improve terrace sizes, the substrates are annealing in a tube furnace at 550° for 12 hr with flowing N_2. In addition, substrates are given a brief fame anneal, in the dark with a H_2 flame to a dull orange glow, prior to use.

Some Cu substrates have been used, including Cu foils, etched foils, and vapor deposited Cu on glass [132,147]. There does not appear to be a significant difference in the quality of deposits formed on Cu vs. Au, beyond that expected to result from considerations of lattice matching.

Single crystal silver substrates have been used exclusively by Foresti et al. [134-136,148]. They use macroscopic Ag single crystals, formed in house. They have formed a number of II-IV compounds using EC-ALE, including: ZnSe, CdS, and ZnS.

Semiconductors such as polycrystalline ITO on glass have been used to form deposits of ZnS [149], CdS and CdTe, by this group. Ideally, lattice matched semiconductor substrates could also be used to form deposits [10]. For instance, InSb is lattice matched with CdTe, and could be used as a substrate. The problems involve adequately preparing the substrate surfaces, and understanding the electrochemistry of a compound semiconductor substrate [150,151]. Present research in our group is focused on using InP single crystal electrodes as substrates for compound semiconductor electrodeposition.

<u>Compound semiconductors, superlattices and nanowires formed by EC-ALE</u>

The first paper on electrodeposition of compound semiconductor thin films by EC-ALE [152] was thin layer electrochemical studies of Cd and Te on poly crystalline Au, Pt and Cu. Gregory et.al [126,127] studied the conditions needed to from II-VI compound

semiconductor CdTe on polycrystalline Au electrode, using the ECALE method. Surface studies on the formation of III-V compound semiconductor GaAs in ultra high vacuum by EC-ALE [153-155] were performed. Surface studies were also performed on atomic layers of Te [156]. The structure of CdTe formed after the deposition Cd on Te atomic layers [157] was analyzed using surface techniques in ultra high vacuum. Thin layer electrochemistry on the formation of CdS was reported by colletti [158] and the first automated flow deposition system to for thin films was reported by Huang [138]. II-VI compounds such as CdTe [126,159-162], CdS [126,160,163-165], ZnSe[136] and CdS / HgS superlattices[164] have been successfully formed using by EC-ALE, as well as some III-V compounds: GaAs[154,155], InAs[145], InSb[8] and superlattices of InAs/InSb[8].

The first project I worked on during my graduate research, was regarding the optimization of the deposition potentials for In and As to promote 2-D growth and stoichiometry of the InAs deposits. Initial studies using thin layer electrochemical cell in the deposition of $CuInSe_2$ thin films was reported by Herrick [166]. In chapters 3 and 4, I will briefly discuss the progress and problems encountered towards the formation of $CuInSe_2$ thin films by EC-ALE. Torimoto et.al. reported the quantum confinement in thin films of ZnS[167], CdS[168], and PbS[169] grown by EC-ALE. We have also reported the quantum confinement of PbSe[170] and PbTe [171] thin films grown by EC-ALE. The first attempt to electrodeposit semiconductor nanowires by EC-ALE is discussed in chapter 4. The formation of quantum confined semiconductor thin films of PbSe, PbTe and PbSe / PbTe superlattices by EC-ALE is also reported in chapters 5-7.

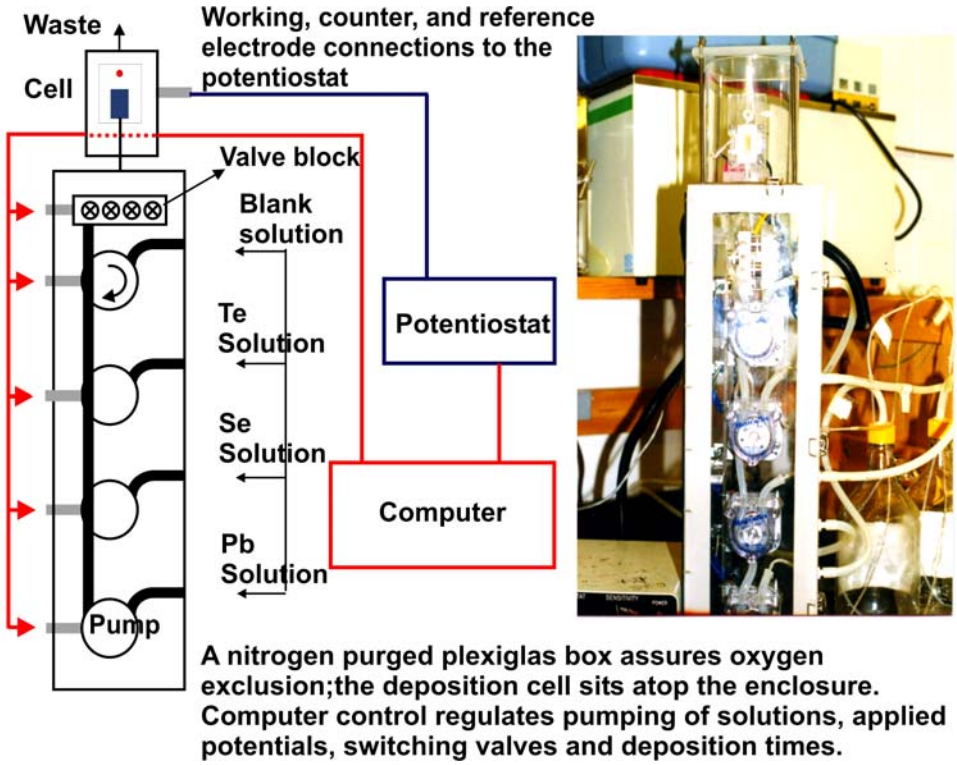

Figure 1.1: Schematic of the automated flow deposition system.

Compound	Band Gap, eV	Lattice Constant, nm	Interatomic Distance,nm	Au Lattice Mismatch, %	Bohr Radius, nm
Au		2.86	4.29		
GaAs	1.43	5.653	3.997	6.83	14
GaSb	0.69	6.095	4.31	-0.47	23.3
InP	1.28	5.8687	4.15	3.26	9.5
InAs	0.36	6.058	4.284	0.14	35.5
InSb	0.17	6.4787	4.581	-6.78	69
ZnS	3.6-3.8	a 3.814, c 6.257	3.814	11.10	1.7
ZnSe	2.58	5.667	3.823	10.89	2.8
ZnTe	2.28	6.101	4.314	-0.56	4.6
CdS	2.53	a 4.136, c 6.713	4.136	3.59	3.1
CdSe	1.74	a 4.299, c 7.010	4.299	-0.21	6.1
CdTe	1.5	6.477	4.58	-6.76	6.5
HgS	2.5				
HgSe	-0.15	6.086	4.303	-0.30	
HgTe	0	6.42	4.568	-6.48	39.3
PbS	0.37	5.936	4.197	2.17	20
PbSe	0.26	6.124	4.33	-0.93	46
PbTe	0.29	6.46	4.568	-6.48	
SnTe	0.18	6.328	4.475	-4.31	

Table 1.1: Bohr radii of semiconductors

References

(1) Goodman, C. H. L.; Pessa, M. V. *J. Appl. Phys.* **1986**, *60*, R65.

(2) Suntola, T.; Antson, J. In *US Patent*: USA, 1977.

(3) Feenstra, R. M.; Collins, D. A.; Ting, D. Z.-Y.; Wang, M. W.; McGill, T. C. *J. Vac. Sci. Technol. B* **1994**, *12*, 2592.

(4) Wei, C.; Rajeshwar, K. *J. Electrochem. Soc.* **1992**, *139*, L40.

(5) Hartmann, J. M.; G., F.; M., C.; H., M. *J. Appl. Phys.* **1996**, *79*, 3035.

(6) Mailhiot, C.; Smith, D. L. *Crit. Rev. Sol. State Mat. Sci.* **1990**, *16*, 131.

(7) Hartmann, J. M.; M., C.; J., C.; H., M. *Appl. Phys. Lett.* **1998**, *72*, 3151.

(8) Wade, T. L.; Vaidyanathan, R.; Happek, U.; Stickney, J. L. *J. Electroanal. Chem.* **2001**, *500*, 322-332.

(9) Dresselhaus, M. S.; Lin, Y. M.; Cronin, S. B.; Rabin, O.; Black, M. R.; Dresselhaus, G.; Koga, T. In *Recent Trends in Thermoelectric Materials Research Iii*; Academic Press Inc: San Diego, 2001; Vol. 71, pp 1-121.

(10) Switzer, J. A.; Hung, C.-J.; Breyfogle, B. E.; Shumsky, M. G.; Leeuwen, R. V.; Golden, T. D. *Science* **1994**, *264*, 1573.

(11) Switzer, J. A. In *Electrochemistry of Nanomaterials*; Hodes, G., Ed.; Wiley-VCH, 2001, pp 67-101.

(12) Peng, X. S.; Meng, G. W.; Zhang, J.; Wang, X. F.; Wang, C. Z.; Liu, X.; Zhang, L. D. *J. Mater. Res.* **2002**, *17*, 1283-1286.

(13) Klein, J. D.; Herrick, R. D.; Palmer, D.; Sailor, M. J.; Brumlik, C. J.; Martin, C. R. *Chem. Mater.* **1993**, *5*, 902-904.

(14) Liu, K.; Nagodawithana, K.; Searson, P. C.; Chien, C. L. *Phys. Rev. B* **1995**, *51*, 7381-7384.

(15) Routkevitch, D.; A., T. A.; J., H.; D., A.; M., M.; M., X. J. *IEEE Trans. Electron Devices* **1996**, *43*, 1646.

(16) Routkevitch, D.; Bigioni, T.; Moskovits, M.; Xu, J. M. *J. Phys. Chem.* **1996**, *100*, 14037.

(17) Blondel, A.; Doudin, B.; Ansermet, J. P. *J. Magn. Magn. Mater.* **1997**, *165*, 34-37.

(18) Ferre, R.; Ounadjela, K.; George, J. M.; Piraux, L.; Dubois, S. *Phys. Rev. B* **1997**, *56*, 14066-14075.

(19) Li, F. Y.; Metzger, R. M.; Doyle, W. D. *Ieee Transactions on Magnetics* **1997**, *33*, 3715-3717.

(20) Piraux, L.; Dubois, S.; Demoustier-Champagne, S. *Nuclear Instruments and Methods in Physics Research B* **1997**, *131*, 357-363.

(21) Schonenberger, C.; van der Zande, B. M. I.; Fokkink, L. G. J.; Henny, M.; Schmid, C.; Kruger, M.; Bachtold, A.; Huber, R.; Birk, H.; Staufer, U. *J. Phys. Chem. B* **1997**, *101*, 5497-5505.

(22) Schonenberger, C.; vanderZande, B. M. I.; Fokkink, L. G. J.; Henny, M.; Schmid, C.; Kruger, M.; Bachtold, A.; Huber, R.; Birk, H.; Staufer, U. *J. Phys. Chem. B* **1997**, *101*, 5497-5505.

(23) Miyazaki, K.; Kainuma, S.; Hisatake, K.; Watanabe, T.; Fukumuro, N. *Electrochim. Acta* **1999**, *44*, 3713-3719.

(24) Sapp, S. A.; Lakshmi, B. B.; Martin, C. R. *Adv. Mater.* **1999**, *11*, 402-404.

(25) Sun, L.; Searson, P. C.; Chien, C. L. *Appl. Phys. Lett.* **1999**, *74*, 2803.

(26) Wang, C. W.; Peng, Y.; Pan, S. L.; Zhang, H. L.; Li, H. L. *Acta Phys. Sin.* **1999**, *48*, 2146-2150.

(27) Metzger, R. M.; Konovalov, V. V.; Sun, M.; Xu, T.; Zangari, G.; Xu, B.; Benakli, M.; Doyle, W. D. *IEEE Transactions on Magnetics* **2000**, *36*, 30-35.

(28) Schwanbeck, H.; Schmidt, U. *Electrochim. Acta* **2000**, *45*, 4389-4398.

(29) Ge, S. H.; Li, C.; Ma, X.; Li, W.; Li, C. X. *Acta Phys. Sin.* **2001**, *50*, 149-152.

(30) Kazadi mukenga Bantu, A.; Rivas, J.; Zaragoza, G.; Lopez-Quintela, M. A.; Blanco, M. C. *J. Non-Crystalline Solids* **2001**, *287*, 5-9.

(31) Kovtyukhova, N. I.; Martin, B. R.; Mbindyo, J. K. N.; Smith, P. A.; Razavi, B.; Mayer, T. S.; Mallouk, T. E. *JPC B* **2001**, *105*, 8762-8769.

(32) Peng, X. S.; Zhang, J.; Wang, X. F.; Wang, Y. W.; Zhao, L. X.; Meng, G. W.; zhang, L. D. *Chem. Phys. Lett.* **2001**, *343*, 470-474.

(33) Richter, J.; Mertig, M.; Pompe, W.; Monch, I.; Schackert, H. K. *Appl. Phys. Lett.* **2001**, *78*, 536.

(34) Santinacci, L.; Djenizian, T.; Schmuki, P. *Appl. Phys. Lett.* **2001**, *79*, 1882.

(35) Schuster, R. *Chemphyschem* **2001**, *2*, 411-412.

(36) Lee, G. H.; Huh, S. H.; Park, J. W.; Ri, H.-C.; Jeong, J. W. *J. Phys. Chem. B* **2001?**, *in press*.

(37) Alperson, B.; Rubinstein, I.; Hodes, G. *Phys. Rev. B* **2001**, *63*, 801303R.

(38) Enders, F.; Abedin, S. Z. E. *Chem. Comm.?* **2002**.

(39) Golan, Y.; Margulis, L.; Rubinstein, I.; Hodes, G. *Langmuir* **1992**, *8*, 749.

(40) Guzelian, A. A.; Banin, U.; Kadavanich, A. V.; Peng, X.; Alivisatos, A. P. *Appl. Phys. Lett.* **1996**, *69*, 1432.

(41) Mizel, A.; L., C. M. *Solid State Commun.* **1997**, *104*, 401.

(42) Rajeshwar, K.; deTacconi, N. R. In *Semiconductor Nanoclusters-Physical, Chemical, and Catalytic Aspects*, 1997; Vol. 103, pp 321-351.

(43) Shi, J.; Zhu, K.; Yao, W.; Zhang, L. *J. Cryst. Growth* **1998**, *186*, 480-486.

(44) Banerjee, S.; Chakravorty, D. *Appl. Phys. Lett.* **1998**, *72*, 1027-1029.

(45) Cachet, H.; Essaaidi, H.; Froment, M.; Maurin, G. *J. Electroanal. Chem.* **1995**, *396*, 175-182.

(46) Dang, X. J.; Massari, A. M.; Hupp, J. T. *Electrochem. Sol. State Lett.* **2000**, *3*, 555-558.

(47) Hodes, G.; Howell, I. D. J.; Peter, L. M. *J. Electrochem. Soc.* **1992**, *139*, 3136.

(48) Hodes, G. *Isr. J. Chem.* **1993**, *3*, 95.

(49) Hodes, G. *Sol. Energy Mater.* **1994**, *32*, 323.

(50) Rajeshwar, K.; deTacconi, N. R. In *Studies in Surface Science and Catalysis*, 1997; Vol. 103, p 321.

(51) Turi, T.; Erb, U. *Mater. Sci. Eng. A-Struct. Mater. Prop. Microstruct. Process.* **1995**, *204*, 34-38.

(52) van Dijken, A.; Vanmaekelbergh, D.; Meijerink, A. *Chem. Phys. Lett.* **1997**, *269*, 494-499.

(53) Wang, N.; Wang, Z. R.; Aust, K. T.; Erb, U. *Mater. Sci. Eng. A-Struct. Mater. Prop. Microstruct. Process.* **1997**, *237*, 150-158.

(54) Zach, M. P.; Penner, R. M. *Advanced Materials* **2000**, *12*, 878-883.

(55) wise, F. W. *Acc. Chem. Res.* **2000**, *2000*, 773-780.

(56) Partovi, A.; Glass, A. M.; Olson, D. H.; Feldman, R. D.; Austin, R. F.; Lee, D.; johnson, A. M.; Miller, D. A. B. *Appl. Phys. Lett.* **1991**, *58*, 334.

(57) Partin, D. L.; Heremans, J.; Thrush, C. M. *Source J. APPL. PHYS.* **1992**, *71*, 2328-2332.

(58) Ochoa, O. R.; Colajacomo, C.; Witkowski, I., E.J.; Simmons, J. H.; Potter, J. B. G. *Solid State Commun.* **1996**, *98*, 717-721.

(59) Mukai, K.; N., O.; M., S.; S., Y. *Jpn. J. Appl. Phys. Part 2 - Lett.* **1994**, *33*, L1710.

(60) Lippens, P. E.; Lannoo, M. *Phys. Rev. B.* **1989**, *39*, 10935-10942.

(61) Hamad, K. S.; R., R.; A., M.; T., v. B.; L., C. L.; M., C.; P., A. A. *Abstr. Pap. Am. Chem. Soc.* **1998**, *216*, U628.

(62) Switzer, J. A.; Shane, M. J.; Phillips, R. J. *Science* **1990**, *247*, 444.

(63) Fedorov A.G, S. I. A., Sipatov A.Yu, Kaidalova E.V *J. Cryst. Growth* **1999**, *198*, 1211-1215.

(64) Rogacheva, E. I.; Tavrina, T. V.; Nashchekina, O. N.; Grigorov, S. N.; Nasedkin, K. A.; Dresselhaus, M. S.; Cronin, S. B. **2002**, *80*, 2690-2692.

(65) Beyer, H.; Nurnus, J.; Bottner, H.; Lambrecht, A.; Roch, T.; Bauer, G. *Appl. Phys. Lett.* **2002**, *80*, 1216-1218.

(66) Broido, D. A.; Reinecke, T. L. *Phys. Rev. B* **2001**, *6404*, art. no.-045324.

(67) Faschinger, W. *Phys. Scr.* **1993**, *T49B*, 492.

(68) Feldman, R. D. *J. Vac. Sci. Technol. A* **1990**, *8*, 1888.

(69) Ueta, A. Y.; Abramof, E.; Boschetti, C.; Closs, H.; Motisuke, P.; Rappl, P. H. O.; Bandeira, I. N.; Ferreira, S. O. *Microelectron. J.* **2002**, *33*, 331-335.

(70) Hartmann, J. M.; F., K.; M., C.; Y., S.; L., R. J.; H., M. *J. Appl. Phys.* **1998**, *84*, 4300.

(71) Goto, S.; K., H.; H., H. *Inst. Phys. Conf. Ser.* **1992**, 547.

(72) Blumina, M.; Lelong, I. O.; Sarfaty, R.; Fekete, D. *J. Appl. Phys.* **1994**, *75*, 357.

(73) Rogacheva, E. I.; Krivulkin, I. M.; Nashchekina, O. N.; Sipatov, A. Y.; Volobuev, V. V.; Dresselhaus, M. S. *Appl. Phys. Lett.* **2001**, *78*, 1661-1663.

(74) Belyansky, M. P.; Gaskov, A. M.; Strelkov, A. V. *Source MATER SCI ENG B SOLID STATE ADV TECHNOL* **1992**, 78-81.

(75) Stickney, J. L.; Rosasco, S. D.; Song, D.; Soriaga, M. P.; Hubbard, A. T. *Surf. Sci.* **1983**, *130*, 326.

(76) Fulop, G. F.; Taylor, R. M. *Ann. Rev. Mater. Sci.* **1985**, *15*, 197.

(77) Mishra, K. K.; Rajeshwar, K. *J. Electroanal. Chem.* **1989**, *273*, 169-182.

(78) Lin, W.-Y.; Mishra, K. K.; Mori, E.; Rajeshwar, K. *Anal. Chem.* **1990**, *62*, 821.

(79) Mori, E.; Mishra, K. K.; Rajeshwar, K. *J. Electrochem. Soc.* **1990**, *137*, 1100.

(80) Eriksson, S.; P., C.; B., H.; K., U. *J. Electroanal. Chem.* **1991**, *313*, 121.

(81) Lokhande, C. D.; Yermune, V. S.; Pawar, S. H. *J. Electrochem. Soc.* **1991**, *138*, 624.

(82) Morris, G. C.; Vanderveen, R. *Sol. Energy Mater.* **1992**, *27*, 305.

(83) Ortega, J. *An. Quim.* **1992**, *88*, 623-627.

(84) Allongue, P.; E., S. *J. Electroanal. Chem.* **1993**, *362*, 79.

(85) Allongue, P.; E., S.; L., A. *J. Electroanal. Chem.* **1993**, *362*, 89.

(86) Gheorghita, L.; Cocivera, M.; Nelson, A. J.; Swartzlander, A. B. *J. Electrochem. Soc.* **1994**, *141*, 529.

(87) Natarajan, C.; Sharon, M.; Levy-Clement, C.; Neumann-Spallart, M. *Thin Solid Films* **1994**, *237*, 118.

(88) Singh, K.; Pathak, R. K. *Electrochim. Acta* **1994**, *39*, 2693.

(89) Elfick, P. V.; Berlouis, L. E. A.; Donald, S. M. M.; Affrossman, S.; Rocabolis, P. *J. Phys. Chem.* **1995**, *99*, 15129.

(90) Fiedler, D. A.; Fritz, H. P. *Electrochim. Acta* **1995**, *40*, 1595.

(91) Guillen, C.; Herrero, J. *J. Electrochem. Soc.* **1995**, *142*, 1834.

(92) Hodes, G. In *"Physical Electrochemistry"*; Rubinstein, I., Ed.; Marcel Dekker: New York, 1995, p 515.

(93) Bhattacharya, R. N.; Fernandez, A. M.; Contreras, M. A.; J.Keane; Tennant, A. L.; Ramanathan, K.; Tuttle, J. R.; Noufi, R. N.; Hermann, A. M. *J. Electrochem. Soc.* **1996**, *143*, 854.

(94) Sugimoto, Y.; Peter, L. M. *J. Electroanal. Chem.* **1995**, *386*, 183.

(95) Dalchiele, E.; Cattarin, S.; Musiani, M.; Casellato, U.; Guerriero, P.; Rossetto, G. *J. Electroanal. Chem.* **1996**, *418*, 83.

(96) Endo, S.; Nagahori, Y.; Nomura, S. *Jpn. J. Appl. Phys.* **1996**, *35*, L1101.

(97) Guillen, C.; Herrero, J. *J. Electrochem. Soc.* **1996**, *143*, 493.

(98) Higgins, S. R.; Hamers, R. J. *J. Vac. Sci. Technol. B* **1996**, *14*, 1360.

(99) You, J. K.; Yang, Y.; Chen, X. G.; Gu, W. D.; Zhuo, X. D.; Lin, X. G. *J. Electroanal. Chem.* **1996**, *405*, 233.

(100) Arico, A. S.; Silvestro, D.; Antonucci, P. L.; Giordano, N.; Antonucci, V. *Advanced Performance Materials* **1997**, *4*, 115.

(101) Streltsov, E. A.; Osipovich, N. P.; Ivashkevich, L. S.; Lyakhov, A. S.; Sviridov, V. V. *Russ. J. Appl. Chem.* **1997**, *70*, 1651-1653.

(102) Gamboa, S. A.; Nguyen-Cong, H.; Chartier, P.; Sebastian, P. J.; Calixto, M. E.; Rivera, M. A. *Sol. Energy Mater.* **1998**, *55*, 95-104.

(103) Streltsov, E. A.; Osipovich, N. P.; Ivashkevich, L. S.; Lyakhov, A. S.; Sviridov, V. V. *Electrochim. Acta* **1998**, *43*, 869.

(104) Yamaguchi, K.; Yoshida, T.; Sugiura, T.; Minoura, H. *J. Phys. Chem. B* **1998**, *102*, 9677.

(105) Myung, N.; Jun, J. H.; Ku, H. B.; Chung, H. K.; Rajeshwar, K. *Microchem J.* **1999**, *62*, 15-25.

(106) Stickney, J. L.; Wade, T. L.; Flowers Jr., B. H.; Vaidyanathan, R.; Happek, U. In *Encyclopedia of Electrochemistry*; Gileadi, E., Urbakh, M., Eds.; Marcel Dekker: New York, 2002; Vol. in press.

(107) Stickney, J. L.; Varazo, K.; Ward, L. C.; Lay, M. D.; Sorenson, T., A. In *Encyclopedia of Surface and Colloid Science*; Hubbard, A. T., Ed.; Marcel Dekker, Inc.: New York, 2002.

(108) Stickney, J. L. In *Advances in Electrochemical Science and Engineering*; Kolb, D. M., Alkire, R., Eds.; Wiley-VCH: Weinheim, 2002; Vol. 7, pp 1-107.

(109) Martin-Gonsalez, M. S.; Perieto, A. L.; Knox, M. S.; Gronsky, R.; Sands, T.; Stacy, A. M. **2002**, *submitted*.

(110) Prieto, A. L.; Sander, M. S.; Martin-Gonzalez, M. S.; Gronsky, R.; Sands, T.; Stacy, A. M. *J. Am. Chem. Soc.* **2001**, *123*, 7160-7161.

(111) Gao, T.; Meng, G. W.; Zhang, J.; Wang, Y. W.; Liang, C. H.; Fan, J. C.; Zhang, L. D. *Appl. PHys. A.* **2001**, *73*, 251-254.

(112) Zangari, G.; Lambeth, D. N. *IEEE Transactions on Magnetics* **1997**, *33*, 3010-3012.

(113) Martin, C. R. *Science* **1994**, *266*, 1961-1996.

(114) Kressin, A. M.; Doan, V. V.; Klein, J. D.; Sailor, M. J. *Chem. Mater.* **1991**, *3*, 1015-1020.

(115) Golan, Y.; Hodes, G.; Rubinstein, I. *J. Phys. Chem.* **1996**, *100*, 2220-2228.

(116) Nicic, I.; Shannon, C.; Bozack, M. J.; Braun, M.; Link, S.; El-Sayed, M. In *National Meeting of the Electrochemical Society*; Andricacos, P. C., Searson, P. C., Reidsema-Simpson, C., Allongue, P., Stickney, J. L., Oleszek, G. M., Eds.; ECS: Washington D.C., 2001.

(117) Streltsov, E. A.; Osipovich, N. P.; Lyakhov, A. S.; Ivashkevich, L. S. *Inorg. Mater.* **1997**, *33*, 442-446.

(118) Ross, C. A. *Ann. Rev. Mat. Sci.* **1994**, *24*, 159.

(119) Doudin, B.; Ansermet, J. P. *Nanostruct. Mater.* **1995**, *6*, 521-524.

(120) Golden, T. D.; Shumsky, M. G.; Zhou, Y. C.; VanderWerf, R. A.; VanLeeuwen, R. A.; Switzer, J. A. *Chem. Mater.* **1996**, *8*, 2499-2504.

(121) Lashmore, D. S.; Dariel, M. P. *J. Electrochem. Soc.* **1988**, *135*, 1219.

(122) McMichael, R. D.; Atzmony, U.; Beauchamp, C.; Bennett, L. H.; Swartzendruber, L. J.; Lashmore, D. S.; Romankiw, L. T. *J. Magn. Magn. Mater.* **1992**, *113*, 149.

(123) Simunovich, D.; Schlesinger, M.; Snyder, D. D. *J. Electrochem. Soc.* **1994**, *141*, L10.

(124) Yahalom, J.; Tessier, D. F.; Timsit, R. S.; Rosenfeld, A. M.; Mitchell, D. F.; Robinson, P. T. *J. Mater. Res.* **1989**, *4*, 755.

(125) Zhou, M.; Myung, N.; Chen, X.; Rajeshwar, K. *J. Electroanal. Chem.* **1995**, *398*, 5-12.

(126) Gregory, B. W.; Stickney, J. L. *J. Electroanal. Chem.* **1991**, *300*, 543.

(127) Gregory, B. W.; Suggs, D. W.; Stickney, J. L. *J. Electrochem. Soc.* **1991**, *138*, 1279.

(128) Kolb, D. M.; Przasnyski, M.; Gerisher, H. *J. Electroanal. Chem.* **1974**, *54*, 25-38.

(129) Kolb, D. M.; Gerisher, H. *Surf. Sci.* **1975**, *51*, 323.

(130) Kolb, D. M. In *Advances in Electrochemistry and Electrochemical Engineering*; Gerischer, H., Tobias, C. W., Eds.; John Wiley: New York, 1978; Vol. 11, p 125.

(131) Juttner, K.; Lorenz, W. J. *Z. Phys. Chem. N. F.* **1980**, *122*, 163.

(132) Wade, T. L.; Flowers Jr., B. H.; Varazo, K.; Lay, M.; Happek, U.; Stickney, J. L. In *Electrochemical Society National Meeting*; Kondo, K., Ed.; Electrochemcial Society: Washington D.C., 2001; Vol. In Press.

(133) Villegas, I.; Stickney, J. L. *J. Electrochem. Soc.* **1991**, *138*, 1310.

(134) Innocenti, M.; Pezzatini, G.; Forni, F.; Foresti, M. L. In *195th meeting of the Electrochemical Society*; Andricacos, P. C., Searson, P. C., Simpson, C. R., Allongue, P., Stickney, J. L., Oleszek, G. M., Eds.; The Electrochemical Society: Seattle, Washington, 1999; Vol. 99-9, pp 294-308.

(135) Foresti, M. L.; Pezzatini, G.; Cavallini, M.; Aloisi, G.; Innocenti, M.; Guidelli, R. *J. Phys. Chem. B* **1998**, *102*, 7413-7420.

(136) Pezzatini, G.; Caporali, S.; Innocenti, M.; Foresti, M. L. *J. Electroanal. Chem.* **1999**, *475*, 164-170.

(137) Villegas, I.; Napolitano, P. *J. Electrochem. Soc.* **1999**, *146*, 117.

(138) Huang, B. M.; Colletti, L. P.; Gregory, B. W.; Anderson, J. L.; Stickney, J. L. *J. Electrochem. Soc.* **1995**, *142*, 3007.

(139) Chidsey, C. E. D.; Loiacono, D. N.; Sleator, T.; Nakahara, S. *Surf. Sci.* **1988**, *200*, 45.

(140) Emch, R.; Nogami, J.; Dovek, M. M.; Lang, C. A.; Quate, C. F. *J. Appl. Phys.* **1988**, *65*, 79.

(141) Putnam, A. l.; Blackford, B. L.; Jericho, M. H.; Watanabe, M. O. *Jpn. J. Appl. Phys.* **1989**, *217*, 276.

(142) Buchholz, S.; Fuchs, H.; Rabe, J. P. *J. Vac. Sci. Technol. B* **1991**, *9*, 857.

(143) DeRose, J. A.; Thundat, T.; Nagahara, L. A.; Lindsay, S. M. *Surf. Sci.* **1991**, *256*, 102.

(144) Holland-Moritz, E.; Gordon-II, J.; Borges, G.; Sonnenfeld, R. *Langmuir* **1991**, *7*, 301.

(145) Wade, T. L.; Ward, L. C.; Maddox, C. B.; Happek, U.; Stickney, J. L. *Electrochem. Sol. State Lett.* **1999**, *2*, 616.

(146) Wade, T. L.; Sorenson, T., A.; Stickney, J. L. In *Interfacial Electrochemistry*; Wieckowski, A., Ed.; Marcel Dekker: New York, 1999, pp 757-768.

(147) Wade, T. L.; Flowers Jr., B. H.; Happek, U.; Stickney, J. L. In *National Meeting of the Electrochemical Society, Spring*; Andricacos, P. C., Searson, P. C., Reidsema-Simpson, C., Allongue, p., Stickney, J. L., Oleszek, G. M., Eds.; The Electrochemical Society: Seattle, Washington, 1999; Vol. 99-9, p 272.

(148) Foresti, M. L.; Innocenti, M.; Forni, F.; Guidelli, R. *Langmuir* **1998**, *14*, 7008-7016.

(149) Colletti, L. P.; Slaughter, R.; Stickney, J. L. *J. Soc. Info. Display* **1997**, *5*, 87.

(150) Ward, L. C.; Stickney, J. L. *Phys. Chem. Chem. Phys.* **2001**, *3*, 3364-3370.

(151) Ward, L. C.; Madhi; Stickney, J. L. *J. Electrochem. Soc.* **2003**, *in preparation.*

(152) Gregory, B. W.; Norton, M. L.; Stickney, J. L. *J. Electroanal. Chem.* **1990**, *293*, 85.

(153) Suggs, D. W.; Villegas, I.; Gregory, B. W.; Stickney, J. L. *Mat. Res. Soc. Symp. Proc.* **1991**, *222*, 283.

(154) Villegas, I.; Stickney, J. L. *J. Electrochem. Soc.* **1992**, *139*, 686.

(155) Villegas, I.; Stickney, J. L. *J. Vac. Sci. Technol. A* **1992**, *10*, 3032.

(156) Suggs, D. W.; Stickney, J. L. *J. Phys. Chem.* **1991**, *95*, 10056.

(157) Suggs, D. W.; Villegas, I.; Gregory, B. W.; Stickney, J. L. *J. Vac. Sci. Technol. A* **1992**, *10*, 886.

(158) Colletti, L. P.; Teklay, D.; Stickney, J. L. *J. Electroanal. Chem.* **1994**, *369*, 145.

(159) Forni, F.; Innocenti, M.; Pezzatini, G.; Foresti, M. L. *Electrochemica Acta* **2000**, *45*, 3225-3231.

(160) Streltsov, E. S.; Labarevich, I. I.; Talapin, D. V. *Dokl. Akad. Nauk Bel.* **1994**, *38*, 64.

(161) Flowers Jr., B. H.; Wade, T. L.; Lay, M.; Garvey, J. W.; Happek, U.; Stickney, J. L. *J. Electroanal. Chem.* **2002**, *in press*.

(162) Varazo, K.; Lay, M. D.; Stickney, J. L. *J. Electroanal. Chem.* **2002**, *in press*.

(163) Boone, B. E.; Shannon, C. *J. Phys. Chem.* **1996**, *100*, 9480-9484.

(164) Gichuhi, A.; Boone, B. E.; Shannon, C. *Langmuir* **1999**, *15*, 763-766.

(165) Innocenti, M.; Pezzatini, G.; Forni, F.; Foresti, M. L. *J. Electrochem. Soc.* **2001**, *148*, c357.

(166) Herrick, R. D. I.; Stickney, J. L. In *New Directions in Electroanalytical Chemistry*; Leddy, J., Wightman, M., Eds.; The Electrochemical Society: Pennington, NJ, 1996; Vol. 96-9, p 186.

(167) Torimoto, T.; Obayashi, A.; Kuwabata, S.; Yasuda, H.; Mori, H.; Yoneyama, H. *Langmuir* **2000**, *16*, 5820-5824.

(168) Torimoto, T.; Nagakubo, S.; Nishizawa, M.; Yoneyama, H. *Langmuir* **1998**, *14*, 7077.

(169) Torimoto, T.; Takabayashi, S.; Mori, H.; Kuwabata, S. *J. Electroanal. Chem.* **2002**, *522*, 33-39.

(170) Vaidyanathan, R.; Happek, U.; Stickney, J. L. *Electrochim. Acta* **2003**, *submitted*.

(171) Vaidyanathan, R.; Happek, U.; Stickney, J. L. *J. Cryst. Growth* **2003**, *submitted*.

Chapter 2

Potential Dependence of InAs formation by EC-ALE at room temperature[1]

[1] Vaidyanathan R, Wade T.L, Happek U and Stickney J.L, Electrochemical Processing in ULSI Fabrication III, Electrochemical Society Proceedings, Vol. 2000-8, 41-52 (Used by permission).

Abstract

Electrodeposition of InAs was carried out at room temperature using EC-ALE. The dependence of deposit stoichiometry, thickness and morphology on the potentials used to deposit Indium and Arsenic were studied. Deposits were characterized using XRD, EPMA, ICP-MS, and AFM. Infrared Absorption measurements were performed to determine the band gap of the material.

Introduction

III-V compound semiconductors and superlattices are widely used for applications in electronic and opto-electronic devices. Atomic level control in the epitaxial growth of these materials is desired for the formation of high quality electronic devices. Techniques such as molecular beam epitaxy (MBE)[1], and metal organic chemical vapor deposition (MOCVD)[2] are some of the methods used for the epitaxial growth of III–V materials like GaAs, InAs and InSb. All the above techniques are carried out at high temperatures and involve the use of hazardous materials during deposition. Some of current issues are formation of strain-layered deposits, lattice mismatch with substrate, and interdiffusion between layers. Electrodeposition has received some attention during the few decades for the successful formation of II-VI and III-V compounds, with some processes reaching commercial applications, such as photovoltaics. Electrodeposition is a low-temperature, low-interdiffusion process and is thus appealing for formation of compound semiconductors. One of standard methods in electrodeposition is co-deposition[3-5], where a set reduction potential or current density is applied to a single solution containing precursors for all the elements involved in the compound. III-V compounds formed by co-deposition from aqueous or nonaqueous solutions are GaAs[6-9], InSb[10-11], InP[12-14], and

InAs[15-17]. Post anneal treatment of the deposit is generally required to obtain stoichiometry and phase formation. Atomic layer epitaxy (ALE) offers greater control over deposit structure. ALE is a method of forming thin films of materials one atomic layer at a time, using surface limited reactions to control the growth rate and morphology. Our group is developing the Electrochemical analog of Atomic Layer Epitaxy (ALE) to form compound thin films, EC-ALE[18-22]. Surface limited reactions are well known in electrochemistry and are referred to as under potential deposition (UPD)[25]. UPD is the deposition of a monolayer or less of an element at a potential prior to bulk deposition. UPD is used in EC-ALE to form compounds one atomic layer at a time. II-VI compounds such as CdTe[18,20-21], CdS[22-23], and ZnSe[24] have been successfully formed by ECALE. Some III-V compounds like GaAs[26-27], and InAs[28] have been explored by this technique. Initial studies in deposition of InAs by ECALE have been reported[28]. This report focuses on better understanding of deposition conditions in EC-ALE formation of InAs.

Experiment

An automated electrochemical flow system for EC-ALE was used for the deposition of InAs thin films and has been described elsewhere[19,20]. $In_2(SO_4)_3$ (Alfa Aesar; Ward Hill, MA) 0.3mM, pH of 3.0, As_2O_3 (J. T. Baker; Phillipsburg, NJ) 2mM, pH of 4.5 were used for deposition. The solutions were made up of 0.1M $NaClO_4$ (Fisher Scientific, Pittsburgh, PA) and buffered with 50mM $CH_3COONa \bullet 3H_2O$ (J. T. Baker; Phillipsburg, NJ). The supporting electrolyte and buffer were used as a blank (pH 3.0). Solution pHs were adjusted with sulphuric acid. All chemicals are reagent grade or better. Solutions were made with water from nanopure water filtration system (Barnstead; Dubuque, IA), fed by a house-distilled water line.

An electrochemical thin layer flow cell was used for deposition[28]. The working electrode was Au vapor deposited on glass, and annealed at 550°C for 12 hrs. This created a predominantly Au(111) substrate. All potentials were measured relative to an Ag/AgCl reference electrode (Bioanalytical Systems, Inc.; West Lafayette, IN). Transparent Indium tin oxide (Delta Technologies, Limited; Stillwater, MN) was used as an auxiliary electrode. The cell was filled with the solution of the element of interest and a surface limited amount was deposited by controlling the potential. The cell was then rinsed with blank and filled with the solution containing the precursor for the next element. A stoichiometric amount of this element was deposited on atomic layer of the previous element to complete one cycle. This cycle was repeated to form the deposit.

Results and discussion

The starting potentials in the deposition program were determined from the cyclic voltammograms of each element (Fig 2.1). Potential of –0.325 V for Arsenic UPD and –0.4 V for Indium UPD were identified for the InAs cycle. After a few cycles, the deposition stopped, because the initial deposition potentials, chosen for Au surface, were no longer optimal for forming atomic layers on the forming compound. It was determined that stepping the potentials more negative by 10 – 25 mV each cycle during deposition (Fig 2.2) was needed to maintain formation of ML (monolayer) each cycle. After 25 cycles, steady state potentials of –0.675 V for arsenic and –0.775 V for Indium were adopted to form the rest of the deposit. Ellipsometry measurements were made to determine the thickness of the deposit. Figure 2.3 shows the variation of thickness (monolayer/cycle) and stoichiometry with with the arsenic steady state deposition potentials at constant steady state indium deposition potentials of –0.775 V. Thickness

drops off at arsenic potentials positive of –0.625 V. Between –0.625 V and –0.775 V, the deposits get thicker and deposition is close to one monolayer (ML) per cycle. At potentials negative of –0.775 V the thickness drops, where bulk deposition of arsenic would be expected. EPMA results indicated that more than 1 mL/cycle was deposited in this potential regime. Roughening of the deposits was observed by optical microscope and ellipsometric measurements were made assuming that deposits were smooth and flat. Apparently, these assumptions are no longer valid accounting for the low ellipsometric thickness readings. EPMA measurements of deposits made between potentials –0.625 V and –0.675 V gave a arsenic to indium atomic ratio of 1.3. ICPMS data showed that the atomic ratio of Arsenic to Indium was closer to 1.1. Figure 2.4 shows the variation of thickness (monolayer/cycle) and stoichiometry at different steady state indium deposition potentials at a constant arsenic steady state deposition potential of –0.675 V. The plateau region extends from –0.750 V to –0.800 V, where less than a ML/cycle is deposited. At potentials positive of –0.750 V, there is the expected drop in deposit thickness and at potentials negative of –0.800 V more than a ML/cycle is deposited as bulk indium begins to form. EPMA indicates constant arsenic to indium atomic ratio of 1.3, between –0.750 V and –0.800 V. Figure 2.5a shows AFM image of gold vapor deposited on glass at 400 C and then annealed in a hydrogen-oxygen flame prior to imaging. Large flat Au terraces (250nm) in diameter are observed. Fig 2.5b shows an AFM image of a 200 cycle InAs, deposited on an annealed Au on glass substrate. The deposit formed appears reasonably conformal with the substrate and some smooth crystallites are found on the surface of the deposit. Glancing angle X-ray diffraction for a 200 cycle InAs film (arsenic at -0.675 V, indium at –0.775 V) is as shown in Figure 2.6. The deposit was 63 nm thick. Diffraction

maxima for InAs are evident, as are maxima for Au[29]. Elemental Indium and Arsenic peaks are absent, suggesting compound formation. Infrared absorption measurements were performed to determine the band gap of the material. Since the films are grown on a gold substrate, transmission measurements were not possible. Reflection measurements were made using a variable angle reflection rig in conjunction with a Bruker 66v FTIR spectrometer, equipped on a cooled InSb detector. The incident angle of the p-polarized radiation was set to the Brewster angle, where the reflectance of parallel-polarized light is zero. The band gap (Fig 2.7) was estimated from absorption measurements by plotting $(\alpha h\upsilon)^2$ versus $h\upsilon$, with α being the experimentally determined absorption co-efficient and $h\upsilon$ the energy of infrared radiation[30]. The analysis gave a film bandgap of 0.36 eV consistent with literature values. In figure 2.8, left is an AFM image of flame annealed Au on glass and the right image indicates the 50 – 100 nm crystallites of Au in the un-annealed Au on glass substrate. InAs was electrodeposited on a substrate (figure 2.9) that had annealed Au on the left and un-annealed Au on the right. Absorption measurements indicated that the band gap of InAs blue shifted on un-anealed Au on glass. This is an example of quantum confinement due to small crystallites of the semiconductor on an un-annealed substrate.

Acknowledgement

We gratefully acknowledge the support of The National Science Foundation divisions of Materials and Chemistry, and The University Of Georgia Research Fund.

References

1. S.P.Grindle, A.H.Clark, S.Rezaic-Serej, E.Falconer, J.McNeily, and L.L.Kazmerski, J. Appl. Phys., **51**, p.5464 (1980).

2. Y.M.Yim and E.J.Stofko, J. Electrochem. Soc., **121**, p.965 (1974)

3.H. Gobrecht, H. D. Liess, and A. Tausend, Ber. Bunsenges. Phys. Chem., **67**, p. 930 (1963).

4. G. Hodes, J. Manassen, and D. Cahen, D. Nature, **261**, p. 403 (1976).

5. M. P. R. Panicker, M. Knaster, and F. A. Kroger, J. Electrochem. Soc., **125,** p. 566 (1978).

6. S. Chandra and N. Khare, Semicond. Sci. Technol., **2**, p. 220 (1987).

7. Y. K. Gao, A. Z. Han, Y. Q. Lin, Y. C. Zhao and J. D. Zhang, Thin Solid Films, **232**, p. 278 (1993).

8. Y. Gao, A. Han, Y. Lin, Y. Zhao and J. Zhang, J. Appl. Phys., **75**, p. 549 (1994).

9. K. R. Murali, V. Subramanian, N. Rangarajan, A. S. Lakshmanan and S. K. Rangarajan, Journal of Materials Science-Materials in Electronics, **2**, p. 149 (1991).

10. J. Ortega and J. Herrero, J. Electrochem. Soc., **136**, p. 3388 (1989).

11. J.McChesney, J.Haigh, I.Dharmadasa, and D.Mowthorpe, Optical Materials, **6**, p. 63 (1996).

12. S. N. Sahu, J. Mater. Sci. Lett., **8**, p. 533 (1989).

13. S. N. Sahu, J. Mater. Sci., **3**, p. 102 (1992).

14. S. N. Sahu, Journal of Materials Science-Materials in Electronics, **3**, p. 102 (1992).

15. G. Mengoli, M. M. Musiani and F. Paolucci, J. Electroanal. Chem., **332**, p. 199 (1992).

16. S. Cattarin, M. Musiani, U. Casellato, G. Rossetto, G. Razzini, F. Decker and B. Scrosati, J. Electrochem. Soc., **142**, p. 1267 (1995).

17. E. Dalchiel, S. Cattarin, M. Musiani, U. Casellato, P. Guerriero, G. Rossetto, J. Electroanal. Chem., **418**, p. 83 (1996).

18. B. W. Gregory, D. W. Suggs and J. L. Stickney, J. Electrochem. Soc., **138**, p. 1279 (1991).

19. B.M. Huang, L. P. Colletti, B. W. Gregory, J. L. Anderson and J. L. Stickney, J. Electrochem. Soc., **142**, p. 3007 (1995).

20. L.P. Colletti, B. H. Flowers Jr. and J. L. Stickney, J. Electrochem. Soc., **145**, p. 1442 (1998).

21. L. P. Colletti and J. L. Stickney, J. Electrochem. Soc., **145,** p. 3594 (1998).

22. U. Demir and C. Shannon, Langmuir, **10**, p. 2794 (1994).

23. M.L.Foresti, G.Pezzatini, M.Cavallini, G.Aloisi, M.Innocenti, and R.J.Guidelli, J. Phys. Chem. B, **102**, p. 7413 (1998).

24. G.Pezzatini, S.Caporali, M.Innocenti, and M.L.Foresti, J. Electroanal. Chem., **475**, p. 164 (1999)

25. D. M. Kolb, in Physical and Electrochemcial Properties of Metal Monolayers on Metallic Substrates; D. M. Kolb, Editor, Vol.11, p.125, John Wiley, New York, (1978).

26. I. Villegas and J.L. Stickney, J.Electrochem.Soc., 139, 686 (1992).

27. I. Villegas and J.L. Stickney, J. Vac. Sci. Technol. A, 10, 3032 (1992).

28. T.L. Wade, L.C. Ward, C.V. Maddox, U. Happek, and J.L. Stickney, Electrochem. Sol. State Lett., 2, 616 (1999).

29. Powder Diffraction File Alphabetical Index, Inorganic Phases; W. F. McClune, Editor, Card Numbers: InAs, (15-869); In, (5-642); Au, (4-784), JCPDS International Center for Diffraction Data, Swarthmore, PA, (1992).

30. K. Seeger, in Semiconductor Physics p. 40, Springer Series in Solid State Science, Springer Verlag, New York, (1982).

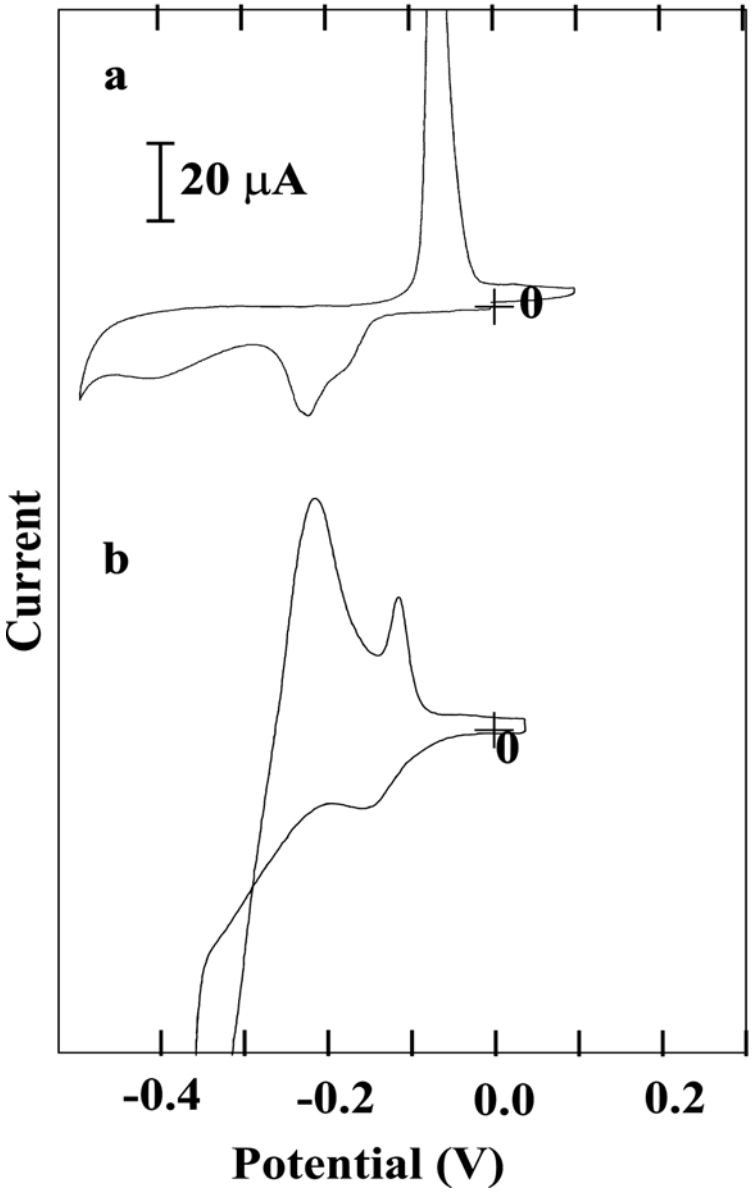

Figure 2.1. Cyclic voltammograms of vapor deposited Au on glass in: (a) 2.0 mM As_2O_3 , 0.5 M $NaClO_4$, 50 mM CH_3COONa, pH 4.5 (b) 0.3 mM $In_2(SO_4)_3$, 0.5 M $NaClO_4$, pH 3.0. Both voltammograms started at 0.2 V and scanned negative at 0.005 V/s.

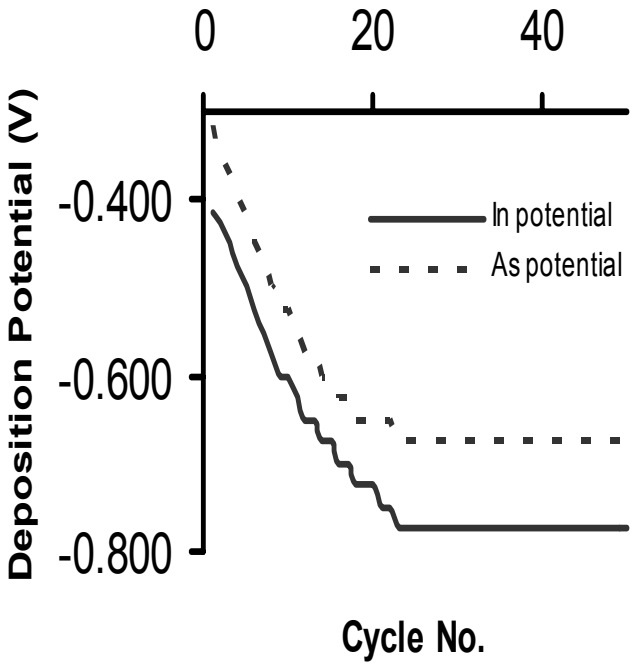

Figure 2.2. First 25 cycles of potential step up program for InAs electrodeposition.

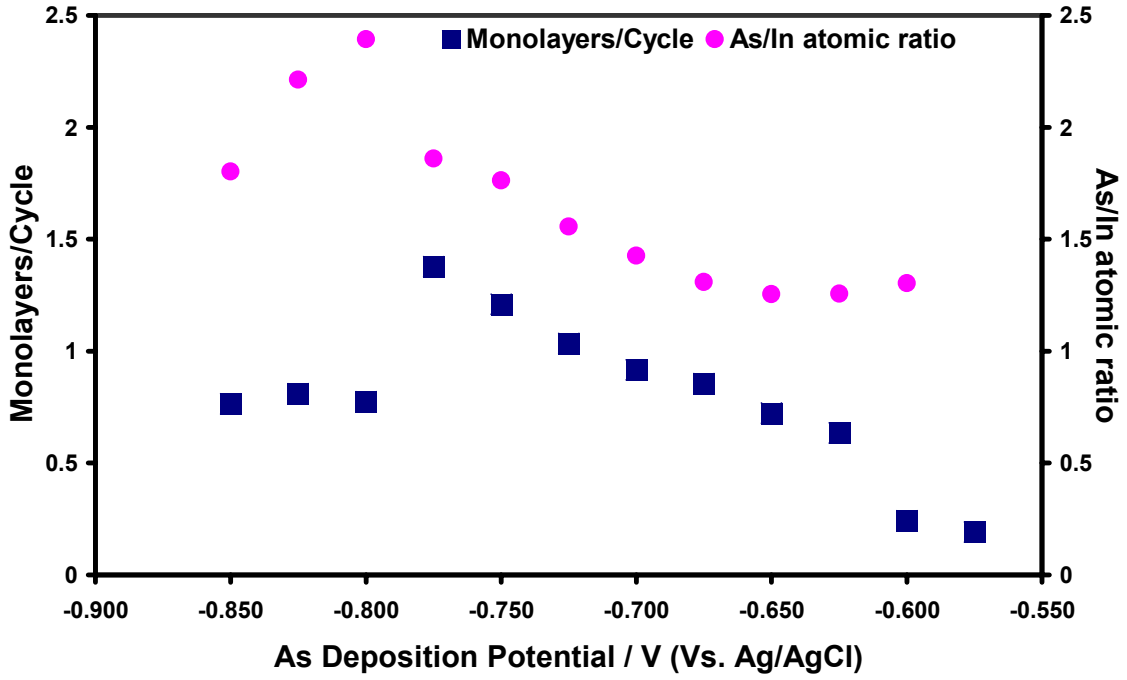

Figure 2.3. Graph of coverage/cycle and arsenic/indium ratio as a function of the arsenic deposition potential. The indium deposition potential was kept at –0.775 V.

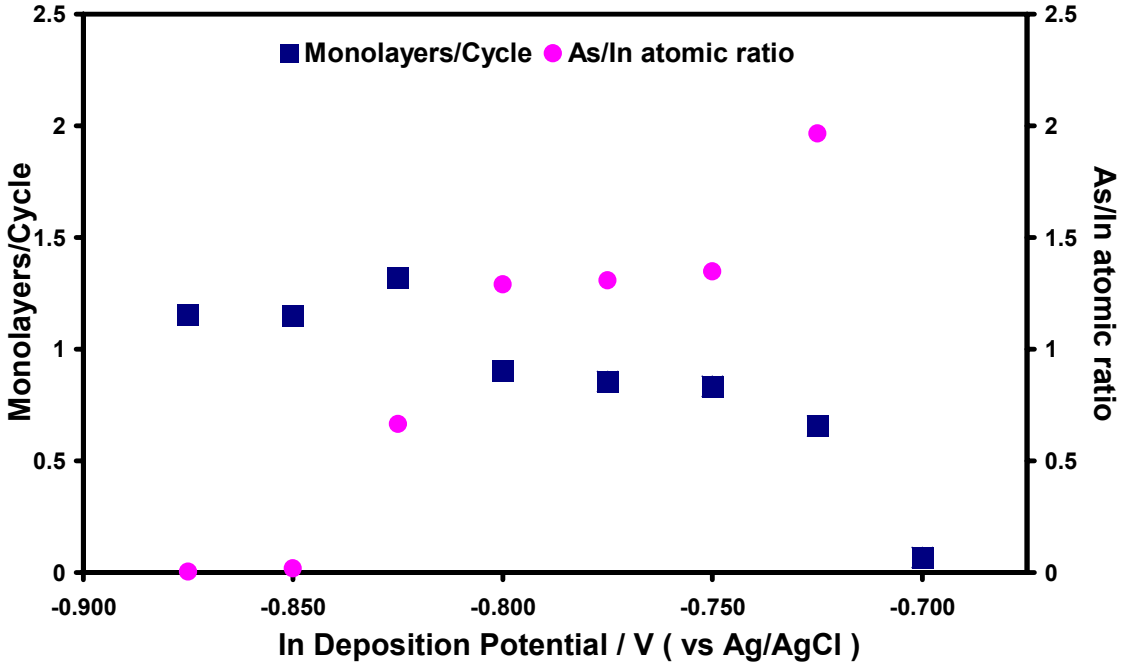

Figure 2.4. Graph of coverage/cycle and arsenic/indium ratio as a function of the indium deposition potential. The arsenic deposition potential was kept at –0.675 V.

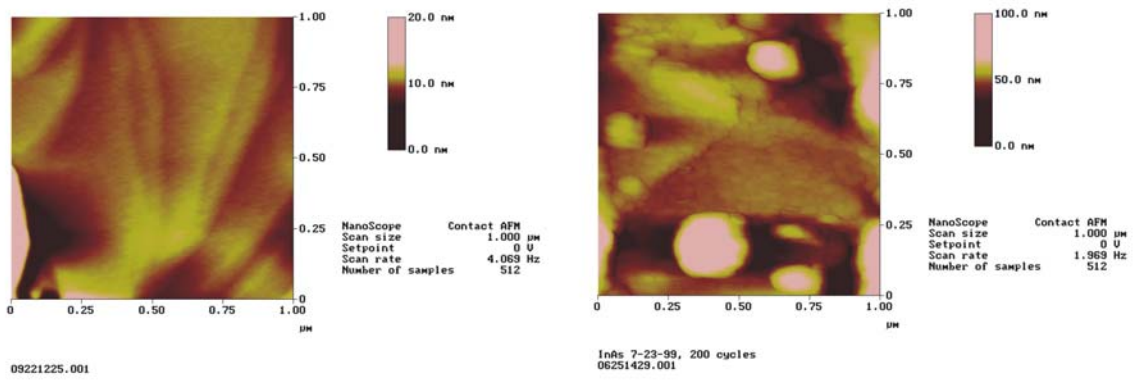

A B

Figure 2.5. AFM images a) Au vapor deposited on glass at 400 °C and annealed in a tube furnace and hydrogen-oxygen flame prior to imaging. b) 200 cycles InAs electrodeposition, on annealed Au on glass.

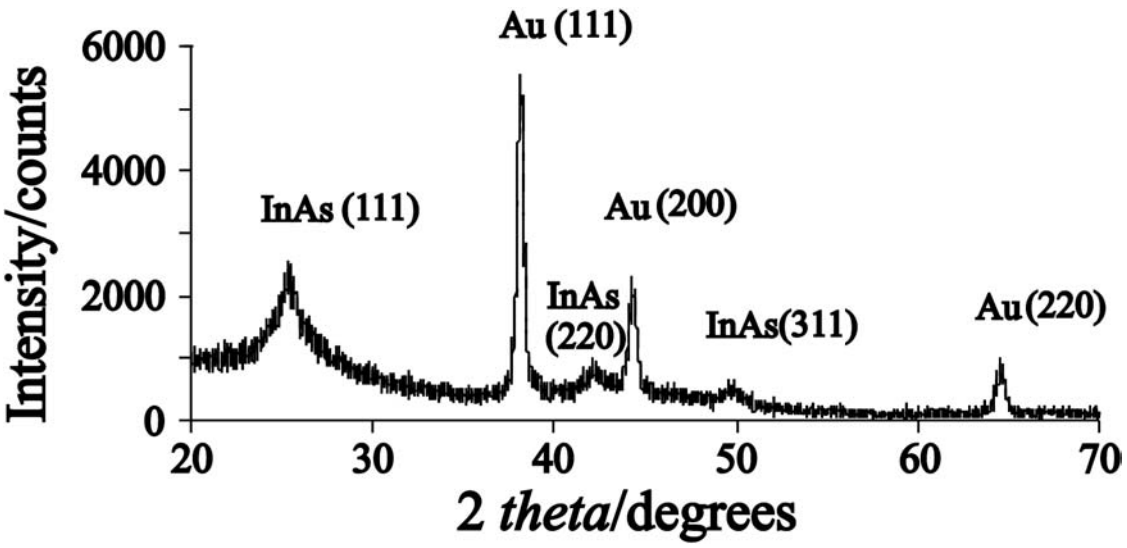

Figure 2.6. Grazing incidence angle diffraction pattern for InAs electrodeposited on Au. The glancing incidence angle was 0.5°.

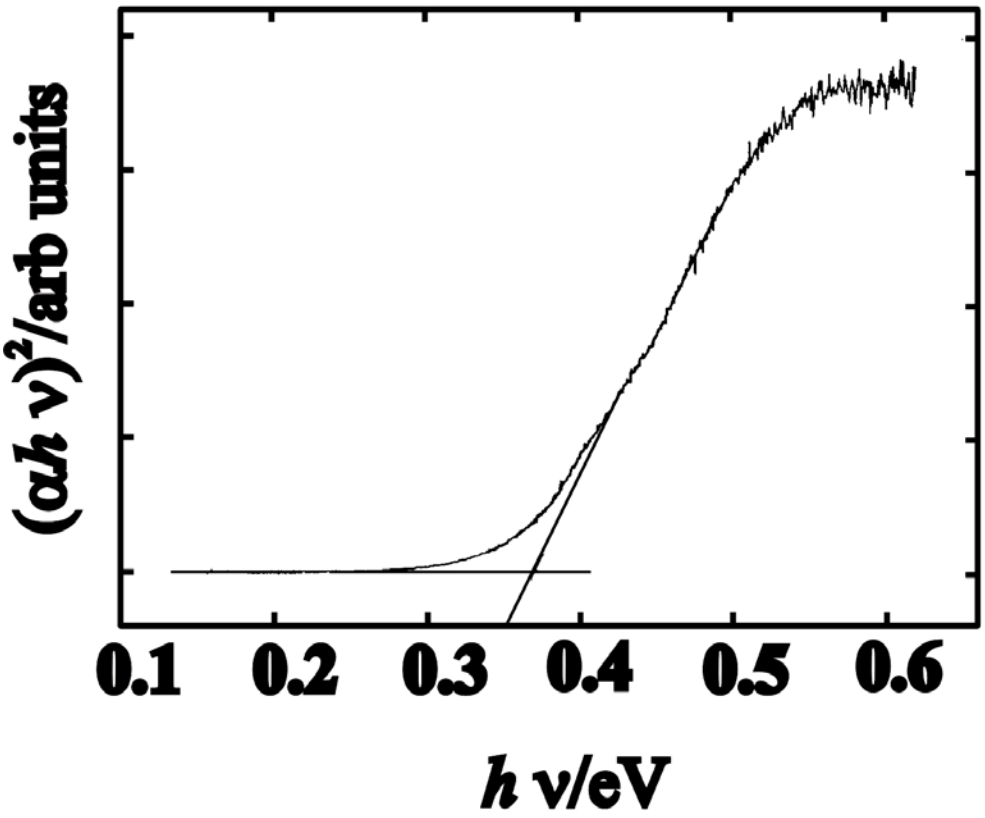

Figure 2.7. Infrared absorption data graphed as absorbtivity versus energy for 200 cycles of InAs electrodeposited on Au.

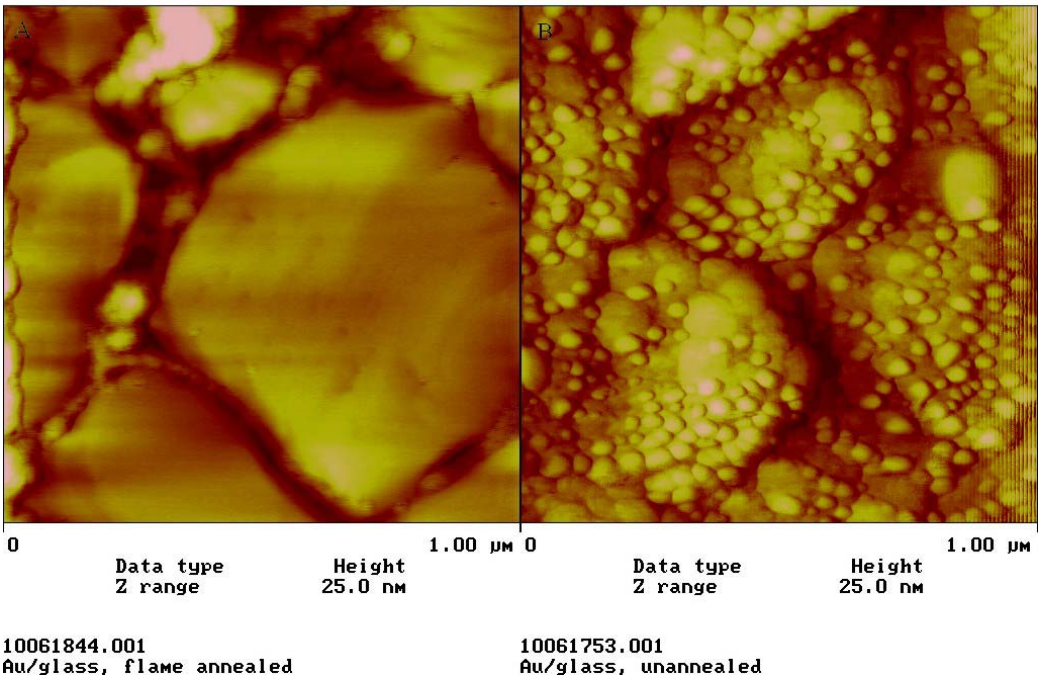

Figure 2.8. AFM image of annealed and un-annealed Au on glass substrate.

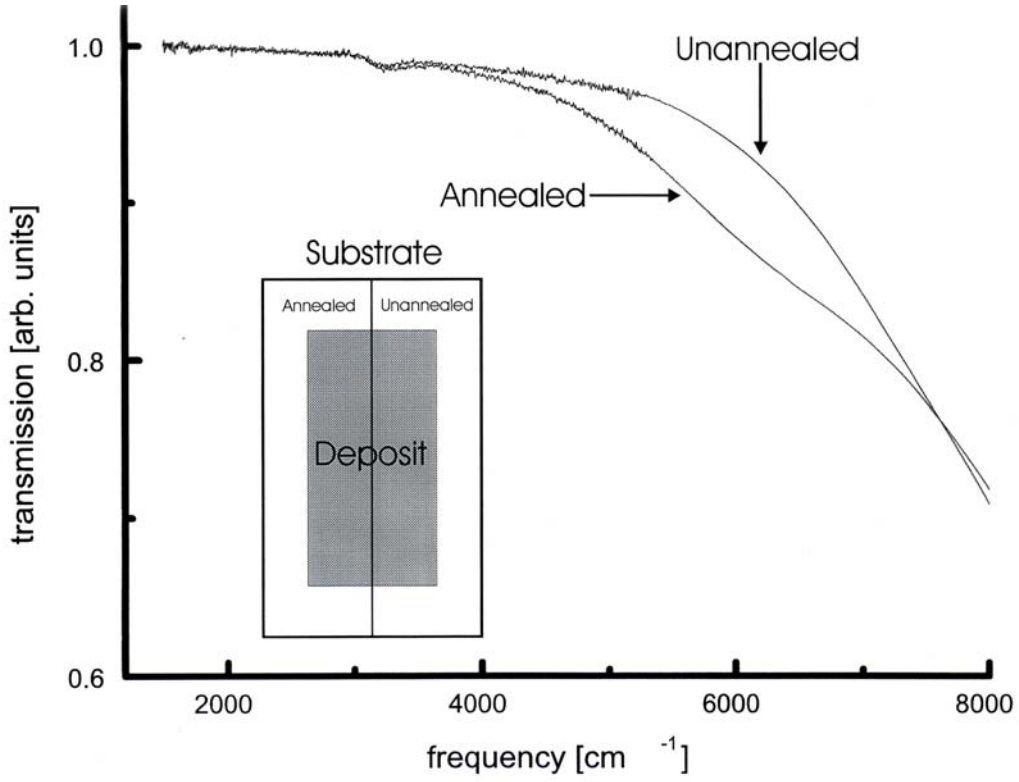

Figure 2.9. Infrared absorption measurements of InAs electrodeposited on annealed and un-annealed Au on glass substrate.

Chapter 3

Electrodeposition of Cu_2Se Thin Films by Electrochemical Atomic Layer Epitaxy (EC-ALE)[2].

[2] Vaidyanathan R, Mathe M.K, Sprinkle P.R, Cox S.M, Happek U and Stickney J.L, MRS Fall Proceedings, Boston 2002, Vol. 44, M5.34 (Used by permission).

Abstract

Electrochemical atomic-layer epitaxy (EC-ALE) is an approach to electrodepositing thin-films of compound semiconductors. It takes advantage of underpotential deposition (UPD), deposition of a surface limited amount (a monolayer or less) of an element at a potential less negative than bulk deposition, to form a thin-film of a compound--one atomic layer at a time. Ideally, the 2-D growth mode should promote epitaxial deposition.

We report the formation of compound Cu_2Se, at room temperature by electrochemical atomic layer epitaxy (EC-ALE). Cyclic voltammograms were used to determine the deposition potentials of each element. An automated deposition program was used to form 750 cycles of Cu_2Se thin films. Electron probe microanalysis was done to determine the stoichiometry of the thin films. X-ray diffraction of the 200 cycle deposit indicated the presence of polycrystalline Cu_2Se. The atomic ratio of Cu/Se in the thin films was found to be 2. Band gap of the thin films were determined by reflection absorption measurements. The band gap of the 200 cycle Cu_2Se films was found to be 1.6 eV. X-ray diffraction of 350 and 750 cycle Cu_2Se films, indicated the deposits consisted of Cu_3Se_2 and Cu_2Se.

Introduction

Electrodeposition of II-VI compounds such as CdTe and chalcopyrite semiconductors $CuInSe_2$ (CIS) has been studied for many years [1-4] and high efficiency photovoltaics, for instance, have been produced commercially. The standard compound electrodeposition methodology, co-deposition, involves the use of a single solution, containing oxidized precursors for all the elements involved in the compound. The deposit is formed by

reduction at a set potential or current density [5-7]. However, reports of the electrodeposition of Cu_2Se have been few, and have generally involved post-electrodeposition annealing or high temperature electrodeposition to produce the compound. CIS has also been formed by sequential evaporation and heat treatment of In_2Se_3 and Cu_2Se layers [8-15]. Cu_2Se has been formed by co-deposition [16-19] and has also been reported to deposit with $CuInSe_2$ during electrodeposition [20, 21], and it has also been used as a precursor for the formation of CIS. Post anneal treatment of the deposit is generally required to obtain stoichiometry and phase formation [17].

As electrodeposited Cu_2Se showed XRD peaks due to mixed phases of Cu_3Se_2 in the deposit and required post annealing and high temperature deposition. This highlights a major problem with compound electrodeposition: the need to maintain stoichiometry and form a phase pure material.

Recently, the electrochemical analog of atomic-layer epitaxy (ALE) has been developed to form compound thin films [22-28]. ALE refers to a methodology developed in the mid 70s for the formation of compounds an atomic layer at a time, using surface limited reactions [29-31]. Surface limited reactions encourage layer-by-layer growth, and thus epitaxial deposition. Surface limited reactions are well known in electrochemistry and are referred to as underpotential deposition (UPD) [32-34]. By selecting a potential prior to (under) that needed to deposit an element on itself, an atomic layer of the element can frequently be formed on a second element. Electrochemical ALE then involves using these underpotentials to form individual atomic layer of the elements making up a compound, using a cycle. Different solutions and potentials are used for each element then they are alternated in a cycle. The cycle is repeated to achieve the desired deposit thickness.

The main benefit of electrochemical ALE is that it breaks the deposition process into a series of controllable steps, each of which can be optimized individually. The degrees of freedom available in compound electrodeposition are thus expanded, allowing the growth of materials that may not have been possible using conventional co-deposition methodologies.

Experimental

Most of the hardware used in the present study has been described in previous articles [23, 24]. The deposition was carried out using an automated flow system, which consists of a series of solution reservoirs, computer controlled pumps, vales and a potentiostat. The system is contained within a nitrogen purged plexiglas box to reduce the influence of oxygen during electrodeposition. A thin-layer electrochemical flow cell, designed to maintain laminar flow was used for the deposition. The electrochemical cell consists of Au working electrode, Au coated indium tin oxide (ITO) auxiliary electrode and Ag/AgCl/3 M reference electrode (Bioanalytical systems, Inc., West Lafayette, IN). The following solutions were used: Cu_2SO_4 solution (Alfa Aesar, Ward Hill, MA): 0.1 mM Cu, with a pH of 5.5, buffered with 50.0 mM sodium citrate (J.T.Baker). SeO_2 solution (Alfa Aesar, Ward Hill, MA): 0.2 mM Se, 50.0 mM $CH_3COONa.3H_2O$, with a pH of 5.5. A pH 5.5 rinse solution was used as well. The pH values of all solutions were adjusted with H_2SO_4 (Fischer Scientific, Pittsburgh, PA). The supporting electrolyte was 0.1 M $NaClO_4$ (Fischer Scientific, Pittsburgh, PA). Solutions were made with water from a nanopure water filtration system (Barnstead, Dubuque, IA), fed by an inline house distilled water system. All chemicals were reagent grade or better.

Substrates were glass micro slides onto which a thin 3 nm film of Ti was first vapor deposited, followed by 700 nm of Au. The substrates were annealed in the deposition chamber at 400 °C for 12 hrs before vapor deposition. The substrates removed from the chamber are dipped in hot nitric acid and rinsed with nanopure water. The substrates were annealed using a H_2 flame and then cleaned in hot nitric acid and rinsed with nanopure water before use. The surface was composed of crystallites with atomically flat terraces as large as 300 nm, observed with an atomic force microscope (AFM) (NanoScope III; Digitial Instruments; Santa Barbara, CA).

Films were deposited on the substrates as follows: The cell was filled by a pump from a reservoir containing an electrolyte solution of the element of interest. A surface limited amount (~0.4 monolayer) of the element was deposited at a set potential. The cell was then rinsed with a blank electrolyte solution and filled with another electrolyte solution of the next element. A stoichiometric amount of this element was then deposited on the previous element and the cycle repeated.

Ellipsometric measurements were performed using a sentech SE 400 (Micro Photonics, Inc., Allentown, PA). Absorption measurements were performed using a variable angle reflection rig in conjunction with a Bruker 66v FTIR spectrometer equipped with Si detector. Glancing angle x-ray diffraction patterns were acquired on a Scintag diffractometer (Co source) equipped with a thin film attachment. Electron probe microanalysis studies were performed using a Joel JXA-8600 super probe.

Results and Discussion

From voltammetry (figure 3.1), a program using –0.1 V for Cu UPD and –0.2 V for Se UPD was suggested for the Cu_2Se cycle. In practice, the program worked for the first few cycles, but then the currents died out. This is understandable, considering that the potentials were chosen for deposition on an Au surface, not for deposition of the elements on the compound. The cycle was sequentially stepped more negative during the deposition by 10mV per cycle. After about 10 cycles final deposition potentials of –0.2 V for Cu and –0.3 V for Se were used for the rest of the deposit. Ellipsometric measurements (Sentech SE 400; Micro Photonics Inc.; Allentown, PA) were used to determine the thickness of the deposits.

Figure 3.2 is a glancing angle X-ray diffraction pattern for a 200, 300 and 750 cycle Cu_2Se film. In figure 3.2A the diffraction maxima for Cu_2Se are evident, as are maxima for Au. The widths of the diffraction maxima suggest that the Cu_2Se crystallites are a few nanometers. The factors controlling deposit grain size are the subject of ongoing studies, but the lattice mismatch is probably a contributing factor. Electron microprobe analysis (EPMA) reveals that the 200 cycle Cu_2Se films are stoichiometric (Se/Cu ~2).

Figure 3.2B and figure 3.2C show the evolution of Cu_3Se_2 phase in the thin film as a function of the deposition cycle. The thin films of 350 and 750 cycles essentially consist of mixed phases of Cu_2Se and Cu_3Se_2. This may be due to the deposition of excess Cu than required to react with Se to form Cu_2Se. Phase transformation of Cu_2Se to Cu_3Se_2 [17] is possible, but was not observed for 200 cycle deposits. The 200 cycle deposits were 70 nm thick.

Reflection absorption measurements (figure 3.3) were performed on the 200 cycle Cu_2Se films to determine the band gap of the obtained material. Since the films are grown on a gold substrate, transmission measurements were not possible. Reflection measurements using a variable angle reflection rig in conjunction with a Bruker 66v FTIR spectrometer equipped with a cooled MCT detector were made. The band gap was estimated from the absorption measurements by plotting $(\alpha h\nu)^2$ versus $h\nu$, with α being the experimentally determined absorption coefficient and $h\nu$ the energy of the infrared radiation. The analysis gave a band gap1.6 eV for the 200 cycle deposit.

Stoichiometric In_2Se_3 thin films have been formed by EC-ALE and have been reported earlier [35]. Formation of $CuInSe_2$ by alternate deposition of Cu_2Se and In_2Se_3 is feasible if deposition potentials of the three elements are close enough so that In does not strip during the deposition of Cu [36, 37]. Initial cycles for the deposition of CIS were attempted by using the UPD potentials of -0.3 V for In, -0.2 V for Cu and -0.2 V for Se. Microprobe analysis indicated that the CIS deposits were rich in Cu (Cu: In: Se ~ 3:1:2). At the potentials used for deposition of Cu and Se atomic layers, In is removed from the deposit and results in a Cu rich film. Investigation is underway to use a strong complexing agent for Cu, the potential for Cu deposition will be shifted to -0.3 V. Se deposition potential could be adjusted by changing the pH of the solution. For the formation of ternary compound CIS by EC-ALE, we need to form stoichiometric Cu_2Se and In_2Se_3 atomic layers and the deposition of single phase Cu_2Se atomic layers at room temperature by EC-ALE, eliminates the use of high temperature deposition and post annealing treatments and indicates the flexibility for atomic level control of CIS formation.

Acknowledgements

Support of the University of Georgia's research foundation (UGARF) is gratefully acknowledged.

References

(1) Fulop, G. F.; Taylor, R. M. *Ann. Rev. Mater. Sci.* **1985**, *15*, 197.

(2) Rajeshwar, K. *Adv. Mater.* **1992**, *4*, 23.

(3) Hodes, G. *SEM* **1994**, *32*, 323.

(4) Pandey, R. K.; Sahu, S. N.; Chandra, S. *Handbook of Semiconductor Electrodeposition*, 1st ed.; Marcel Dekker, Inc.: New York, 1996.

(5) Gobrecht, H.; Liess, H. D.; Tausend, A. *Ber. Bunsenges. Phys. Chem.* **1963**, *67*, 930.

(6) Hodes, G.; Manassen, J.; Cahen, D. *Nature* **1976**, *261*, 403.

(7) Panicker, M. P. R.; Knaster, M.; Kroger, F. A. *J. Electrochem. Soc.* **1978**, *125*, 566.

(8) Adurodija, F. O.; Carter, M. J.; Hill, R. *Solar Energy Materials and Solar Cells* **1995**, *37*, 203-216.

(9) Ashida, A.; Hachiuma, Y.; Yamamoto, N.; Ito, T.; Cho, Y. *Japanese Journal of Applied Physics Part 1-Regular Papers Short Notes & Review Papers* **1993**, *32*, 84-85.

(10) Ashida, A.; Hachiuma, Y.; Yamamoto, N.; Ito, T.; Cho, Y. *Journal of Materials Science Letters* **1994**, *13*, 1181-1184.

(11) Hachiuma, Y.; Ashida, A.; Yamamoto, N.; Ito, T.; Cho, Y. *Solar Energy Materials and Solar Cells* **1994**, *35*, 247-254.

(12) Lim, J. W.; Choi, J. H.; Choi, I. H. *Journal of the Korean Physical Society* **1997**, *30*, 293-298.

(13) Park, S. C.; Kwon, S. H.; Song, J. S.; Ahn, B. T. *Solar Energy Materials and Solar Cells* **1998**, *50*, 43-49.

(14) Park, J. S.; Dong, Z.; Kim, S.; Perepezko, J. H. *Journal of Applied Physics* **2000**, *87*, 3683-3690.

(15) Park, S. C.; Lee, D. Y.; Ahn, B. T.; Yoon, K. H.; Song, J. *Solar Energy Materials and Solar Cells* **2001**, *69*, 99-105.

(16) Massaccesi, S.; Sanchez, S.; Vedel, J. *Journal of the Electrochemical Society* **1993**, *140*, 2540-2546.

(17) Lippkow, D.; Strehblow, H. H. *Electrochimica Acta* **1998**, *43*, 2131-2140.

(18) Pottier, D.; Maurin, G. *J. Appl. Electrochem.* **1989**, *19*, 361.

(19) Sebastian, P. J.; Pattabi, M. *Journal of Physics D-Applied Physics* **1992**, *25*, 981-985.

(20) Bhattacharya, R. N.; Batchelor, W.; Wiesner, H.; Hasoon, F.; Granata, J. E.; Ramanathan, K.; Alleman, J.; Keane, J.; Mason, A.; Matson, R. J.; Noufi, R. N. *Journal of the Electrochemical Society* **1998**, *145*, 3435-3440.

(21) Guillen, C.; Martinez, M. A.; Herrero, J. *Vacuum* **2000**, *58*, 594-601.

(22) Gregory, B. W.; Suggs, D. W.; Stickney, J. L. *J. Electrochem. Soc.* **1991**, *138*, 1279.

(23) Huang, B. M.; Colletti, L. P.; Gregory, B. W.; Anderson, J. L.; Stickney, J. L. *Journal of the Electrochemical Society* **1995**, *142*, 3007.

(24) Colletti, L. P.; Flowers Jr., B. H.; Stickney, J. L. *Journal of the Electrochemical Society* **1998**, *145*, 1442-1449.

(25) Colletti, L. P.; Stickney, J. L. *Journal of the Electrochemical Society* **1998**, *145*, 3594.

(26) Demir, U.; Shannon, C. *Langmuir* **1994**, *10*, 2794-2799.

(27) Aloisi, G. D.; Cavallini, M.; Innocenti, M.; Foresti, M. L.; Pezzatini, G.; Guidelli, R. *Journal of Physical Chemistry B* **1997**, *101*, 4774-4780.

(28) Hayden, B. E.; Nandhakumar, I. S. *Journal of Physical Chemistry B* **1998**, *102*, 4897.

(29) Goodman, C. H. L.; Pessa, M. V. *JAP* **1986**, *60*, R65.

(30) Sakaue, H.; Asami, K.; Ichihara, T.; Ishizuka, S.; Kawamura, K.; HJoriike, Y. In *Atomic Layer Growth and Processing*; Kuech, T. F., Dapkus, P. D., Aoyagi, Y., Eds.; Mater. Res. Soc.: Pittsburgh, 1991; Vol. 222, pp 195.

(31) Bedair, S. *Atomic Layer Epitaxy*; Elsevier: Amsterdam, 1993.

(32) Kolb, D. M. In *Advances in Electrochemistry and Electrochemical Engineering*; Gerischer, H., Tobias, C. W., Eds.; John Wiley: New York, 1978; Vol. 11, pp 125.

(33) Adzic, R. R. In *Advances in Electrochemistry and Electrochemical Engineering*; Gerishcher, H., Tobias, C. W., Eds.; Wiley-Interscience: New York, 1984; Vol. 13, pp 159.

(34) Gewirth, A. A.; Niece, B. K. *Chem. Rev.* **1997**, *97*, 1129-1162.

(35) Vaidyanathan, R.; Stickney, J. L.; Happek, U. *J. Electroanal. Chem.* **2002**, *accepted*.

(36) Herrick, R. D. I.; Stickney, J. L. In *New Directions in Electroanalytical Chemistry*; Leddy, J., Wightman, M., Eds.; The Electrochemical Society: Pennington, NJ, 1996; Vol. 96-9, pp 186.

(37) Oliveira, M. C. F.; Azevedo, M.; Cunha, A. *TSF* **2002**, *405*, 129-134.

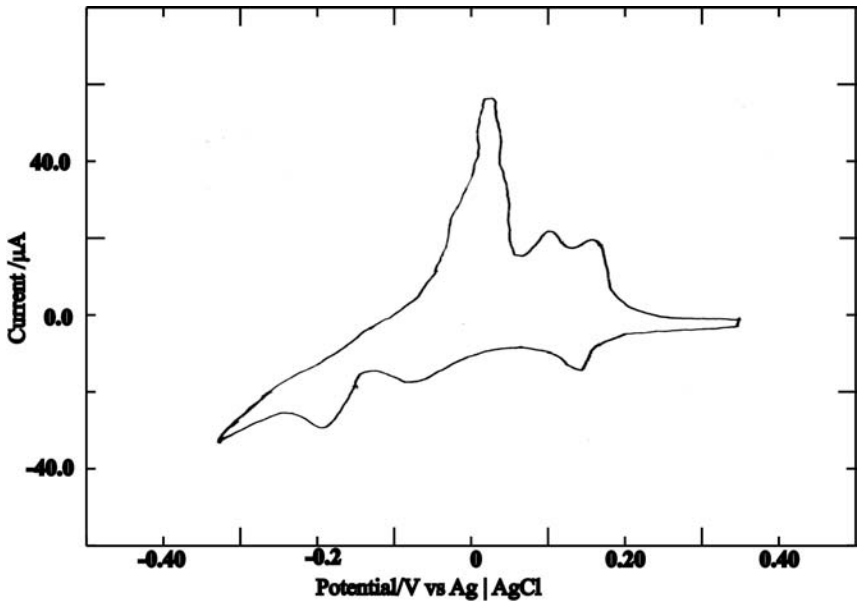

Figure 3.1. Voltammogram of a Au electrode in 0.1 mM Cu_2SO_4, 50 mM sodium citrate solution, pH 5.5.

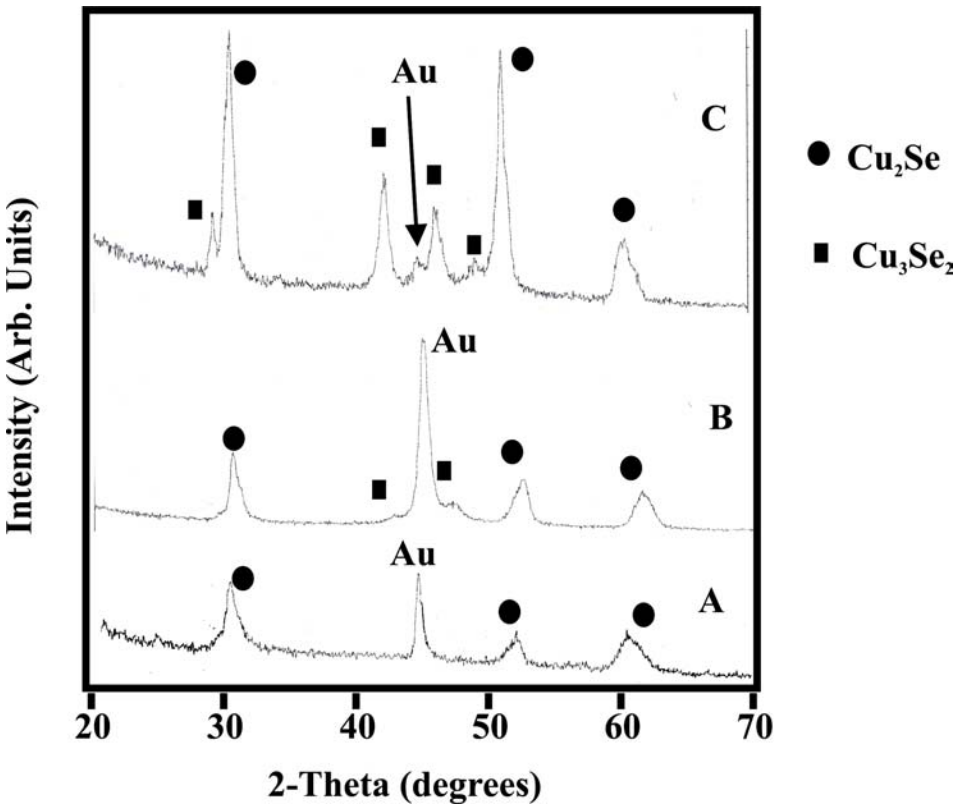

Figure 3.2. Glancing angle XRD pattern of A) 200 cycle B) 350 cycle C) 750 cycle electrodeposited Cu_2Se.

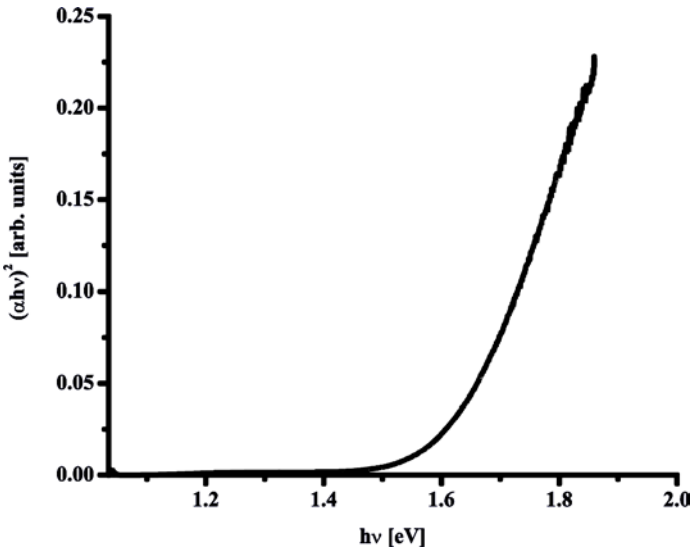

Figure 3.3. Infrared absorption measurements for a 200 cycle Cu_2Se deposit electrodeposited on annealed Au on glass substrate.

Chapter 4

Formation of In_2Se_3 Thin Films and Nanostructures using Electrochemical Atomic Layer Epitaxy (EC-ALE)[3].

[3] Vaidyanathan R, Stickney J.L, Cox S.M, Compton S.P, Happek U, Journal of Electroanalytical Chemistry, August 1, 2003 (Used by permission).

Abstract

The formation of the III-VI compound In_2Se_3, at room temperature by electrochemical atomic layer epitaxy (EC-ALE) is reported here. EC-ALE involves the use of surface limited reactions to form atomic layers of the elements making up a compound (In and Se) in a cycle. In Electrodeposition, surface limited reactions are referred to as under potential deposition (upd), and generally result in the formation of an atomic layer of the depositing element. These layers are deposited alternately in a cycle, resulting in the formation of a one monolayer (ML) of the compound, In_2Se_3. Cyclic voltammograms were used to determine approximate deposition potentials for each element. An automated deposition program was used to form thin films of In_2Se_3, with from up to 350 cycles. Electron probe microanalysis was performed to determine the stoichiometry of the thin-films. The atomic ratio of Se/In in the thin films was found to be 3/2. X-ray diffraction of 350 cycle films indicated the deposits contained beta phase In_2Se_3. Band gaps were determined by FT-IR reflection absorption measurements, and found to be 1.73 eV. Surface morphology was determined by atomic force microscopy (AFM), suggesting the deposits consist of 100 nm crystallites. Deposits on rougher substrates resulted in still smaller crystallites, and a blue shift in the band gap, possibly due to quantum confinement. Photoelectrochemical measurements suggested a band gap of 1.82 eV. In_2Se_3 nanostructures were electrodeposited inside the pores (200 nm) of commercial polycarbonate membrane using EC-ALE. AFM images indicated that nano-structures were higher then expected, for 200 cycles of deposition. Studies of the Au vapor deposited on the membrane showed that it had ingressed into the holes, accounting

for most of the extra height. Microprobe data suggested that the total coverage was 1/6th that observed for a thin film, consistent with the observed coverage of nanostructures.

Keywords

Electrodeposition, Compound Semiconductor, III-VI, Thin films, ECALE, upd, Nanostructures, Template synthesis, Polycarbonate membrane

Introduction

III-VI compound semiconductors have received much attention in recent years for applications in photovoltaic and photoelectrochemical devices [1-10]. Atomic level control in the epitaxial growth of these materials is desired for the formation of high efficiency solar cells. Techniques such as molecular beam epitaxy (MBE) [11-13], vapor deposition [14], spray pyrolysis [15] and evaporation techniques [16-23] are some of the methods used for the growth of III–VI materials like In_2Se_3 and In_2Te_3. These compound semiconductors have been formed, by sequential evaporation of In and Se layers, followed by post deposition annealing at high temperatures. Chalcopyrite semiconductors ($CuInSe_2$) have also been formed by sequential evaporation and heat treatment of In_2Se_3 and Cu_2Se layers [2, 3, 8]. Various phases of the compound In_2Se_3 exist and have been reported in previous publications [24, 25].

Device structures composed of different materials are generally formed at elevated temperatures (by MBE, MOCVD…). At high temperatures, the boundaries between these materials blur, due to interdiffusion of the component elements, degrading the quality of the device. Interdiffusion is minimized for devices formed near room temperature. Electrodeposition is a low-temperature technique, minimizing interdiffusion, and is thus appealing for the formation of complex compound semiconductors structures, including some photovoltaics [6, 7, 9, 26-29]. One of the standard methods for compound electrodeposition is co-deposition, where a set reduction potential or current density is applied to a single solution containing precursors for all the elements in a compound. In_2Se_3 has been formed by Co-deposition [1, 30], as has $CuInSe_2$ [29, 31]. Post deposition

annealing of the deposits was generally required to adjust stoichiometry, crystallinity, and the phase formed.

Atomic layer epitaxy (ALE) is a method used to form compound thin films one atomic layer at a time. Surface limited reactions are used to control the growth rate and morphology. ALE offers greater control over deposit structure then methods based on controlling reactant fluxes for all elements simultaneously. Our group has been developing the electrochemical analog of ALE, electrochemical atomic layer epitaxy (EC-ALE) [32-34]. Surface limited reactions are well known in electrochemistry and are referred to as underpotential deposition (upd) [35-39]. Upd is the deposition of an atomic layer of one element on a second, at a potential prior to that needed to form bulk deposits of the first. Upd facilitates the formation of compounds one atomic layer at a time in EC-ALE. II-VI compounds such as CdTe [33, 40-45], CdS[46-50], and ZnSe[51, 52] have been successfully formed using by EC-ALE, as well as some III-V compounds: GaAs[53-55], InAs[56], InSb and superlattices of InAs/InSb [57]. Initial studies for the development of a cycle for $CuInSe_2$ formation [58] were reported earlier, where difficulties were found in starting the second cycle without stripping out In. It was then decided to try and deposit Cu_2Se and In_2Se_3, to create $CuInSe_2$ via a superlattice of the two compounds. Cu_2Se was formed, but controlling the phase and stoichiometry proved difficult. In this publication we report the room temperature formation of In_2Se_3 using EC-ALE.

Template based electrochemical synthesis of semiconductor nano-structures has been investigated in several research laboratories. Those studies generally involved electrodeposition into commercial template membranes. The first example appears to be

that of Sailor and Martin, where a nanoelectrode array based on an anodized aluminum membrane was used to form an array of nano diode wires, based on the compounds CdSe and CdTe [59]. A unique compound electrodeposition methodology, sequential monolayer electrodeposition (SMED), was used. SMED is based on a cyclic potential program and a single solution. The potential program was designed to improve stoichiometry in the deposits by stripping excess Se each cycle [60]. There have been several other examples of compound electrodeposition into template electrodes [61-64]. The first attempt to electrodeposit compounds into nanotemplates using EC-ALE is presented here.

Experimental

Depositions were carried out using an automated electrochemical thin-layer flow deposition system, consisting of a series of solution reservoirs, computer controlled pumps, valves and a potentiostat. Most of the hardware used has been described in previous articles [56, 65]. The system is contained within a nitrogen purged Plexiglas box, to reduce the influence of oxygen during electrodeposition. A thin-layer electrochemical flow cell, designed to maintain laminar flow was used for the depositions, and consisted of a Au working electrode, Au coated indium tin oxide (ITO) auxiliary electrode and Ag | AgCl (3M NaCl) reference electrode (Bioanalytical systems, Inc., West Lafayette, IN).

Solutions used include: 0.3 mM $In_2(SO_4)_3$ (Alfa Aesar, Ward Hill, MA), pH 3.0, buffered with 50.0 mM $CH_3COONa{\cdot}3H_2O$ (J.T.Baker); 0.2 mM SeO_2 (Alfa Aesar, Ward Hill, MA), pH 5.5, also buffered with 50.0 mM $CH_3COONa{\cdot}3H_2O$. A pH 3.0 rinse solution was used as well. The pH values of all solutions were adjusted with H_2SO_4

(Fischer Scientific, Pittsburgh, PA). Supporting electrolyte, 0.1 M $NaClO_4$ (Fischer Scientific, Pittsburgh, PA), was added to each solution. Solutions were made with water from a Nanopure water filtration system (Barnstead, Dubuque, IA), fed from the house distilled water system. All chemicals were reagent grade or better.

Substrates were glass microscope slides (Gold Seal products), etched in HF briefly prior to insertion into the deposition chamber. The substrates were annealed in the deposition chamber at 400 °C for 12 hrs before vapor deposition. Thin, 3 nm thick, films of Ti were first vapor deposited, followed by 600 nm of Au, while the substrates were held at 400 °C. The substrates, removed from the chamber, were dipped in nitric acid and rinsed with nanopure water. Prior to use, the substrates were annealed using a H_2 flame (to a dull orange glow in the dark), cleaned again in hot nitric acid and rinsed with nanopure water. The templates used for electrodeposition were track etched polycarbonate membranes (Poretics Inc.) with an average pore size of 200 nm and 6 to 14 μm thick. Gold was vapor deposited at room temperature on to the back of the membrane. The template was glued onto a glass slide using silver paint and mounted into electrochemical flow cell described earlier.

AFM studies were performed using a Nanoscope 2000 (Digital Instruments, Santa Barbara, CA) in the tapping mode. Ellipsometric measurements were performed using a Sentech SE 400 (Micro Photonics, Inc., Allentown, PA). Absorption measurements were performed using a variable angle reflection rig in conjunction with a Bruker 66v FTIR spectrometer equipped with a Si detector. Glancing angle X-ray diffraction patterns were acquired on a Scintag PAD V diffractometer, equipped with a 6” long set of Sola slits on

the detector to improve resolution in this asymmetric diffraction configuration. Electron probe microanalysis (EPMA) studies were performed using a Joel JXA-8600 super probe.

Results and Discussion

In_2Se_3 thin films

The starting potentials in the deposition program were determined from cyclic voltammograms for each element. Potentials of -0.3 V for In (Fig. 4.1) and -0.3 V for Se (Fig. 4.2) were identified as reasonable potentials for upd in a cycle for In_2Se_3.

The cycle involved filling the cell with the In solution at a potential of -0.3 V and holding the solution for 15 sec for deposition. The cell was then rinsed with the blank for 2 sec and filled with the Se solution, again at –0.3 V for 15 sec, for deposition. This cycle was intended to form a ML of the III-VI semiconductor In_2Se_3.

The deposition currents, however, decreased over the first few cycles, resulting in less then a monolayer of compound each cycle. This could be the simple result of depending on potentials chosen for upd on Au, not for upd on the compound. However, similar phenomena have been observed with most of the compound formed using EC-ALE: the potentials have to be shifted more negatively over the first 25-30 cycles in order to maintain ML/cycle deposition. The justification for this is that some of the applied potential is being dropped across a growing space charge layer (SCL)/schotky barrier, between the Au electrode and the developing semiconductor. This would correspond to a very thin SCL, which should be a function of the doping in the deposit, and suggests a highly doped material. Doping studies are planed, to better understand the conditions in the deposit. To keep the deposition charges sufficient for the formation of a full monolayer with each cycle, the potentials were stepped negative after each of the first 30

cycles (Fig. 4.3). After 30 cycles, steady state potentials of -0.650 V for In and –0.720 V for Se were attained, and used to form the rest of the deposit.

Ellipsometric measurements of 350 cycle deposits indicated that the films were 100 nm thick. EPMA of the deposits indicated an Se/In atomic ratio of 3/2 (standard deviation = 0.03). Fig. 4.4 shows the X-ray diffraction patterns for a 350 cycle In_2Se_3 deposit. The peaks for the (211) and (301) planes of In_2Se_3 [JCPDS 20-0494] are seen as shoulders on the Au diffraction peaks. No other diffraction peaks were seen for In_2Se_3. Given the intensity of the peaks, it appears the quality of the structure is not high. Prelimary raman studies suggested some of the material may be amorphous, and a more extensive study is planned. Fig. 4.5a shows an AFM image of the flame annealed Au on glass substrate, while Fig. 4.5b shows an AFM image of a 350 cycle deposit of In_2Se_3. The thin film consists of particles that are between 70-200 nm in diameter, which are conformal with the Au substrate. These results suggest 2-D growth of In_2Se_3 thin films.

Fig. 4.6 shows a plot of the square of the absorption data for a 350 cycle deposit of In_2Se_3, times energy, vs. energy. The band gap for the In_2Se_3 deposit was estimated to be 1.73 eV. The band gaps for In_2Se_3 films reported in the literature range between 1.2-1.8 eV. The band gap from photoelectrochemical measurements (Fig. 4.7) was found to be 1.82 eV.

<u>In_2Se_3 nano-structures</u>

Fig. 4.9 shows the AFM image of a polycarbonate membrane with 200 nm diameter pores, at randomly oriented angles to the surface. A 1μm thick Au film was deposited on the back, using a 45 degree angle of incidence, helping to cover the holes (Fig. 4.10). The cell was filled with the In precursor solution and a monolayer of the element was

deposited. After the deposition, the cell is rinsed with a blank solution. After the blank rinse, the cell was filled with the Se precursor solution and an atomic layer was deposited. The cell was again rinsed with blank. This program was repeated, to form nano-structures inside the polycarbonate membrane. A schematic for formation of the nanostructures is shown in Fig. 4.8. The Au was vapor deposited onto the back of the membrane and electrodeposition was carried out from the top. The membrane was dissolved in methylene chloride solution and the nanostructures were retained on the gold surface. Fig. 4.11 shows an AFM image of In_2Se_3 nanostructures, after dissolving the membrane. The diameter of these structures range between 180- 200 nm. For a 200 cycle EC-ALE experiment, the expected deposit thickness inside a pore is 70 nm. The AFM shows that structures are about 1μm tall. There also appears to be extra deposition on the edges compared to the centers of the clusters, as indicated by a dip in the center of each structure, imaged with AFM.

Initially, it was felt that the deposits were much thicker then expected, because of the high aspect ratio of the templates. There may not have been sufficient time for the ions to diffuse in and back out during rinsing. However, to better understand the morphology of the deposits, the polycarbonate membrane was dissolved from the vapor deposited Au film (substrate), without having deposited any compound. The Au surface that had been in contact with the polycarbonate was imaged with AFM, and showed that the vapor deposited Au ingressed into the holes in the polycarbonate template, resulting in a ring with a hole in the center. Observed nanocluster heights were revieled to be excessively high because of the ingressed Au. The dips in the centers of the clusters were shown to simply be the result of depositing on a ring electrode (Figure 4.11). Analysis of the

EPMA data suggested the coverages of In_2Se_3 for the clusters was about $1/6^{th}$ that expected for a thin film formed with the same number of cycles. This is consistent with coverages observed with AFM, and suggest that diffusion problems due to the high aspect ratio were only a minority issue.

Conclusions

In_2Se_3 thin films have been successfully formed using EC-ALE. The deposits appear to be composed of 100 nm In_2Se_3 crystallites on the Au substrate. The band gap of the thin film is in reasonable agreement with the bulk value. The room temperature phase, β-In_2Se_3, has been formed with up to 350 cycles of deposition. Studies designed to form $CuInSe_2$ by alternating layers of In_2Se_3 and Cu_2Se are presently underway. Semiconductor nanoclusters have been formed using EC-ALE in the pores of polycarbonate membranes. Technical problems with ingression of Au into the holes in the polycarbonate membrane were responsible for the excessive vertical height of the nanoclusters, and the dips in the centers. The high aspect ratio of these pores may have also caused some problems with ion exchange between steps in the EC-ALE cycle, possibly resulting in a small amount of co-deposition during formation of the nanostructures. The possibility of forming low aspect ratio template materials (30-50 nm diameter holes, but only and 100-500 nm tall) is being pursued.

Acknowledgements

Acknowledgement is gratefully made to support from the National Science Foundation, Divisions of Materials and Chemistry.

References

1. J. Herrero and J. Ortega, Solar Energy Materials 16:477 (1987).

2. A. Ashida, Y. Hachiuma, N. Yamamoto, T. Ito, and Y. Cho, Jpn. J. Appl. Phys. Part 1 - Regul. Pap. Short Notes Rev. Pap. 32:84 (1993).

3. Y. Hachiuma, A. Ashida, N. Yamamoto, T. Ito, and Y. Cho, Sol. Energy Mater. Sol. Cells 35:247 (1994).

4. J.W. Lim, J.H. Choi, and I.H. Choi, J. Korean Phys. Soc. 30:293 (1997).

5. P. Gallon, F. Ouchen, M.C. Artaud, and S. Duchemin, in Ternary and Multinary Compounds, Vol. 152, IOP PUBLISHING LTD, Bristol, 1998, p. 365.

6. S.H. Kwon, S.C. Park, B.T. Ahn, K.H. Yoon, and J.S. Song, Sol. Energy 64:55 (1998).

7. S.H. Kwon, B.T. Ahn, S.K. Kim, K.H. Yoon, and J. Song, Thin Solid Films 323:265 (1998).

8. S.C. Park, S.H. Kwon, J.S. Song, and B.T. Ahn, Sol. Energy Mater. Sol. Cells 50:43 (1998).

9. A.M. Hermann, M. Mansour, V. Badri, B. Pinkhasov, C. Gonzales, F. Fickett, M.E. Calixto, P.J. Sebastian, C.H. Marshall, and T.J. Gillespie, Thin Solid Films 361:74 (2000).

10. A. Kampmann, V. Sittinger, J. Rechid, and R. Reineke-Koch, Thin Solid Films 361:309 (2000).

11. T. Ohtsuka, T. Okamoto, A. Yamada, and M. Konagai, in Compound Semiconductors 1997, Vol. 156, IOP PUBLISHING LTD, Bristol, 1998, p. 183.

12. T. Ohtsuka, K. Nakanishi, T. Okamoto, A. Yamada, M. Konagai, and U. Jahn, Jpn. J. Appl. Phys. Part 1 - Regul. Pap. Short Notes Rev. Pap. 40:509 (2001).

13. T. Okamoto, A. Yamada, and M. Konagai, J. Cryst. Growth 175:1045 (1997).

14. J.W. Cheon, J. Arnold, K.M. Yu, and E.D. Bourret, Chem. Mat. 7:2273 (1995).

15. H. Bouzouita, N. Bouguila, S. Duchemin, S. Fiechter, and A. Dhouib, Renew. Energy 25:131 (2002).

16. C.H. de Groot and J.S. Moodera, J. Appl. Phys. 89:4336 (2001).

17. M. Emziane and R. Le Ny, J. Phys. D-Appl. Phys. 32:1319 (1999).

18. M. Emziane, S. Marsillac, and J.C. Bernede, Mater. Chem. Phys. 62:84 (2000).

19. D. Manno, G. Micocci, R. Rella, P. Siciliano, and A. Tepore, Vacuum 46:997 (1995).

20. S. Marsillac, J.C. Bernede, R. Leny, and A. Conan, Vacuum 46:1315 (1995).

21. A.F. Qasrawi, M. Parlak, C. Ercelebi, and I. Gunal, J. Mater. Sci.-Mater. Electron. 12:473 (2001).

22. S. Marsillac, J.C. Bernede, M. Emziane, J. Wery, E. Faulques, and P. Le Ray, Appl. Surf. Sci. 151:171 (1999).

23. M. Emziane and R. Le Ny, Thin Solid Films 385:312 (2001).

24. J. Vanlanduyt, G. Vantendeloo, and S. Amelinckx, Phys. Status Solidi A-Appl. Res. 30:299 (1975).

25. J.P. Ye, S. Soeda, Y. Nakamura, and O. Nittono, Jpn. J. Appl. Phys. Part 1 - Regul. Pap. Short Notes Rev. Pap. 37:4264 (1998).

26. O. Savadogo, Sol. Energy Mater. Sol. Cells 52:361 (1998).

27. A. Kampmann, A. Abken, G. Leimkuhler, J. Rechid, V. Sittinger, T. Wietler, and R. Reineke-Koch, Prog. Photovoltaics 7:129 (1999).

28. R. Herberholz, U. Rau, H.W. Schock, T. Haalboom, T. Godecke, F. Ernst, C. Beilharz, K.W. Benz, and D. Cahen, Eur. Phys. J.-Appl. Phys 6:131 (1999).

29. R.N. Bhattacharya, A.M. Fernandez, M.A. Contreras, J. Keane, A.L. Tennant, K. Ramanathan, J.R. Tuttle, R.N. Noufi, and A.M. Hermann, J. Electrochem. Soc. 143:854 (1996).

30. S. Massaccesi, S. Sanchez, and J. Vedel, J. Electroanal. Chem. 412:95 (1996).

31. L. Thouin, S. Massaccesi, S. Sanchez, and J. Vedel, J. Electroanal. Chem. 374:81 (1994).

32. B.W. Gregory and J.L. Stickney, J. Electroanal. Chem. 300:543 (1991).

33. B.W. Gregory, D.W. Suggs, and J.L. Stickney, J. Electrochem. Soc. 138:1279 (1991).

34. J.L. Stickney, T.L. Wade, B.H. Flowers Jr, R. Vaidyanathan, and U. Happek, in Encyclopedia of Electrochemistry, Vol. 1 (A. J. a. S. BARD, ed.), 2002, p. 1.

35. E. Herrero, L.J. Buller, and H.D. Abruna, Chemical Reviews 101:1897 (2001).

36. A.A. Gewirth and B.K. Niece, Chem. Rev. 97:1129 (1997).

37. R.R. Adzic, in Advances in Electrochemistry and Electrochemical Engineering, Vol. 13 (H. Gerishcher and C. W. Tobias, eds.), Wiley-Interscience, New York, 1984, p. 159.

38. D.M. Kolb, in Advances in Electrochemistry and Electrochemical Engineering, Vol. 11 (H. Gerischer and C. W. Tobias, eds.), John Wiley, New York, 1978, p. 125.

39. K. Juttner and W.J. Lorenz, Z. Phys. Chem. N. F. 122:163 (1980).

40. L.P. Colletti, B.H. Flowers, and J.L. Stickney, J. Electrochem. Soc. 145:1442 (1998).

41. D.W. Suggs and J.L. Stickney, Surf. Sci. 290:362 (1993).

42. D.W. Suggs and J.L. Stickney, Surf. Sci. 290:375 (1993).

43. L.P. Colletti and J.L. Stickney, J. Electrochem. Soc. 145:3594 (1998).

44. B.E. Hayden and I.S. Nandhakumar, J. Phys. Chem. B 102:4897 (1998).

45. I. Villegas and P. Napolitano, J. Electrochem. Soc. 146:117 (1999).

46. U. Demir and C. Shannon, Langmuir 10:2794 (1994).

47. U. Demir and C. Shannon, Langmuir 12:594 (1996).

48. U. Demir and C. Shannon, Langmuir 12:6091 (1996).

49. A. Gichuhi, B.E. Boone, U. Demir, and C. Shannon, J. Phys. Chem. B 102:6499 (1998).

50. T. Torimoto, S. Nagakubo, M. Nishizawa, and H. Yoneyama, Langmuir 14:7077 (1998).

51. L.P. Colletti, S. Thomas, E.M. Wilmer, and J.L. Stickney, in Electrochemical Synthesis and Modification of Materials, Vol. 451 (P. C. Searson, T. P. Moffat, P. C. Andricacos, S. G. Corcoran, and J. L. Delplancke, eds.), Materials Research Society, Boston, 1996, p. 235.

52. G. Pezzatini, S. Caporali, M. Innocenti, and M.L. Foresti, JEC 475:164 (1999).

53. I. Villegas and J.L. Stickney, J. Electrochem. Soc. 139:686 (1992).

54. D.W. Suggs, I. Villegas, B.W. Gregory, and J.L. Stickney, Mat. Res. Soc. Symp. Proc. 222:283 (1991).

55. I. Villegas and S. J.L, J. Vac. Sci. Technol. A-Vac. Surf. Films 10:3032 (1992).

56. T.L. Wade, L.C. Ward, C.B. Maddox, U. Happek, and J.L. Stickney, Electrochemical and Solid State Letters 2:616 (1999).

57. T.L. Wade, R. Vaidyanathan, U. Happek, and J.L. Stickney, J. Electroanal. Chem. 500:322 (2001).

58. R.D. Herrick II and J.L. Stickney, in New Directions in Electroanalytical Chemistry, Vol. 96-9 (J. Leddy and M. Wightman, eds.), The Electrochemical Society, Pennington, NJ, 1996, p. 186.

59. J.D. Klein, R.D. Herrick, D. Palmer, M.J. Sailor, C.J. Brumlik, and C.R. Martin, Chem. Mat. 5:902 (1993).

60. A.M. Kressin, V.V. Doan, J.D. Klein, and M.J. Sailor, Chem. Mater. 3:1015 (1991).

61. D. Routkevitch, A.A. Tager, J. Haruyama, D. Almawlawi, M. Moskovits, and J.M. Xu, IEEE Trans. Electron Devices 43:1646 (1996).

62. D. Routkevitch, T.L. Haslett, L. Ryan, T. Bigioni, C. Douketis, and M. Moskovits, Chemical Physics 210:343 (1996).

63. D. Routkevitch, T. Bigioni, M. Moskovits, and J.M. Xu, J. Phys. Chem. 100:14037 (1996).

64. P.V. Braun and P. Wiltzius, Nature 402:603 (1999).

65. T.L. Wade, B.H. Flowers.Jr, M. Lay, J.W. Garvey, U. Happek, and J.L. Stickney, CM in prep (2000).

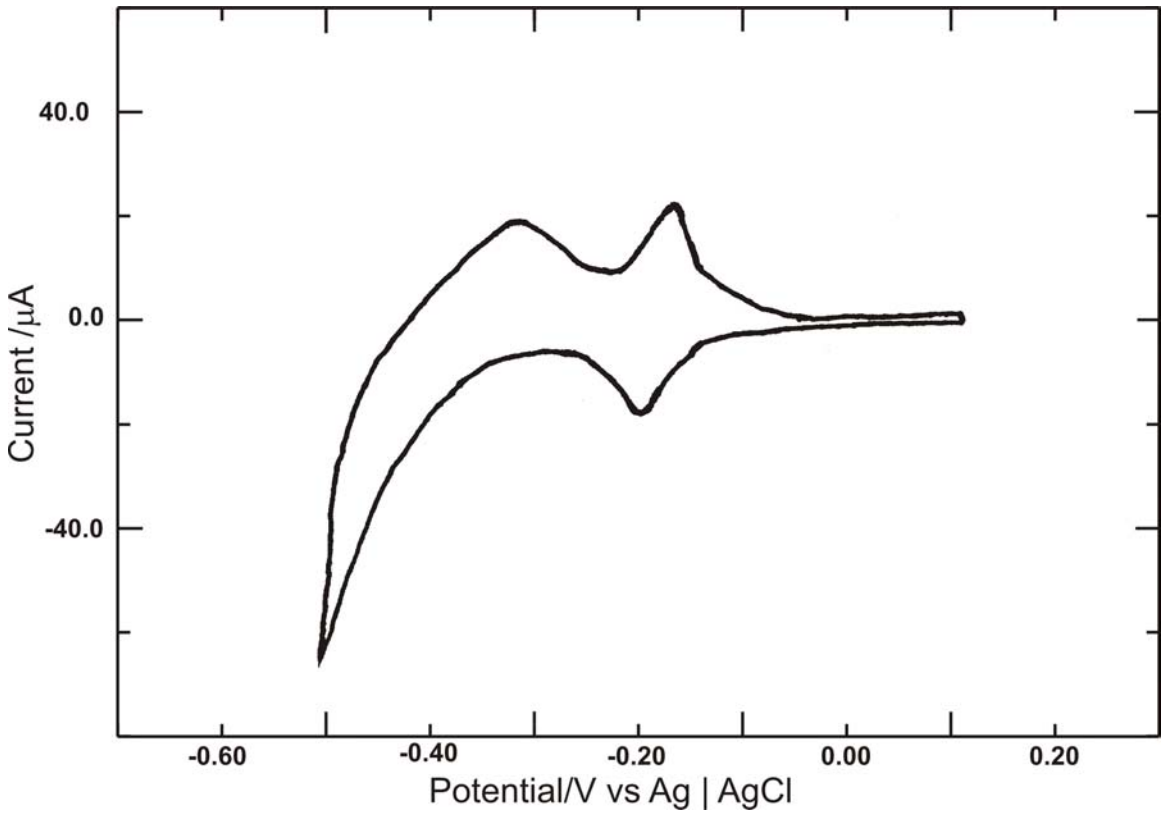

Figure 4.1. Cyclic voltammogram of In on annealed Au on glass substrate in a flow cell. The scan rate was 5 mV s^{-1} and the reference electrode was BAS Ag | AgCl | 3 M NaCl (-0.035 V vs. SCE).

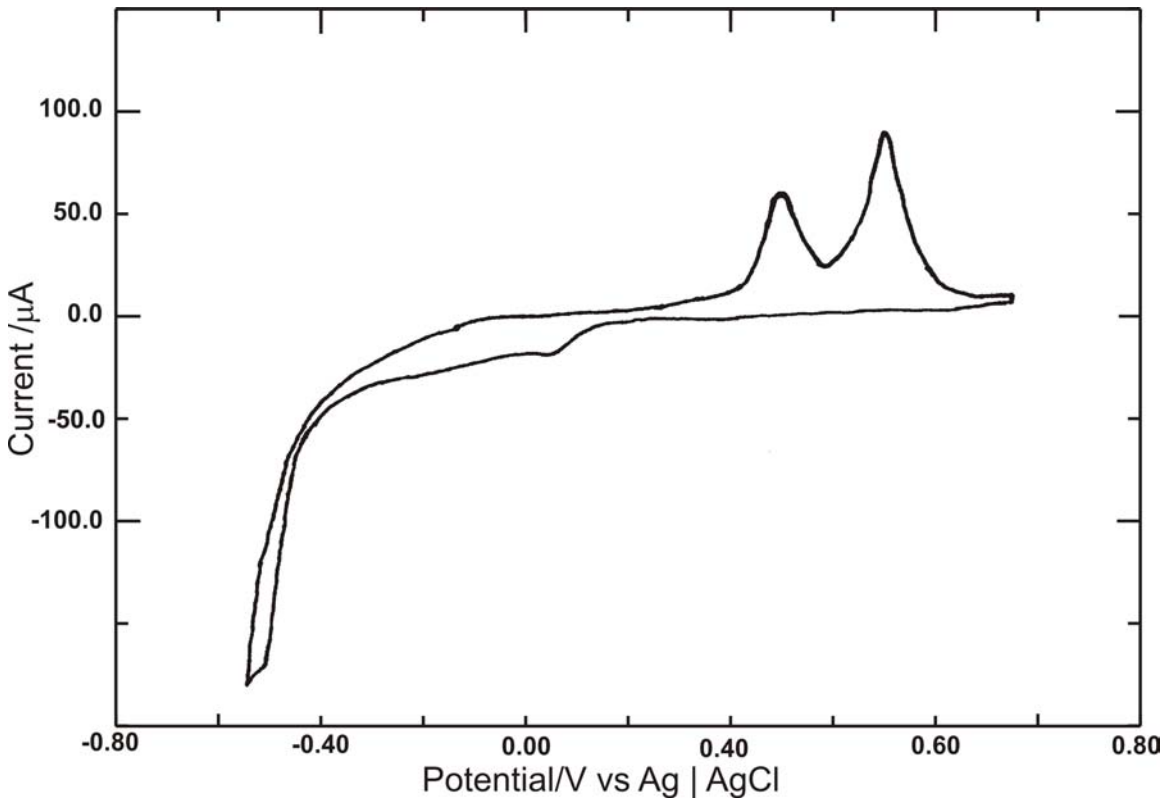

Figure 4.2. Cyclic voltammogram of Se on annealed Au on glass substrate in a flow cell. The scan rate was 5 mV s^{-1} and the reference electrode was BAS Ag | AgCl | 3 M NaCl (-0.035 V vs. SCE).

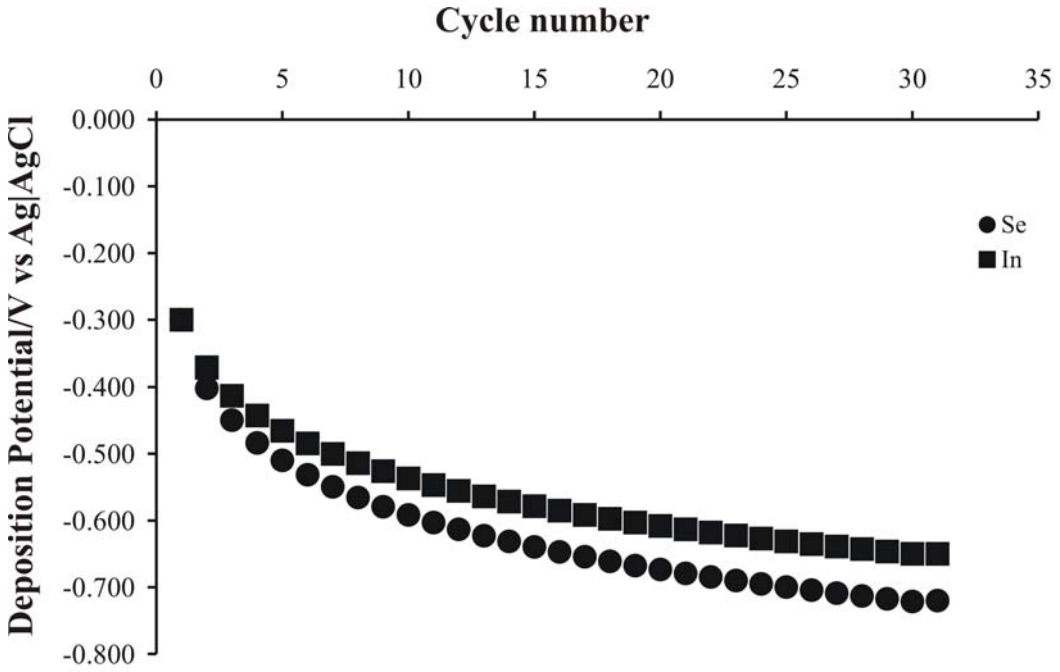

Figure 4.3. Deposition potential versus cycle number for In_2Se_3 electrodeposition

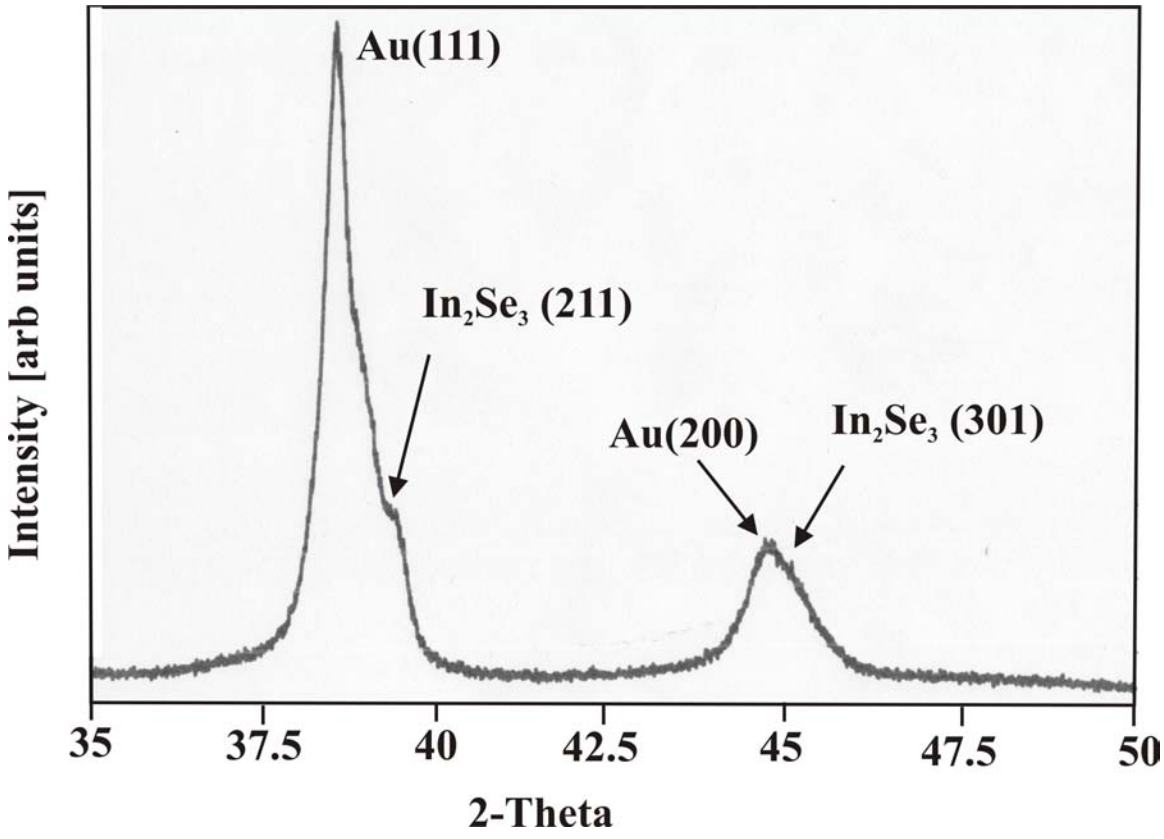

Figure 4.4. Grazing angle x-ray diffraction pattern of 350 cycle In_2Se_3 thin film.

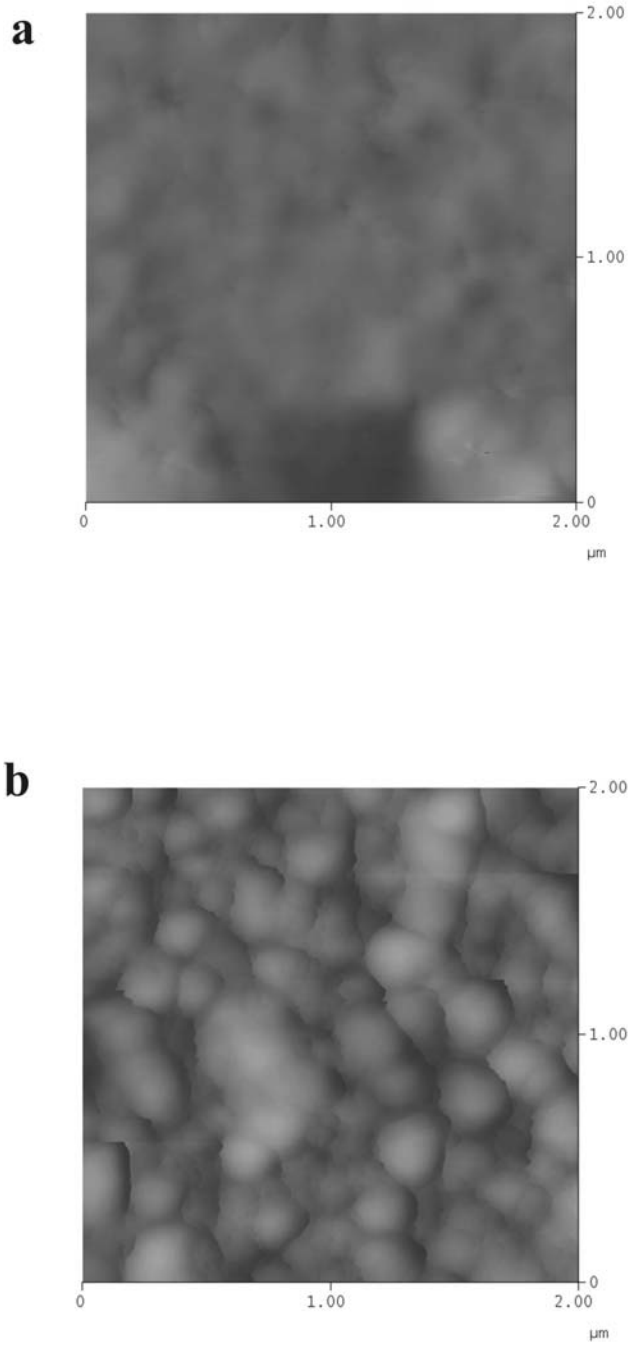

Figure 4.5. a) AFM image of annealed Au on glass substrate. b) AFM image of 350 cycle In_2Se_3 electrodeposited on annealed Au on glass. Data scale is 125 nm.

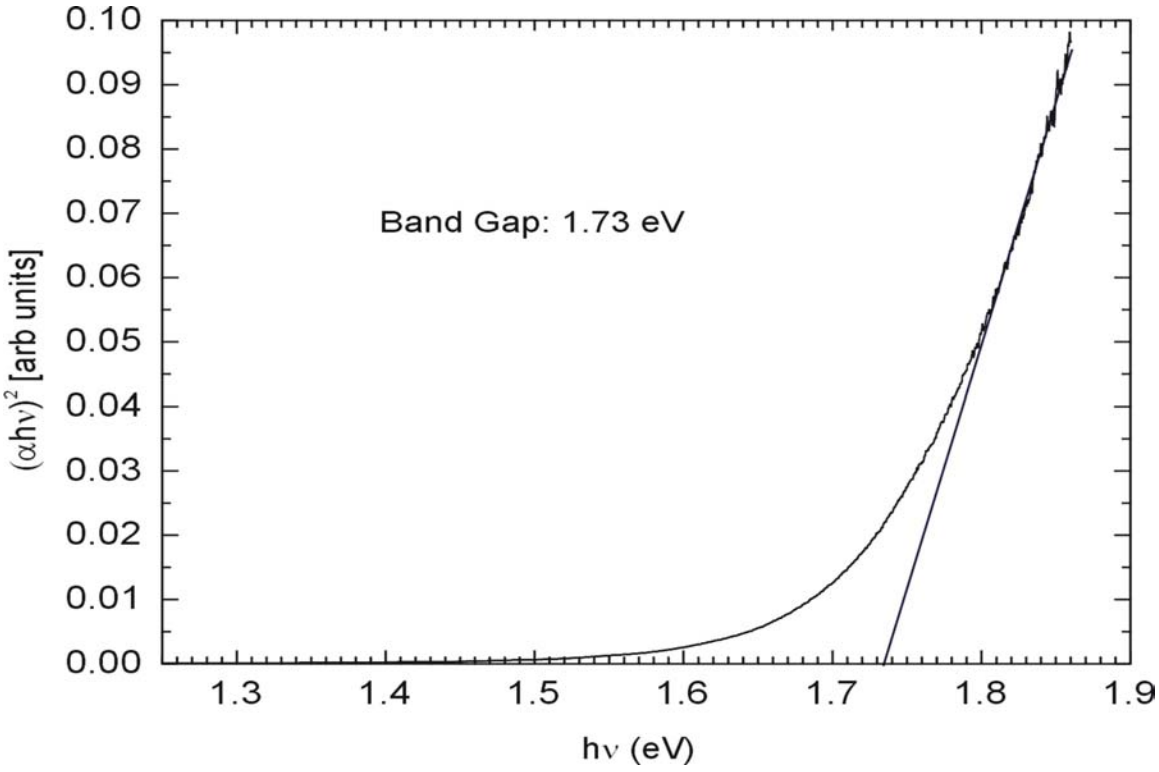

Figure 4.6. Absorbance spectrum of a 350-cycle In_2Se_3 deposit. The band gap of the film was determined to be 1.73 eV.

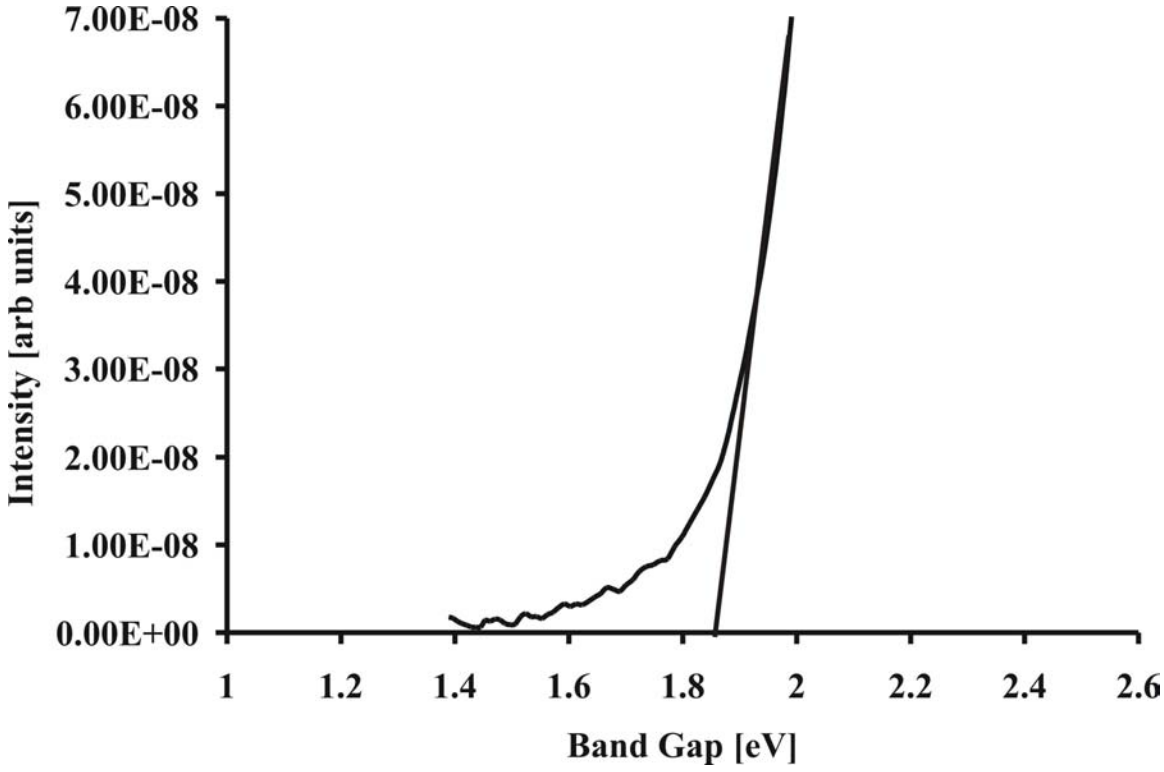

Figure 4.7. Photoelectrochemical spectrum of a 350-cycle In_2Se_3 deposit. The measurements gave a band gap of 1.82 eV for the electrodeposited film.

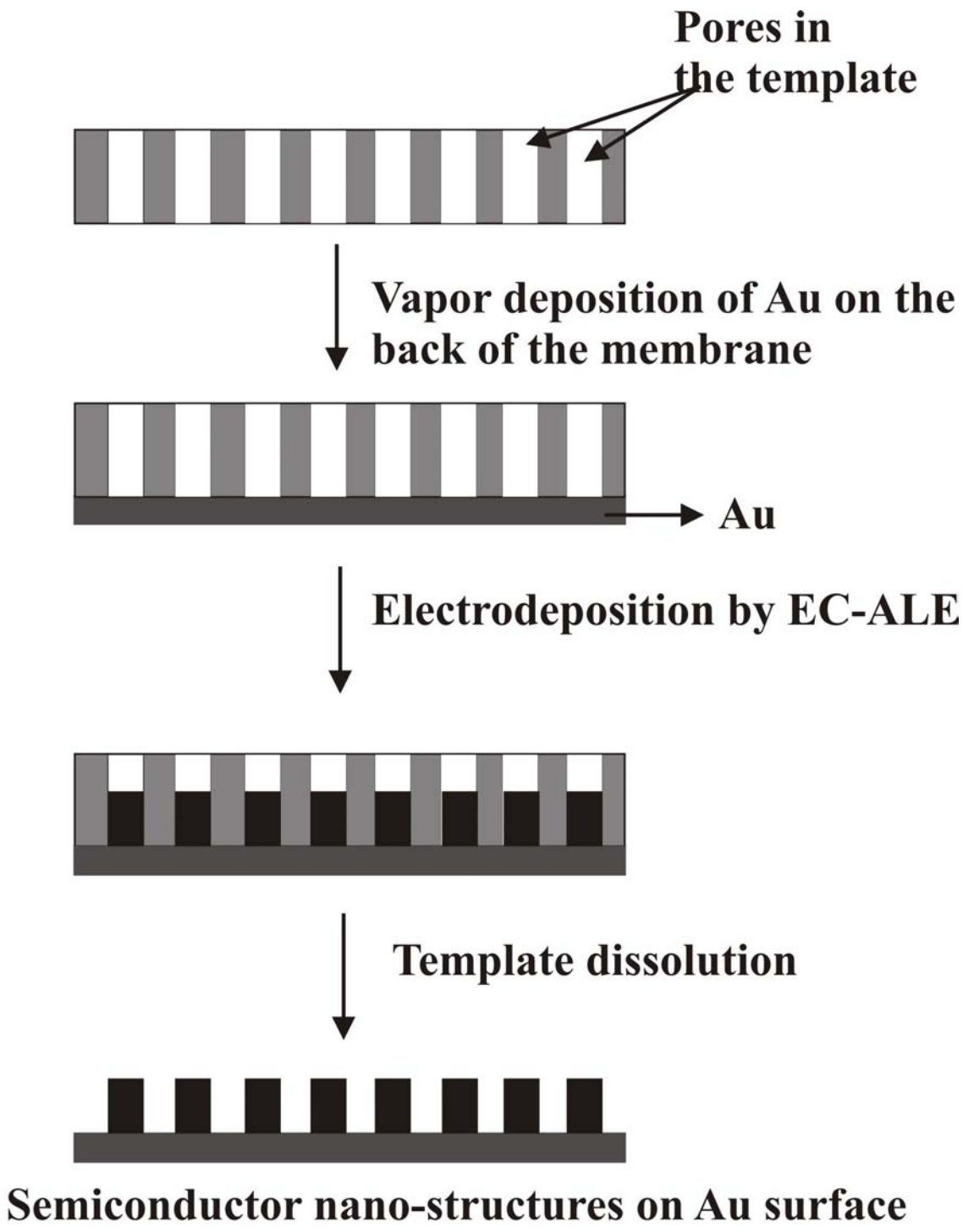

Figure 4.8. Template based formation of semiconductor nanostructures on Au, by EC-ALE.

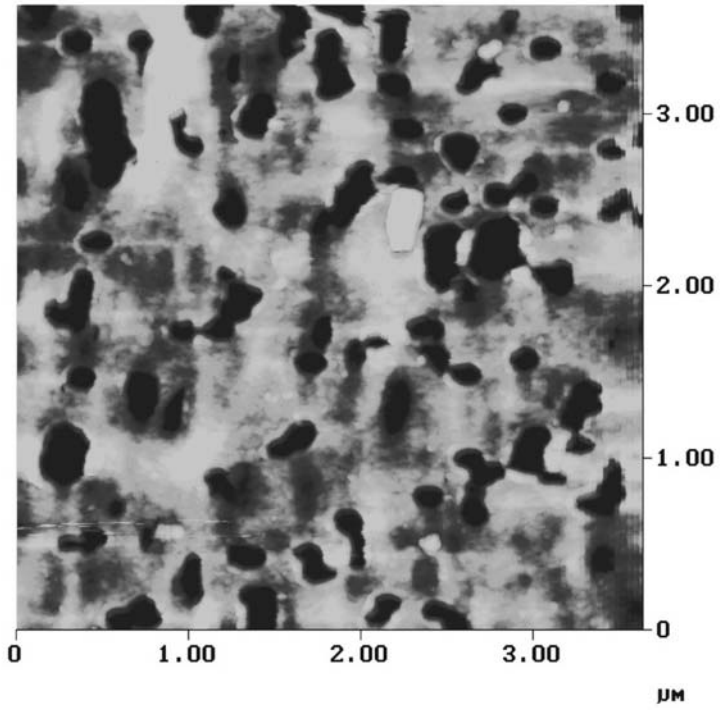

Figure 4.9. AFM image of a polycarbonate membrane. The data scale is 75nm

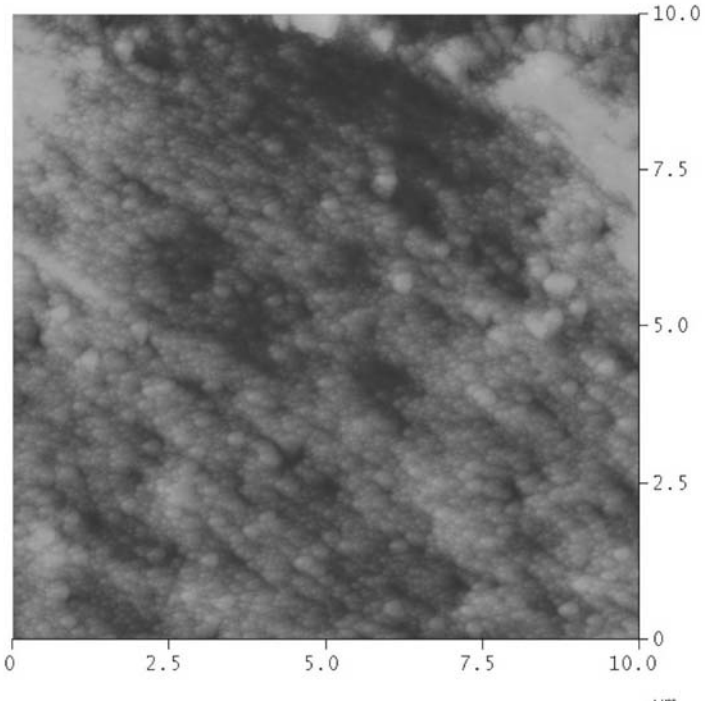

Figure 4.10. AFM image of Au vapor deposited on back of the membrane. The data scale is 350 nm.

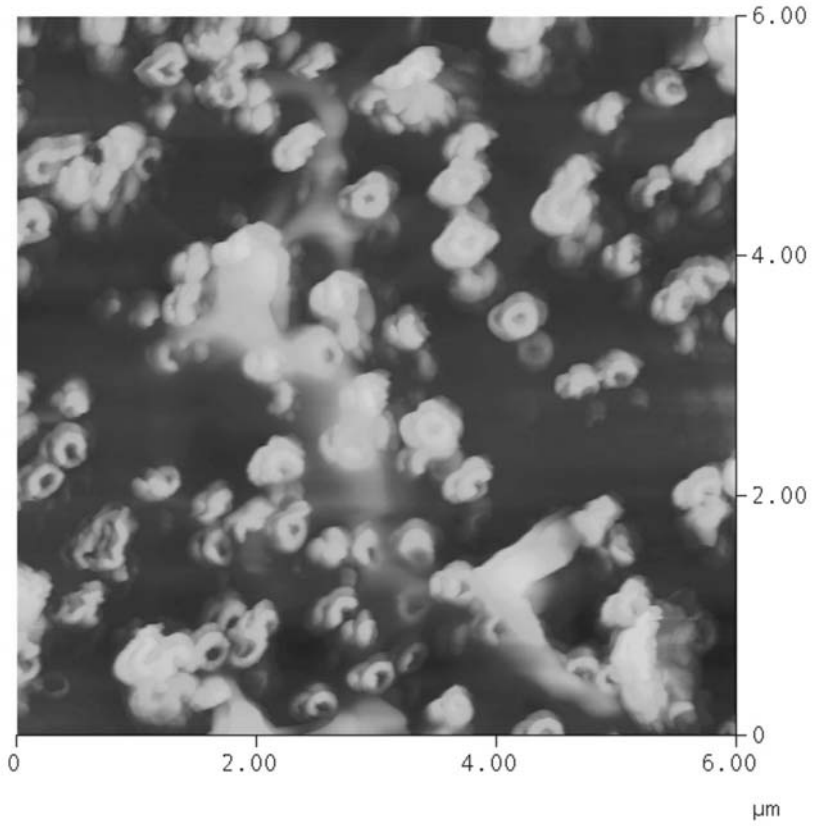

Figure 4.11. AFM image of 6 µm scan of In_2Se_3 nanostructures after dissolving the polycarbonate membrane. The data scale is 1 µm.

Chapter 5

Quantum Confinement In PbSe Thin Films Electrodeposited By Electrochemical Atomic Layer Epitaxy (EC-ALE)[4].

[4] Vaidyanathan R, Happek U, and Stickney J.L, Electrochimica Acta submitted (2003).

Abstract

Electrochemical atomic-layer epitaxy (EC-ALE) is an approach to electrodepositing thin-films of compound semiconductors. It is based on the use of underpotential deposition (UPD), the electrodeposition of a surface limited amount (a monolayer or less) of one element on a second, at a potential prior to that for deposition of the element on itself. A compound monolayer (ML) is formed by the underpotential deposition of each element, in turn, an atomic layer at a time. Knowing the thickness of a ML, this cycle can then be repeated a sufficient number of times to grow a film of the desired thickness. PbSe has a narrow band gap (0.26 eV) and is an IV-VI compound semiconductor, used in photodetectors, photoresistors and photoemitters in the infrared range. This paper is a report of the first instance of PbSe formation by EC-ALE. The films were characterized using electron probe microscope analysis (EPMA) and X- ray diffraction (XRD), and the optical properties were studied via infrared absorption measurements. The ratio of Pb to Se was one, stoichiometric, via EPMA. XRD showed PbSe with the expected rock salt structure, and a primary (200) orientation. In adsorption studies with films grown with 10 to 50 cycles, strong blue shifts of the fundamental absorption edge were observed, believed to be due to quantum confinement.

Keywords

Electrodeposition, Compound Semiconductor, PbSe, Thin films, ECALE, upd, Quantum Confinement, and XRD

Introduction

Lead chalcogenide (IV-VI) semiconductors are used in photodetectors, photoresistors and photoemitters in the infrared range. Strong quantum confinement effects in IV-VI compound semiconductors are well known [1-3]. These IV-VI compound semiconductors have large Bohr radii (a_o), 46 nm for PbSe. When the dimensions of the semiconductor are less than or near the Bohr radius, the optical properties of the semiconductor change due to quantum confinement[3, 4].

Molecular beam epitaxy[5-7] and chemical vapor deposition use temperature for control of deposition, where room temperature would be considered low temperature. One of the drawbacks to the use of higher temperatures is a tendency for interdiffusion between adjacent compounds. The boundaries between materials blur, degrading the quality of the device structures [7]. Interdiffusion is minimized for devices formed near room temperature. Electrodeposition is a low-temperature technique, minimizing interdiffusion, and is thus appealing for the formation of complex compound semiconductors structures. One of the standard methods for compound electrodeposition is co-deposition, where a set reduction potential or current density is applied to a single solution containing precursors for all the elements in a compound. Co-deposition of PbSe have been reported [8-16] and post deposition annealing or the use of Cd was generally required to adjust stoichiometry, crystallinity, and the phase formation.

Atomic layer epitaxy (ALE) is a method used to form compound thin films one atomic layer at a time. Surface limited reactions are used to control the growth rate and morphology. ALE offers greater control over deposit structure than methods based simply on controlling reactant fluxes for all elements simultaneously. This and other

groups have been developing the electrochemical analog of ALE, electrochemical atomic layer epitaxy (EC-ALE) [17]. Surface limited reactions are well known in electrochemistry and are referred to as underpotential deposition (upd) [18-21]. Upd is the deposition of an atomic layer of one element on a second, at a potential prior to that needed to form bulk deposit of the first element. Upd facilitates the formation of compounds one atomic layer at a time in EC-ALE.

II-VI compounds such as CdTe [22-26], CdS [23, 24, 27-29], and ZnSe [30] have been successfully formed using by EC-ALE, as well as some III-V compounds: GaAs [31, 32], InAs [33], InSb and superlattices of InAs/InSb [34]. Torimoto et.al. reported quantum confinement in thin films of ZnS [35], CdS [36] and PbS [37] grown by EC-ALE. Upd of Pb on Se electrodes has been reported by Strelsov et.al [15]. In this paper we report quantum confinement in PbSe thin films electrodeposited by Electrochemical Atomic Layer Epitaxy.

Experimental

An automated electrochemical thin-layer flow deposition system was used for the formation of the thin films described below. The system consists of a series of solution reservoirs, computer controlled pumps, valves and a potentiostat. Most of the hardware used has been described in previous articles [33, 34, 38]. The system is contained within a nitrogen purged Plexiglas box, to reduce the influence of oxygen during electrodeposition. A thin-layer electrochemical flow cell, designed to maintain laminar flow was used for the depositions, and consisted of a Au working electrode, Au coated indium tin oxide (ITO) auxiliary electrode and Ag | AgCl (3M NaCl) reference electrode (Bioanalytical systems, Inc., West Lafayette, IN).

Solutions used include: 0.2 mM $Pb(ClO_4)_2$ (Alfa Aesar, Ward Hill, MA), pH 5.5, buffered with 50.0 mM $CH_3COONa{\cdot}3H_2O$ (J.T.Baker); 0.2 mM SeO_2 (Alfa Aesar, Ward Hill, MA), pH 5.5, also buffered with 50.0 mM $CH_3COONa{\cdot}3H_2O$. A pH 5.5 rinse solution was used as well. The pH values of all solutions were adjusted with CH_3COOH (Fischer Scientific, Pittsburgh, PA). Supporting electrolyte, 0.1 M $NaClO_4$ (Fischer Scientific, Pittsburgh, PA), was added to each solution. Solutions were made with water from a Nanopure water filtration system (Barnstead, Dubuque, IA), fed from the house distilled water system. All chemicals were reagent grade or better.

Substrates were glass microscope slides (Gold Seal products), etched in HF and rinsed with HNO_3 briefly prior to insertion into the vapor deposition chamber. The substrates were annealed in the deposition chamber at 400 °C for 12 hrs before vapor deposition. Thin, 3 nm thick, films of Ti were first vapor deposited, followed by 600 nm of Au, while the substrates were held at 400 °C. The substrates, removed from the chamber, were dipped in nitric acid and rinsed with nanopure water. Prior to use, the substrates were annealed using a H_2 flame (to a dull orange glow in the dark), cleaned again in hot nitric acid and rinsed with nanopure water.

AFM studies were performed using a Nanoscope 2000 (Digital Instruments, Santa Barbara, CA) in the tapping mode. Absorption measurements were performed using a variable angle reflection rig in conjunction with a Bruker 66v FTIR spectrometer equipped with a Si detector. Glancing angle X-ray diffraction patterns were acquired on a Scintag PAD V diffractometer, equipped with a 6” long set of Sola slits on the detector to improve resolution in this asymmetric diffraction configuration. Electron probe microanalysis (EPMA) studies were performed using a Joel JXA-8600 super probe.

Results and Discussion

Starting potentials in the deposition program were determined from cyclic voltammograms for each element. Potentials of -0.2 V for Pb (Fig. 5.1) and -0.2 V for Se (Fig. 5.2) were identified as upd potentials for the deposition of PbSe on the Au substrates.

The cycle involved filling the cell with the Pb solution at a potential of -0.2 V and depositing Pb for 15 secs. The cell was then rinsed with blank for 2 sec, followed by filling with Se solution at –0.2 V, and holding for 15 sec without flow. Se ions were then rinsed from the cell with blank for 2 sec. This cycle was intended to form a ML of the IV-VI semiconductor PbSe and was repeated to form PbSe thin films. The definition of a compound monolayer is somewhat ambiguous. However, in the present case, PbSe crystallizes in the rock salt structure, with a predominate (200) orientation, as will be shown below. The thickness of a monolayer would then be half of the thickness of the PbSe unit cell (a = 0.6124 nm). This is just an approximation, dependent on the surface roughness of the substrate and the degree of polycrystallinity in the deposit. Overall, deposit quality has proven to be similar as long as the deposited amounts do not exceed a monolayer/cycle, however the deposition rate will be maximized, the closer to a monolayer/cycle that can be maintained. Exceeding a monolayer/cycle generally results in 3D growth, obvious after 200 cycles with the eye, or optical microscopy.

In the present study, deposition currents decreased over the first few cycles, resulting in less then a ML of compound/cycle. Presently, this appears to be due to differences in the underpotentials for the elements on Au vs. on each other, needed to form the compound. Similar potential shifts during the first cycles appear to be required to deposit thin films

of most of the compounds formed via EC-ALE [38]. In the present study, small negative potential shifts were used for the first 10 cycles in order to maintain a deposition rate close to a ML/cycle. Experience has shown that potential shifts tend to decrease exponentially for the first 10 to 30 cycles, depending on the compound. These changes appear to be due to a decrease in the driving force for deposition, the underpotentials, the thicker the deposit gets, relative to UPD of the elements on the Au substrates. However, the closer the potentials get to the formal potentials for the reversible element, Pb in this case, steady state potentials can be maintained. Steady state potentials are obtained in the present case after about ten cycles. An alternative justification for these potential changes, suggested by this group, involves dropping some of the applied potential across a growing space charge layer (SCL), or schottky barrier, between the Au electrode and the growing semiconductor thin film. However, given the extremely thin films present by the point where steady state potentials are achieved, it is unrealistic to think that a space charge layer has been fully developed [39].

To keep the deposition charges sufficient for the formation of a full monolayer with each cycle, the potentials were stepped negative after each of the first 10 cycles (Fig. 5.3). After 10 cycles, steady state potentials of -0.3 V for Pb and –0.3 V for Se were attained, and used to form the rest of the deposit.

Pb is referred to here as the reversible element, as its coverage is directly dependent on the potential, prior to bulk deposition, or the formal potential for the element, it deposits in a truly surface limited equilibrium. While Se, is actually deposited at an overpotential, as it is irreversibly deposited. Thus Se deposition is not a truly surface limited reaction. However, experience has shown that the majority of the Se needed to form a compound

ML deposits rapidly on the previously deposited Cd atomic layer, while subsequent Se deposition is much slower and can be controlled by using low concentrations and short deposition times. Some extra Se, a fraction of a monolayer, may deposit, but this appears to quantitatively react with Pb, as will be shown below.

ICP-MS measurements of a 50 cycle thin film deposit showed it to be 22 nm thick and the stoichiometry was 1:1 (standard deviation = 0.01). EPMA of the deposits indicated a Se/Pb atomic ratio of 1/1 (standard deviation = 0.01). Fig. 5.4 shows the X-ray diffraction patterns for the 50 cycle PbSe deposit. X-ray diffraction peaks, correspond to the rock salt structure, were recorded, including peaks for the (200), (111), (222), (400) and (311) planes of PbSe [JCPDS 20-0494], along with peaks for the Au substrate, the (111) most prominent. Elemental peaks for Pb and Se are absent. The number and relative intensities of the PbSe peaks suggest a nearly polycrystalline deposit, although the (200) was somewhat prominent. Fig. 5.5 shows an AFM image of a 50 cycle deposit of PbSe on flame annealed Au on glass substrate. The thin film consists of crystallites that are 300 nm in diameter and 2-D growth, suggesting a deposit relatively conformal with the Au substrate [33, 40]. These results suggest 2-D growth of PbSe thin films.

Fig. 5.6 shows a plot of the square of the absorption data for 5, 10, 15, 25, and 50 cycle deposits of PbSe. The bulk value of the band gap for PbSe is 2100 cm^{-1}. The band gaps measured for the 30 and 50 cycle deposits are blue shifted to 8500 cm^{-1} and 8000 cm^{-1} respectively. We observe a strong blue shift in the band gap even for the thick film, 50 cycle, apparently due to quantum confinement. For the 5, 10, 15 and 20 cycle films, the absorption was insufficient in the range of the IR spectrometer used, for an accurate measurement of the bandgap, which was shifted into the visible. The band gap of the

materials is directly related to the thickness or the number of cycles of the deposit [36, 37]. Simple calculations showed that a 50 cycle PbSe deposit must be 16 nm thick for an atomic layer growth each cycle and the band gap must be 1 eV. IC-PMS results (22nm) suggest that the deposit is thicker than theoretical value. This may be due to the fact that the Se deposition potentials are in the over potential region as described earlier and we may have a 3-D growth, even though AFM results do not show any 3-D growth of the deposit and optimization of the deposition potentials for Pb and Se is required.

Conclusions

A series of stoichiometric PbSe thin films have been electrodeposited using electrochemical atomic layer epitaxy, as shown using XRD, on Au on glass substrates. Strong quantum confinement, even for a 50 cycle PbSe thin film deposit, was observed. The band gap for the 50 cycle deposit was a factor of 4 greater then that for the bulk deposit, and those for the thinner were even greater, shifted into the visible. The monolayer/cycle growth provided by EC-ALE is a very attractive candidate for controlling the growth and optical properties, via quantum confinement, of PbSe thin films.

Acknowledgements

Support from the NSF and the Nanoscale Exploratory Research program, is gratefully acknowledged.

References

1. E. I. Rogacheva, T. V. Tavrina, O. N. Nashchekina, S. N. Grigorov, K. A. Nasedkin, M. S. Dresselhaus, and S. B. Cronin, 80:2690 (2002).

2. X. S. Peng, G. W. Meng, J. Zhang, X. F. Wang, C. Z. Wang, X. Liu, and L. D. Zhang, J. Mater. Res. 17:1283 (2002).

3. F. W. wise, Acc. Chem. Res. 2000:773 (2000).

4. K. S. Hamad, R. R., M. A., v. B. T., C. L. L., C. M., and A. A. P., Abstracts of Papers of the American Chemical Society 216:U628 (1998).

5. A. Y. Ueta, E. Abramof, C. Boschetti, H. Closs, P. Motisuke, P. H. O. Rappl, I. N. Bandeira, and S. O. Ferreira, Microelectron. J. 33:331 (2002).

6. G. Springholz and K. Wiesauer, Phys. Rev. Letters 88:015507 (2002).

7. M. P. Belyansky, A. M. Gaskov, and A. V. Strelkov, Source MATER SCI ENG B SOLID STATE ADV TECHNOL:78 (1992).

8. E. A. Streltsov, N. P. Osipovich, L. S. Ivashkevich, A. S. Lyakhov, and V. V. Sviridov, Russian Journal of Applied Chemistry 70:1651 (1997).

9. H. Saloniemi, T. Kanniainen, M. Ritala, M. Leskela, and R. Lappalainen, J. Materials Chemistry 8:651 (1998).

10. E. A. Streltsov, N. P. Osipovich, L. S. Ivashkevich, and A. S. Lyakhov, EA 44:407 (1998).

11. E. A. Streltsov, N. P. Osipovich, L. S. Ivashkevich, A. S. Lyakhov, and V. V. Sviridov, Electrochimica Acta 43:869 (1998).

12. E. A. Streltsov, N. P. Osipovich, L. S. Ivashkevich, and A. S. Lyakhov, Electrochimica Acta 44:2645 (1999).

13. H. Saloniemi, M. Kemell, M. Ritala, and M. Leskela, J. Materials Chemistry 10:519 (2000).

14. L. Beaunier, H. Cachet, and M. Froment, Mater. Sci. Semicond. Process 4:433 (2001).

15. E. A. Streltsov, S. K. Poznyak, and N. P. Osipovich, JEC 518:103 (2002).

16. M. Froment, L. Beaunier, H. Cachet, and A. Etcheberry, 150:C89 (2003).

17. R. Vaidyanathan, U. Happek, and J. L. Stickney, Electrochimica Acta submitted (2003).

18. R. R. Adzic, in Advances in Electrochemistry and Electrochemical Engineering, Vol. 13 (H. Gerishcher and C. W. Tobias, eds.), Wiley-Interscience, New York, 1984, p. 159.

19. E. Herrero, L. J. Buller, and H. D. Abruna, Chemical Reviews 101:1897 (2001).

20. A. A. Gewirth and B. K. Niece, Chem. Rev. 97:1129 (1997).

21. D. M. Kolb, in Advances in Electrochemistry and Electrochemical Engineering, Vol. 11 (H. Gerischer and C. W. Tobias, eds.), John Wiley, New York, 1978, p. 125.

22. F. Forni, M. Innocenti, G. Pezzatini, and M. L. Foresti, Electrochemica Acta 45:3225 (2000).

23. B. W. Gregory and J. L. Stickney, Journal of Electroanalytical Chemistry 300:543 (1991).

24. E. S. Streltsov, I. I. Labarevich, and D. V. Talapin, Doklady Akademii Nauk Belarusi 38:64 (1994).

25. B. H. Flowers Jr., T. L. Wade, M. Lay, J. W. Garvey, U. Happek, and J. L. Stickney, JEC in press (2002).

26. K. Varazo, M. D. Lay, and J. L. Stickney, JEC in press (2002).

27. M. Innocenti, G. Pezzatini, F. Forni, and M. L. Foresti, JECS 148:c357 (2001).

28. B. E. Boone and C. Shannon, Journal of Physical Chemistry 100:9480 (1996).

29. A. Gichuhi, B. E. Boone, and C. Shannon, Langmuir 15:763 (1999).

30. G. Pezzatini, S. Caporali, M. Innocenti, and M. L. Foresti, JEC 475:164 (1999).

31. I. Villegas and J. L. Stickney, Journal of the Electrochemical Society 139:686 (1992).

32. I. Villegas and J. L. Stickney, Journal of Vacuum Science & Technology A 10:3032 (1992).

33. T. L. Wade, L. C. Ward, C. B. Maddox, U. Happek, and J. L. Stickney, Electrochemical and Solid State Letters 2:616 (1999).

34. T. L. Wade, R. Vaidyanathan, U. Happek, and J. L. Stickney, JEC 500:322 (2001).

35. T. Torimoto, A. Obayashi, S. Kuwabata, H. Yasuda, H. Mori, and H. Yoneyama, Langmuir 16:5820 (2000).

36. T. Torimoto, S. Nagakubo, M. Nishizawa, and H. Yoneyama, Langmuir 14:7077 (1998).

37. T. Torimoto, S. Takabayashi, H. Mori, and S. Kuwabata, JEC 522:33 (2002).

38. J. L. Stickney, T. L. Wade, B. H. Flowers Jr., R. Vaidyanathan, and U. Happek, in Encyclopedia of Electrochemistry, Vol. in press (E. Gileadi and M. Urbakh, eds.), Marcel Dekker, New York, 2002.

39. S. M. Sze, Physics of Semiconductor Devices, john Wiley & Sons, New York, 1981.

40. T. L. Wade, B. H. Flowers Jr., K. Varazo, M. Lay, U. Happek, and J. L. Stickney, in Electrochemical Society National Meeting, Vol. In Press (K. Kondo, ed.), Electrochemcial Society, Washington D.C., 2001.

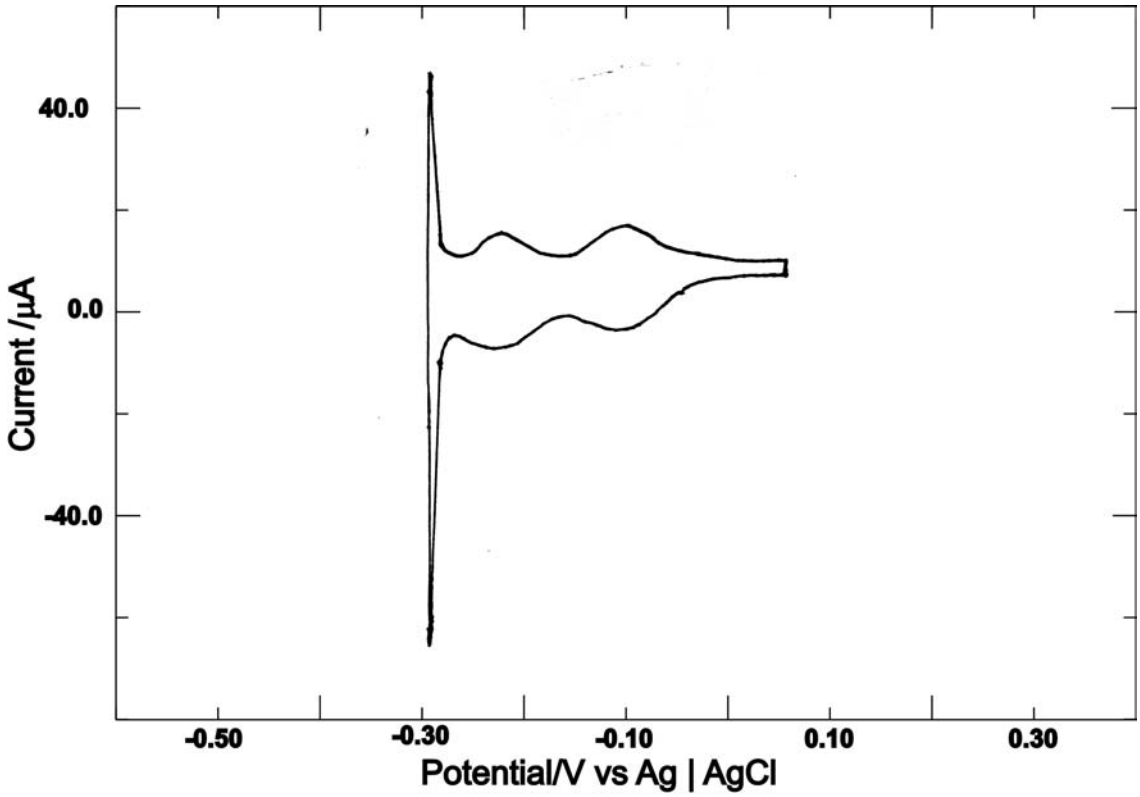

Figure 5.1. Cyclic voltammogram of a Au electrode in a pH 5.5 solution containing 0.2 mM $Pb(ClO_4)_2$, 50 mM CH_3COONa and 0.1 M $NaClO_4$. Scan rate 5 mV/sec

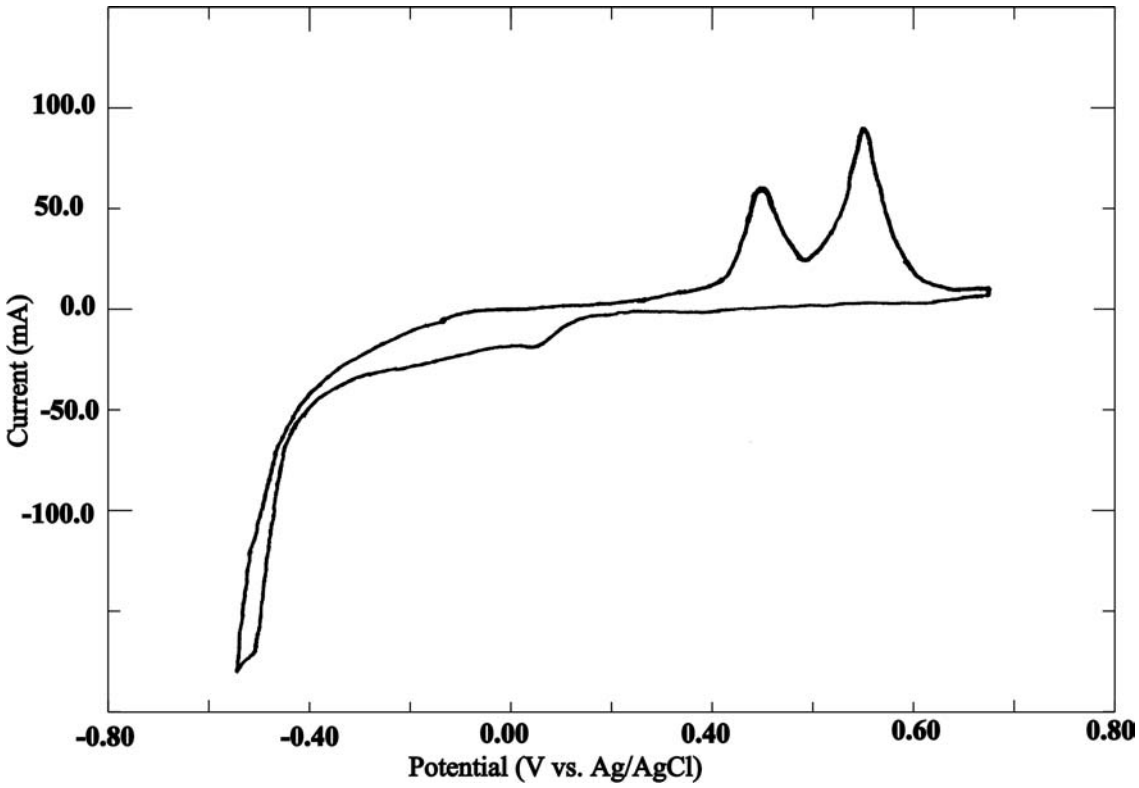

Figure 5.2. Cyclic voltammogram of a Au electrode in a pH 5.5 solution containing 0.2 mM SeO_2, 50 mM CH_3COONa and 0.1 M $NaClO_4$. Scan rate 5 mV/sec

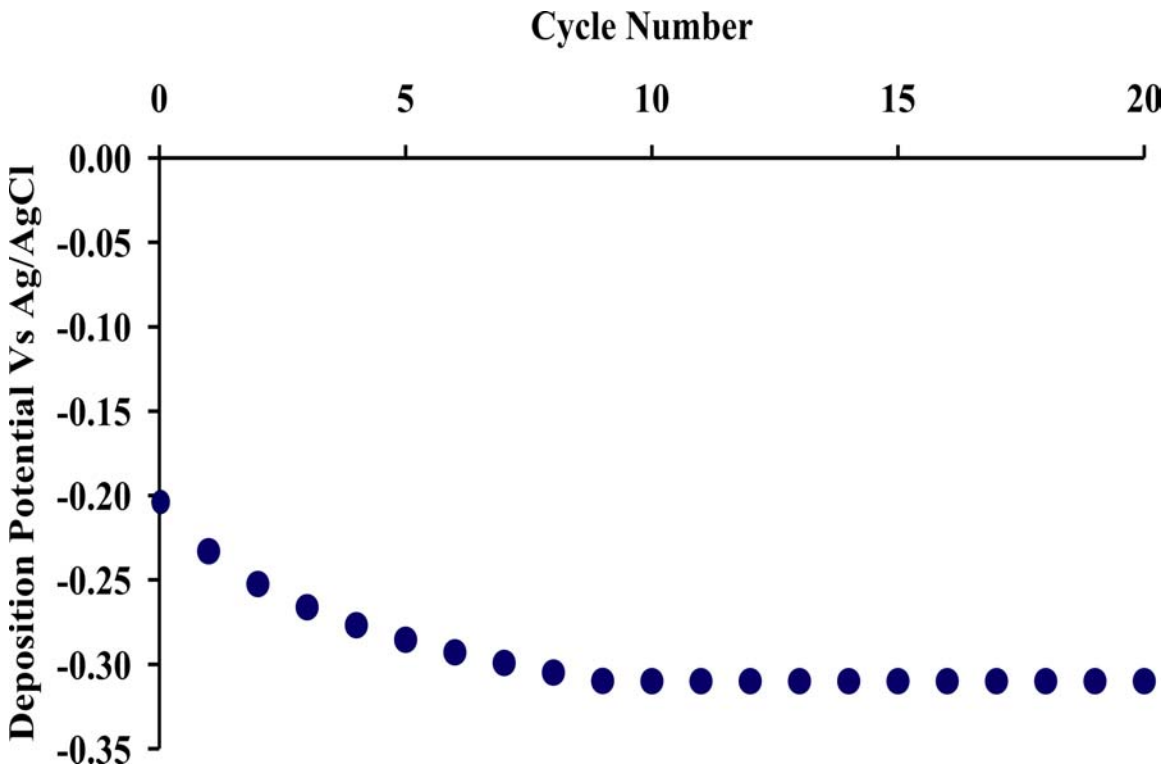

Figure 5.3. Graph of change in deposition potential of Pb and Se versus cycle number

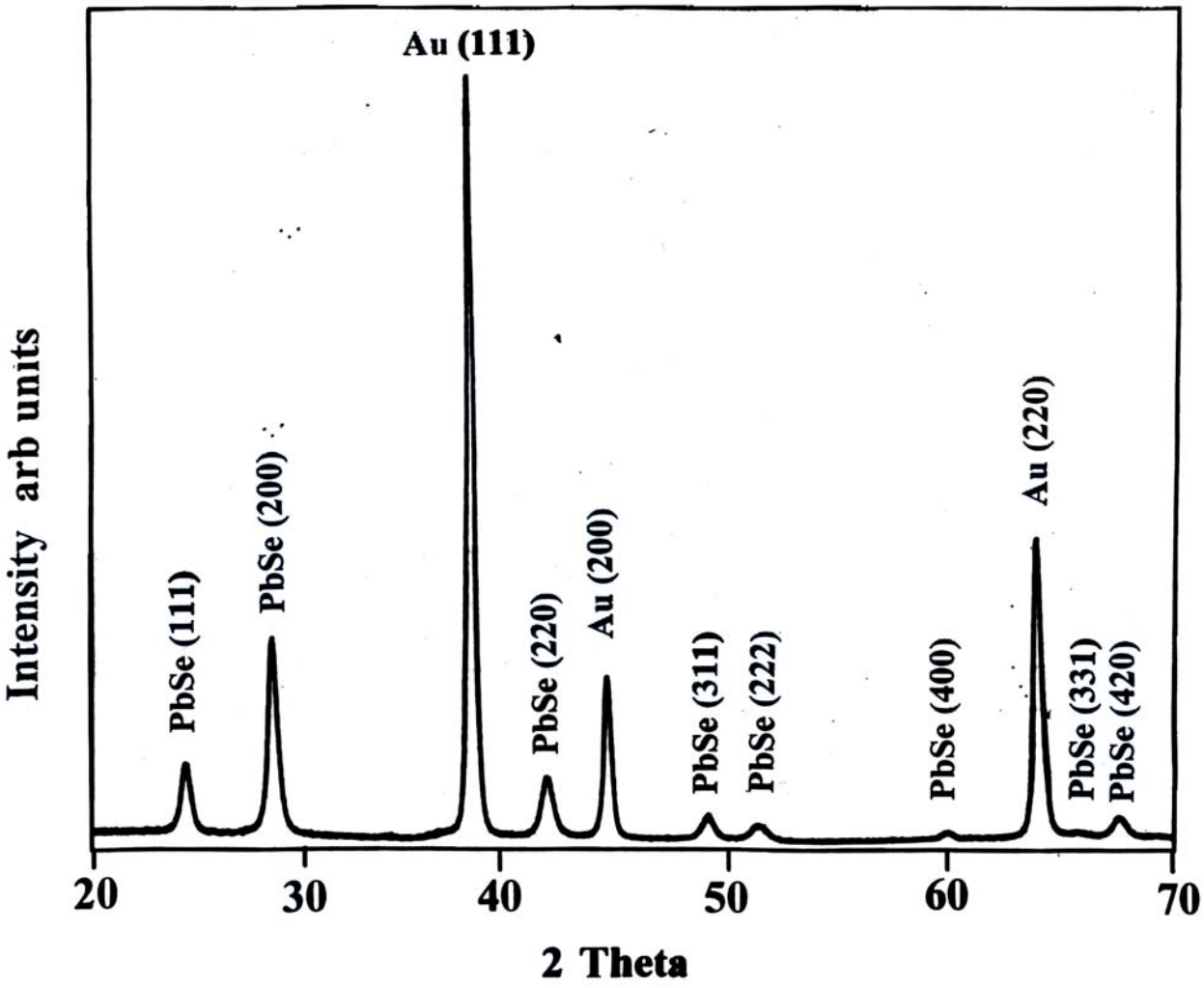

Figure 5.4. X-ray diffraction of a 50 cycle electrodeposited PbSe thin film. Angle of incidence is 1°, Cu Kα source.

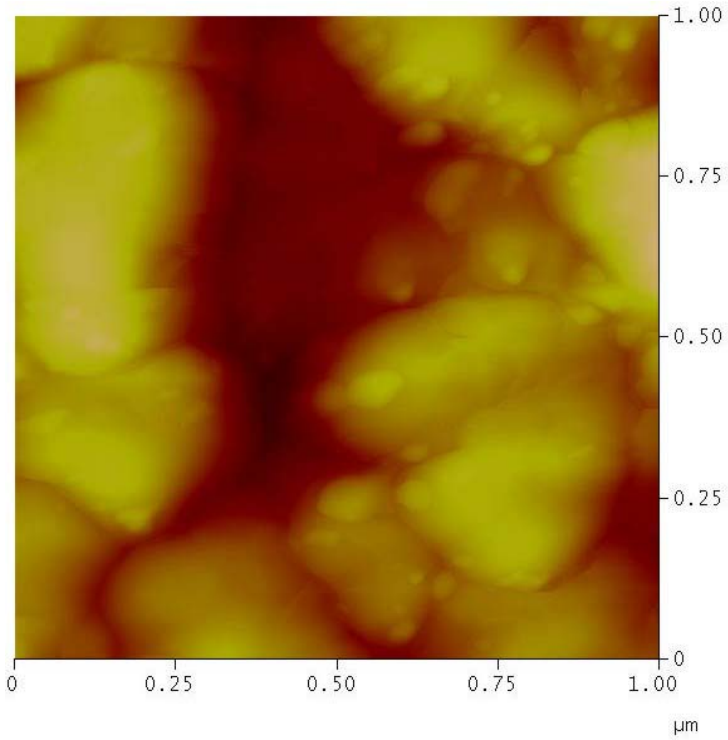

Figure 5.5. AFM of a 50 cycle electrodeposited PbSe thin film on annealed Au substrate. The scan size is 1µm and the data scale is 50 nm.

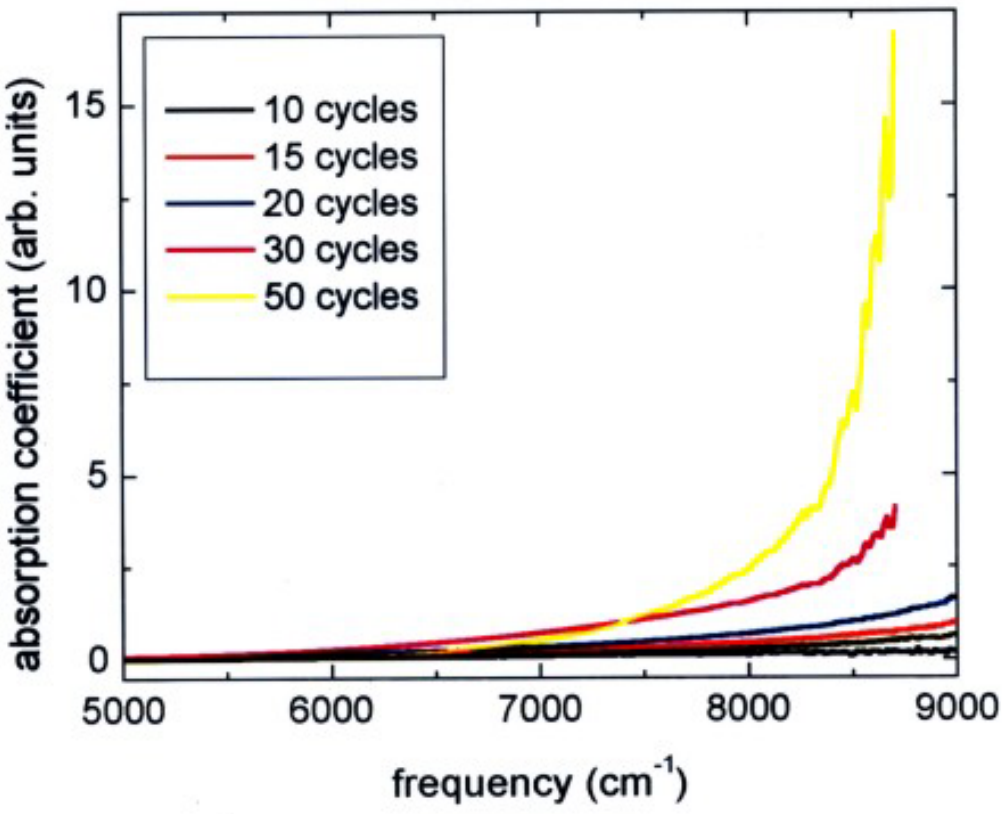

Figure 5.6. Absorption spectrum of a) 10 cycle b) 15 cycle c) 20 cycle d) 30 cycle and e) 50 cycle electrodeposited PbSe thin film.

Chapter 6

Electrodeposition of quantum confined PbTe Thin Films by Electrochemical Atomic Layer Epitaxy (EC-ALE)[5]

[5] Vaidyanathan R, Happek U, and Stickney J.L, Journal of Crystal Growth submitted (2003).

Abstract

Electrochemical atomic-layer epitaxy (EC-ALE) is an analog to atomic layer epitaxy, to electrodeposit thin-films of compound semiconductors. It takes advantage of underpotential deposition (UPD), a surface limited reaction in electrochemistry, to deposit one monolayer or less of an element at a potential less negative than bulk deposition, to form a thin-film of a compound--one atomic layer at a time. PbTe is a narrow bandgap semiconductor (E_g = 0.29 eV) and is an important thermoelectric material. We report the electrodeposition and quantum confinement of PbTe thin films by EC-ALE. The films were characterized using electron probe microscope analysis (EPMA), x- ray diffraction (XRD), atomic force microscopy (AFM) and the optical properties of the films were studied via infrared absorption measurements. The ratio of Pb and Te atoms in the thin films were found to be stoichiometric by EPMA. In the thin films of even 100 cycles of electrodeposited PbTe, we observe a strong blue shift of the fundamental absorption edge due to quantum confinement. X-ray diffraction measurements indicate that the thin films are rock salt structure and have a preferential (200) orientation. AFM indicates that the crystallite size of the thin films is 300 nm corresponding to that of the Au substrate.

Keywords

PbTe, IV-VI, Thermoelectric materials, Quantum confinement, UPD, Electrodeposition, EC-ALE, and X-ray diffraction.

Introduction

PbTe an important IV-VI compound semiconductor, used in thermoelectric applications [1-11], infrared sensors[12], photovoltaics [13-15] etc. and the properties of IV-VI compound semiconductor change with the strong confinement effects. These IV-VI compound semiconductor materials have a large Bohr radius and the typical Bohr radius (a_o) for PbTe is 50 nm. When the dimension of the semiconductor material is less than that of the Bohr radius, the electron is confined in the lattice, and there is a change in optical, mechanical or magnetic properties of the semiconductor material due to quantum confinement[16]. IV-VI compound semiconductors like PbSe, PbTe and PbS, have small and equal electron and hole masses compared to III-V or II-VI compound semiconductors, which enables large confinement energies to be split equally between the carriers and they exhibit better confinement effects compared to InSb, InAs or CdS[16]. The band gap of the quantum confined material will be larger compared to the bulk lead chalcogenides (0.2 – 0.3 eV).

Molecular beam epitaxy [14, 17], chemical vapor deposition and hot-wall epitaxy [18-20] use high temperatures for deposition, and the boundaries between these materials blur, due to interdiffusion[19] of the component elements, degrading the quality of the device. Interdiffusion is minimized for devices formed near room temperature. Electrodeposition is a low-temperature technique, minimizing interdiffusion, and is thus appealing for the formation of complex compound semiconductors structures, including thermoelectric devices. One of the standard methods for compound electrodeposition is co-deposition, where a set reduction potential or current density is applied to a single solution containing precursors for all the elements in a compound. Co-deposition of PbTe has been reported

[21-26] and post deposition annealing or the use of Cd was generally required to adjust stoichiometry, crystallinity, and the phase formation.

Atomic layer epitaxy (ALE) is a method [27-30] used to form compound thin films one atomic layer at a time. Surface limited reactions are used to control the growth rate and morphology. ALE offers greater control over deposit structure than methods based on controlling reactant fluxes for all elements simultaneously. Our group has been developing the electrochemical analog of ALE, electrochemical atomic layer epitaxy (EC-ALE) [31-33], which uses surface limited reactions for one atomic layer of compound semiconductor. Surface limited reactions are well known in electrochemistry and are referred to as underpotential deposition (upd). Upd [34-38] is the deposition of an atomic layer of one element on a second, at a potential prior to that needed to form bulk deposit of the first element. Upd facilitates the formation of compounds one atomic layer at a time in EC-ALE.

II-VI compounds such as CdTe[33, 39-42], CdS[33, 40, 43-45], ZnSe[46] and CdS / HgS superlattices[44] have been successfully formed using by EC-ALE, as well as some III-V compounds: GaAs[47, 48], InAs[49], InSb[50] and superlattices of InAs/InSb[50]. Torimoto et.al. reported quantum confinement in thin films of ZnS[51], CdS[52], and PbS[53] grown by EC-ALE. We have also reported the quantum confinement of PbSe[54] thin films grown by EC-ALE. In this paper we report the quantum confinement properties of PbTe thin films electrodeposited by Electrochemical Atomic Layer Epitaxy.

Experimental

An automated electrochemical thin-layer flow deposition system was used for the formation of thin films. The system consists of a series of solution reservoirs, computer

controlled pumps, valves and a potentiostat. Most of the hardware used has been described in previous articles[32, 50, 55]. The system is contained within a nitrogen purged plexiglas box, to reduce the influence of oxygen during electrodeposition. A thin-layer electrochemical flow cell, designed to maintain laminar flow was used for the depositions, and consisted of a Au working electrode, Au coated indium tin oxide (ITO) auxiliary electrode and Ag | AgCl (3M NaCl) reference electrode (Bioanalytical systems, Inc., West Lafayette, IN).

Solutions used include: 0.2 mM $Pb(ClO_4)_2$ (Alfa Aesar, Ward Hill, MA), pH 5.5, buffered with 50.0 mM $CH_3COONa{\cdot}3H_2O$ (J.T.Baker); 0.2 mM TeO_2 (Alfa Aesar, Ward Hill, MA), pH 9.2, buffered with 50.0 mM Sodium borate. A pH 7.0 rinse solution was used as well. The pH values of all solutions were adjusted with CH_3COOH and KOH (Fischer Scientific, Pittsburgh, PA). Supporting electrolyte, 0.1 M $NaClO_4$ (Fischer Scientific, Pittsburgh, PA), was added to each solution. Solutions were made with water from a Nanopure water filtration system (Barnstead, Dubuque, IA), fed from the house distilled water system. All chemicals were reagent grade or better.

Substrates were glass microscope slides (Gold Seal products), etched in HF and rinsed with HNO_3 briefly prior to insertion into the vapor deposition chamber. The substrates were annealed in the deposition chamber at 400 °C for 12 hrs before vapor deposition. Thin, 3 nm thick, films of Ti were first vapor deposited, followed by 600 nm of Au, while the substrates were held at 400 °C. The substrates, removed from the chamber, were dipped in nitric acid and rinsed with nanopure water. Prior to use, the substrates were annealed using a H_2 flame (to a dull orange glow in the dark), cleaned again in hot nitric acid and rinsed with nanopure water.

AFM studies were performed using a Nanoscope 2000 (Digital Instruments, Santa Barbara, CA) in the tapping mode. Absorption measurements were performed using a variable angle reflection rig in conjunction with a Bruker 66v FTIR spectrometer equipped with a Si detector. Glancing angle X-ray diffraction patterns were acquired on a Scintag PAD V diffractometer, equipped with a 6" long set of Sola slits on the detector to improve resolution in this asymmetric diffraction configuration. Electron probe microanalysis (EPMA) studies were performed using a Joel JXA-8600 super probe.

Results and Discussion

The starting potentials in the deposition program were determined from cyclic voltammograms for each element. Potentials of -0.2 V for Pb (Fig. 1) and -0.3 V for Te (Fig. 2) were identified as upd potentials for the deposition of PbTe.

The cycle involved filling the cell with the Pb solution at a potential of -0.2 V and depositing Pb for 15 secs. The cell was then rinsed with the blank for 2 sec and filled with the Se solution at –0.2 V, and depositing Se for 15 secs. The Te ions were rinsed out of the cell by flowing the blank solution for 2 secs. This cycle was intended to form a ML of the IV-VI semiconductor PbTe and was repeated to form PbTe thin films.

The deposition currents, however, decreased over the first few cycles, resulting in less then a monolayer of compound each cycle. This could be the simple result of depending on potentials chosen for upd on Au, not for upd on the compound. In the present study, deposition currents decreased over the first few cycles, resulting in less then a ML of compound/cycle. Presently, this appears to be due to differences in the underpotentials for the elements on Au vs. on each other, needed to form the compound. Similar potential shifts during the first cycles appear to be required to deposit thin films of most

of the compounds formed via EC-ALE [55, 56]. In the present study, small negative potential shifts were used for the first 10 cycles in order to maintain a deposition rate close to a ML/cycle. Experience has shown that potential shifts tend to decrease exponentially for the first 10 to 30 cycles, depending on the compound. These changes appear to be due to a decrease in the driving force for deposition, the underpotentials, the thicker the deposit gets, relative to UPD of the elements on the Au substrates. However, the closer the potentials get to the formal potentials for the reversible element, Pb in this case, steady state potentials can be maintained. Steady state potentials are obtained in the present case after about ten cycles. An alternative justification for these potential changes, suggested by this group, involves dropping some of the applied potential across a growing space charge layer (SCL), or schottky barrier, between the Au electrode and the growing semiconductor thin film. However, given the extremely thin films present by the point where steady state potentials are achieved, it is unrealistic to think that a space charge layer has been fully developed [57]. To keep the deposition charges sufficient for the formation of a full monolayer with each cycle, the potentials were stepped negative after each of the first 10 cycles. After 10 cycles, steady state potentials of -0.3 V for Pb and –0.4 V for Te were attained, and used to form the rest of the deposit. EPMA of the deposits indicated an Te/Pb atomic ratio of 1/1 (standard deviation = 0.01). Fig. 3 and Fig. 4 shows the X-ray diffraction patterns for a 50, 65, 85 and 100 cycle PbTe deposit. The x-ray diffraction peaks of 50 (figure 3a), and 65 cycle PbTe deposit (figure 3b) correspond to the rock salt structure peaks for the (200), (111), (222), (400) and (311) planes of PbTe [JCPDS 20-0494], along with polycrystalline Au substrate peaks. Elemental peaks for Pb and Se are absent and the peaks indicate the polycrystalline

nature of the deposit. The 50 and 65 cycle PbTe deposit have a preferential (200) orientation in the deposit. The 85 (figure 4a) and 100 cycle PbTe deposit (figure 4b) is essentially (200) oriented. Fig. 5 shows an AFM image of the AFM image of a 100 cycle deposit of PbTe. The scan size is 5μm and the data scale is 50 nm. The thin film consists of crystallites that are 300 nm in diameter, which are conformal with the Au substrate. Also we can see that there is beginning of 3-D growth associated with the deposit, and as described earlier excess Te may have been deposited being in the overpotential region. Fig. 6 shows a plot of the square of the absorption data for a 50, 65 and 100 cycle deposit of PbTe, times energy, vs. energy. Bulk value of the band gap of PbTe is 0.29 eV. The 50 and 65 cycle thin film band gap is blue shifted to 1 eV and 0.9 eV respectively. We observe a strong blue shift in the band gap (0.7 eV) even for a 100 cycle thin film due to quantum confinement.

Conclusions

PbTe thin films have been successfully formed by EC-ALE. The films were had a preferential (200) orientation and the AFM image indicated that there may be 3-D growth in the grain boundaries of the Au substrate. Further studies involving the optimization of deposition potentials for Te is presently being pursued. We also observe strong quantum confinement effects even in the 100 cycle electrodeposited PbTe thin film. Formation of quantum confined nanowires of PbTe and PbSe and PbSe / PbTe superlattice thin films are presently underway.

Acknowledgements

NSF is gratefully acknowledged for its nano scale exploratory research grant (NERT #024755-01) support for the project.

References

1. M. Orihashi, Y. Noda, L. D. Chen, and T. Hirai, Mater. Trans. JIM 41:1282 (2000).

2. T. C. Harman, P. J. Taylor, D. L. Spears, and M. P. Walsh, J. Electron. Mater. 29:L1 (2000).

3. D. A. Broido and T. L. Reinecke, Appl. Phys. Lett. 77:705 (2000).

4. D. A. Broido and T. L. Reinecke, Phys. Rev. B 6404:art. no. (2001).

5. M. S. Dresselhaus, Y. M. Lin, S. B. Cronin, O. Rabin, M. R. Black, G. Dresselhaus, and T. Koga, in Recent Trends in Thermoelectric Materials Research Iii, Vol. 71, Academic Press Inc, San Diego, 2001, p. 1.

6. S. Yoneda, E. Ohta, H. T. Kaibe, I. J. Ohsugi, I. Shiota, and I. A. Nishida, Mater. Trans. JIM 42:329 (2001).

7. E. I. Rogacheva, I. M. Krivulkin, O. N. Nashchekina, A. Y. Sipatov, V. V. Volobuev, and M. S. Dresselhaus, Appl. Phys. Lett. 78:1661 (2001).

8. H. Beyer, J. Nurnus, H. Bottner, A. Lambrecht, T. Roch, and G. Bauer, Appl. Phys. Lett. 80:1216 (2002).

9. Z. H. Dughaish, Physica B 322:205 (2002).

10. T. C. Harman, P. J. Taylor, M. P. Walsh, and B. E. LaForge, Science 297:2229 (2002).

11. P. W. Zhu, X. Jia, H. Y. Chen, W. L. Guo, L. X. Chen, D. M. Li, H. A. Ma, G. Z. Ren, and G. T. Zou, Solid State Commun. 123:43 (2002).

12. V. I. Rudakov and I. M. Smirnov, J. Phys. IV 12:75 (2002).

13. Y. A. Ugai, A. M. Samoilov, Y. V. Synorov, and O. B. Yatsenko, Inorg. Mater. 36:449 (2000).

14. C. Boschetti, I. N. Bandeira, H. Closs, A. Y. Ueta, P. H. O. Rappl, P. Motisuke, and E. Abramof, Infrared Phys. Technol. 42:91 (2001).

15. D. Zimin, K. Alchalabi, and H. Zogg, Physica E 13:1220 (2002).

16. F. W. wise, Acc. Chem. Res. 2000:773 (2000).

17. S. O. Ferreira, B. R. A. Neves, R. Magalhaes-Paniago, A. Malachias, P. H. O. Rappl, A. Y. Ueta, E. Abramof, and M. S. Andrade, J. Cryst. Growth 231:121 (2001).

18. C. Teichert, B. Jamnig, and J. Oswald, Surf. Sci. 454:823 (2000).

19. M. P. Belyansky, A. M. Gaskov, and A. V. Strelkov, Source MATER SCI ENG B SOLID STATE ADV TECHNOL:78 (1992).

20. A. Belenchuk, A. Fedorov, H. Huhtinen, V. Kantser, R. Laiho, O. Shapoval, and V. Zakhvalinskii, Thin Solid Films 358:277 (2000).

21. E. A. Streltsov, N. P. Osipovich, L. S. Ivashkevich, A. S. Lyakhov, and V. V. Sviridov, Russian Journal of Applied Chemistry 70:1651 (1997).

22. H. Saloniemi, T. Kanniainen, M. Ritala, and M. Leskela, Thin Solid Films 326:78 (1998).

23. H. Saloniemi, M. Kemell, P. Ritala, and M. Leskela, Journal of Electroanalytical Chemistry 482:139 (2000).

24. L. Beaunier, H. Cachet, R. Cortes, and M. Froment, J. Electroanal. Chem. 532:215 (2002).

25. M. N. Mamedov, Russ. J. Appl. Chem. 75:1075 (2002).

26. I. Nick, J. Liang, V. Cammarata, and C. Shannon, Abstr. Pap. Am. Chem. Soc. 223:263 (2002).

27. F. Herman, R. L. Kortum, C. D. Kuglin, and J. P. Van Dyke, in Methods in Computational Physics, Vol. 8 (B. Alder, S. Fernbach, and M. Rotenberg, eds.), Acamdemic Press, New York, 1968, p. 193.

28. T. Suntola and J. Antson, in US Patent, USA, 1977.

29. C. H. L. Goodman and M. V. Pessa, JAP 60:R65 (1986).

30. H. Sitter and F. W., Festkorperprobleme-Advances in Solid State Phyics 30:219 (1990).

31. J. L. Stickney, in Advances in Electrochemical Science and Engineering, Vol. 7 (D. M. Kolb and R. Alkire, eds.), Wiley-VCH, Weinheim, 2002, p. 1.

32. J. L. Stickney, T. L. Wade, B. H. Flowers Jr., R. Vaidyanathan, and U. Happek, in Encyclopedia of Electrochemistry, Vol. in press (E. Gileadi and M. Urbakh, eds.), Marcel Dekker, New York, 2002.

33. B. W. Gregory and J. L. Stickney, Journal of Electroanalytical Chemistry 300:543 (1991).

34. D. M. Kolb, M. Przasnyski, and H. Gerisher, JEC 54:25 (1974).

35. R. R. Adzic, D. N. Simic, A. R. Despic, and D. M. Drazic, JEC 65:587 (1975).

36. D. M. Kolb and H. Gerisher, SS 51:323 (1975).

37. D. M. Kolb, in Advances in Electrochemistry and Electrochemical Engineering, Vol. 11 (H. Gerischer and C. W. Tobias, eds.), John Wiley, New York, 1978, p. 125.

38. R. R. Adzic, in Advances in Electrochemistry and Electrochemical Engineering, Vol. 13 (H. Gerishcher and C. W. Tobias, eds.), Wiley-Interscience, New York, 1984, p. 159.

39. F. Forni, M. Innocenti, G. Pezzatini, and M. L. Foresti, Electrochemica Acta 45:3225 (2000).

40. E. S. Streltsov, I. I. Labarevich, and D. V. Talapin, Doklady Akademii Nauk Belarusi 38:64 (1994).

41. B. H. Flowers Jr., T. L. Wade, M. Lay, J. W. Garvey, U. Happek, and J. L. Stickney, JEC in press (2002).

42. K. Varazo, M. D. Lay, and J. L. Stickney, JEC in press (2002).

43. B. E. Boone and C. Shannon, Journal of Physical Chemistry 100:9480 (1996).

44. A. Gichuhi, B. E. Boone, and C. Shannon, Langmuir 15:763 (1999).

45. M. Innocenti, G. Pezzatini, F. Forni, and M. L. Foresti, JECS 148:c357 (2001).

46. G. Pezzatini, S. Caporali, M. Innocenti, and M. L. Foresti, JEC 475:164 (1999).

47. I. Villegas and J. L. Stickney, Journal of Vacuum Science & Technology A 10:3032 (1992).

48. I. Villegas and J. L. Stickney, Journal of the Electrochemical Society 139:686 (1992).

49. T. L. Wade, L. C. Ward, C. B. Maddox, U. Happek, and J. L. Stickney, Electrochemical and Solid State Letters 2:616 (1999).

50. T. L. Wade, R. Vaidyanathan, U. Happek, and J. L. Stickney, JEC 500:322 (2001).

51. T. Torimoto, A. Obayashi, S. Kuwabata, H. Yasuda, H. Mori, and H. Yoneyama, Langmuir 16:5820 (2000).

52. T. Torimoto, S. Nagakubo, M. Nishizawa, and H. Yoneyama, Langmuir 14:7077 (1998).

53. T. Torimoto, S. Takabayashi, H. Mori, and S. Kuwabata, JEC 522:33 (2002).

54. R. Vaidyanathan, U. Happek, and J. L. Stickney, Electrochimica Acta submitted (2003).

55. T. L. Wade, B. H. Flowers Jr., R. Vaidyanathan, K. Mathe, C. B. Maddox, U. Happek, and J. L. Stickney, in Materials Research Society, Vol. 581, Materials Research Society, 2000, p. 145.

56. T. L. Wade, B. H. Flowers Jr., K. Varazo, M. Lay, U. Happek, and J. L. Stickney, in Electrochemical Society National Meeting, Vol. In Press (K. Kondo, ed.), Electrochemcial Society, Washington D.C., 2001.

57. S. M. Sze, Physics of Semiconductor Devices, john Wiley & Sons, New York, 1981.

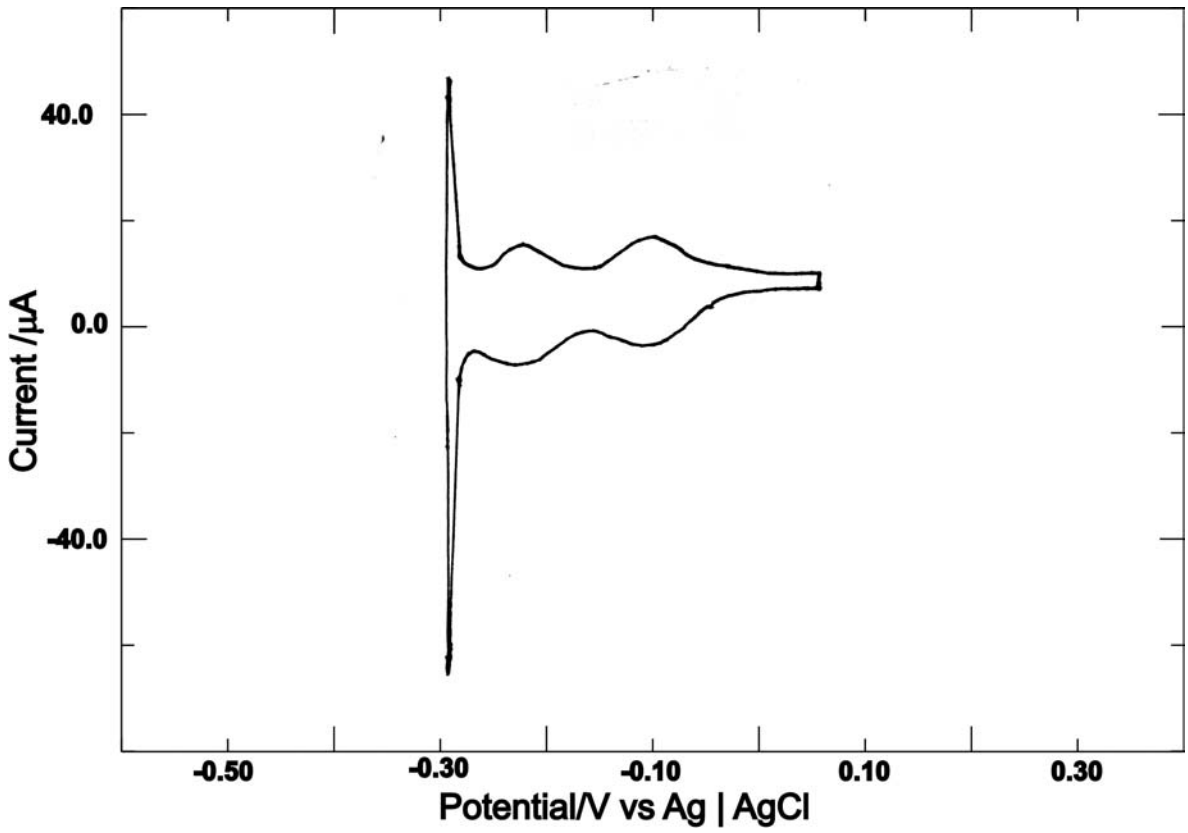

Figure 6.1. Cyclic voltammogram of a Au electrode in a pH 5.5 solution containing 0.2 mM $Pb(ClO_4)_2$, 50 mM CH_3COONa and 0.1 M $NaClO_4$. Scan rate 5 mV/sec

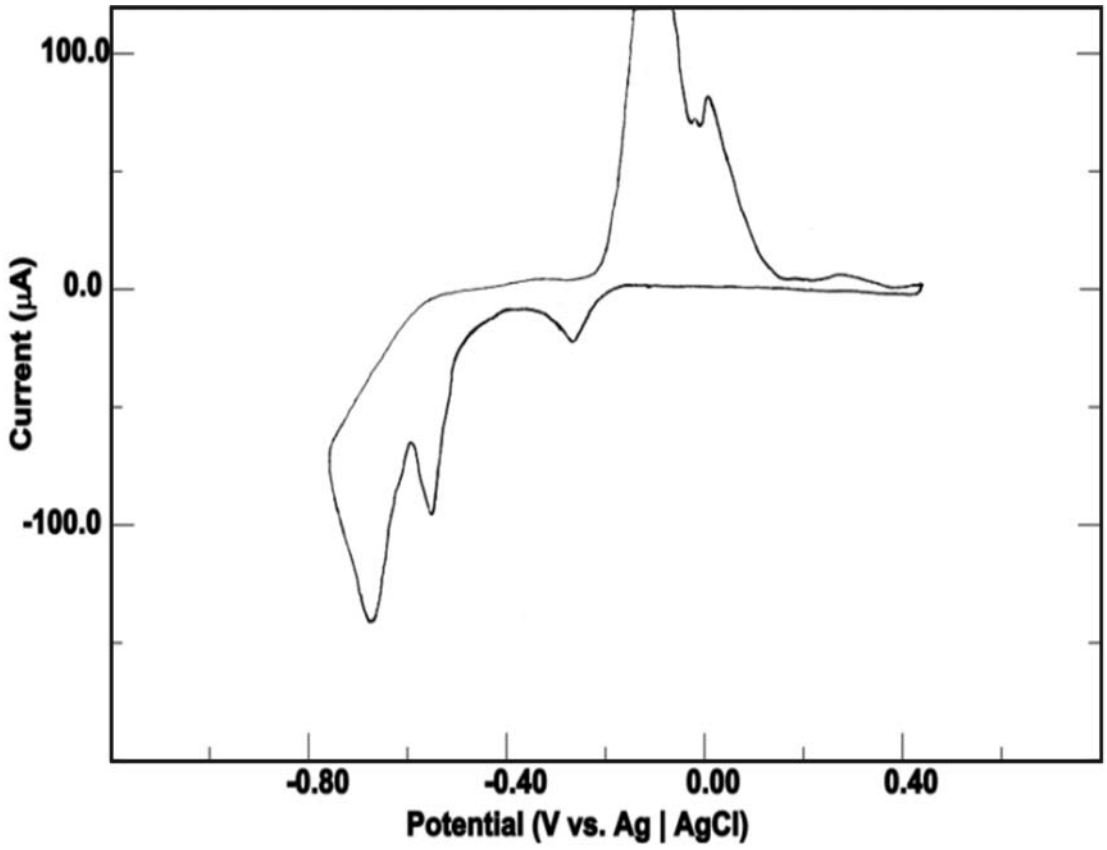

Figure 6.2. Cyclic voltammogram of a Au electrode in a pH 9.2 solution containing 0.2 mM TeO_2, 50 mM Sodium borate and 0.1 M $NaClO_4$. Scan rate 5 mV/sec

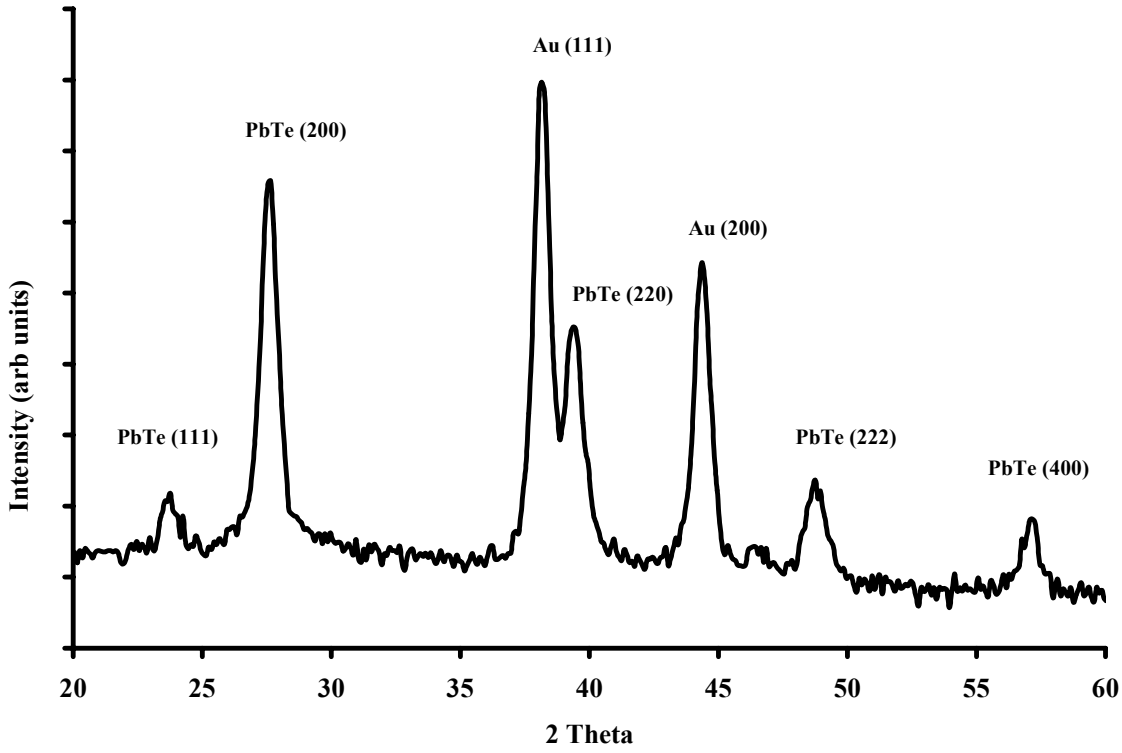

Figure 6.3a. X-ray diffraction of 50 cycle electrodeposited PbTe thin film. Angle of incidence is 1°, Cu Kα source.

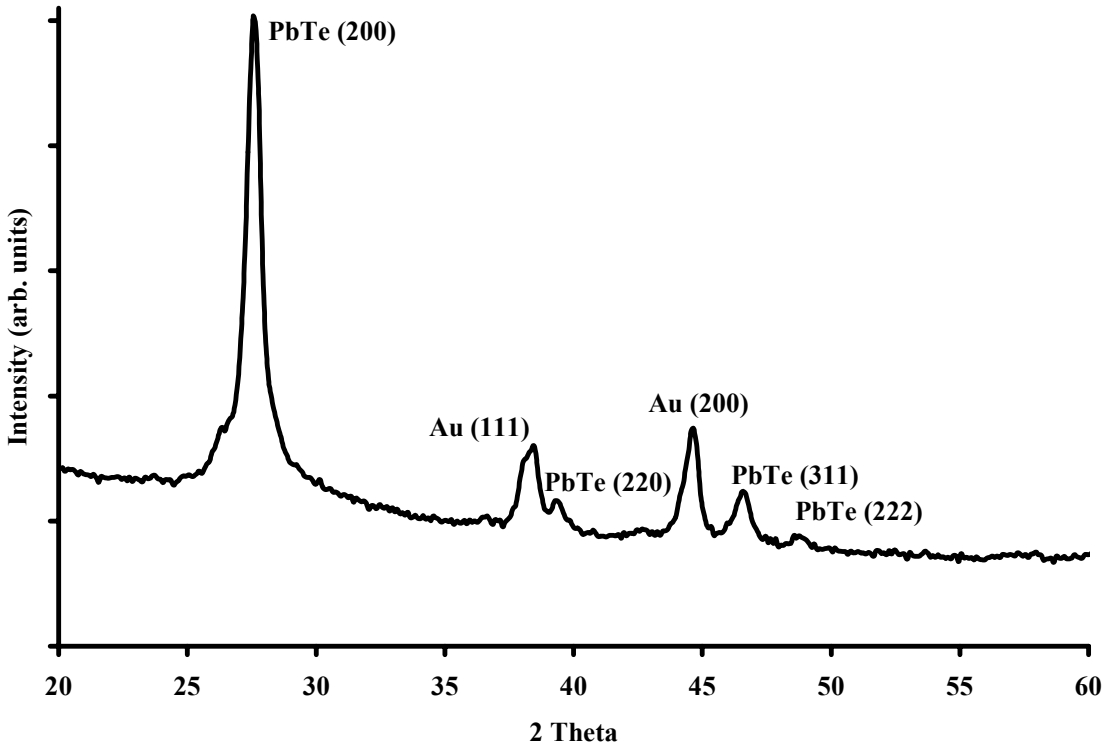

Figure 6.3b. X-ray diffraction of 65 cycle electrodeposited PbTe thin film. Angle of incidence is 1°, Cu Kα source.

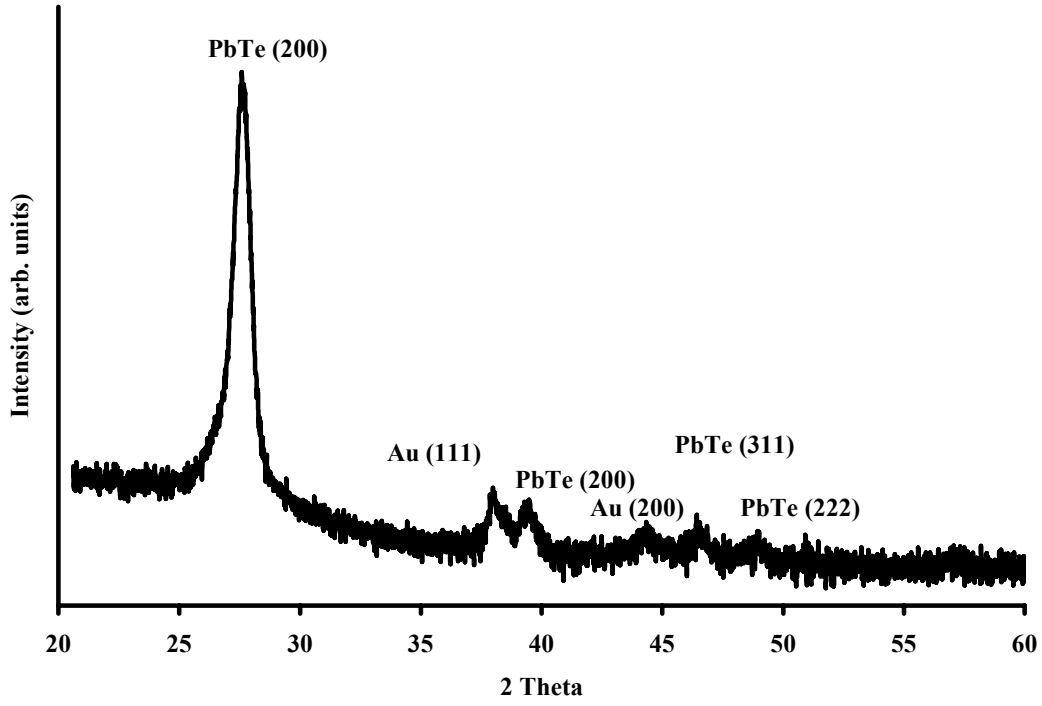

Figure 6.4a. X-ray diffraction of 85 cycle electrodeposited PbTe thin film. Angle of incidence is 1°, Cu Kα source.

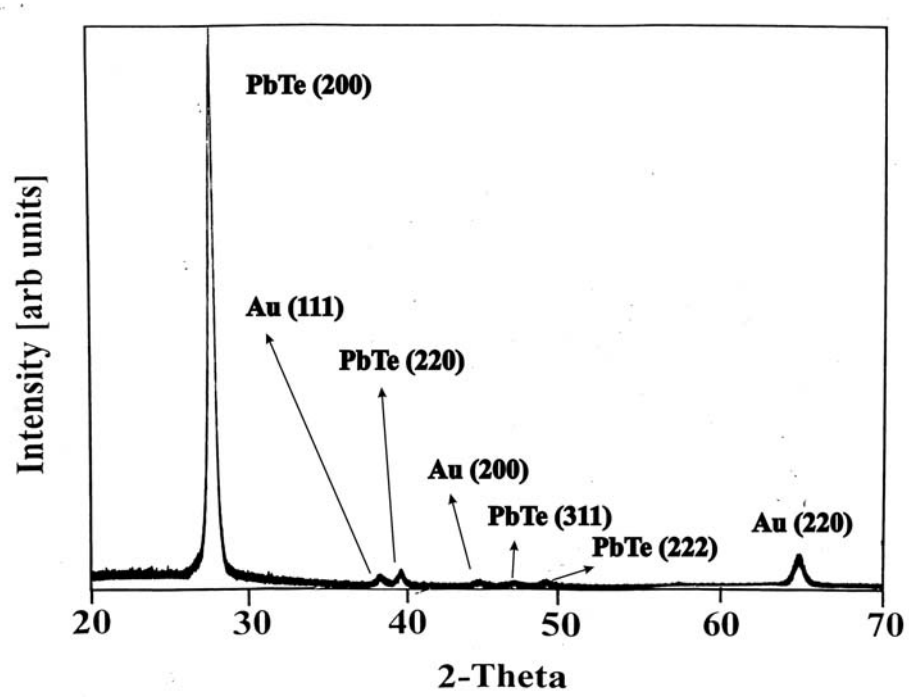

Figure 6.4b. X-ray diffraction of 100 cycle electrodeposited PbTe thin film. Angle of incidence is 1°, Cu Kα source.

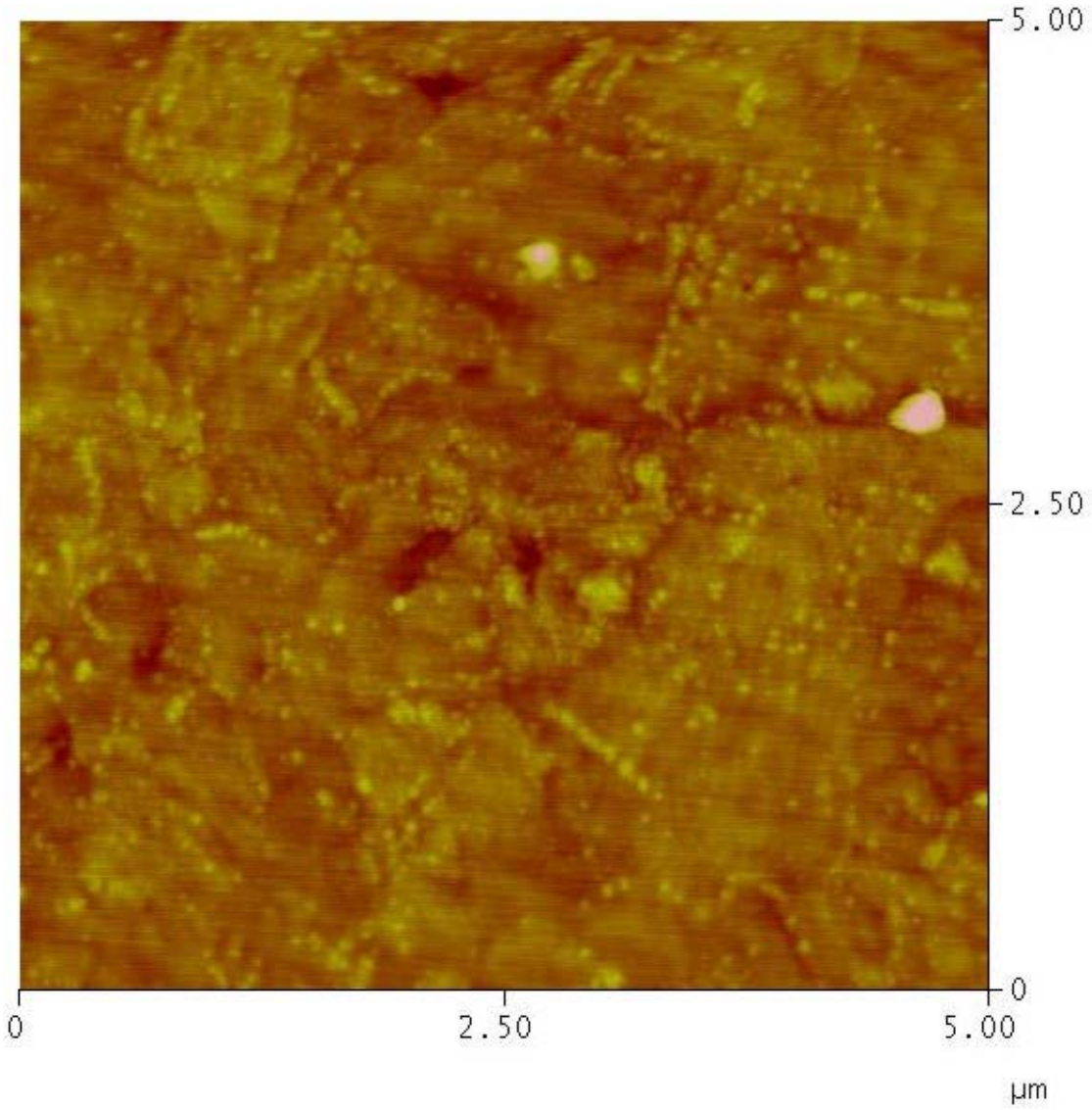

Figure 6.5. AFM of 100 cycle electrodeposited PbTe thin film on annealed Au substrate. The scale is 5µm and data scale is 50 nm.

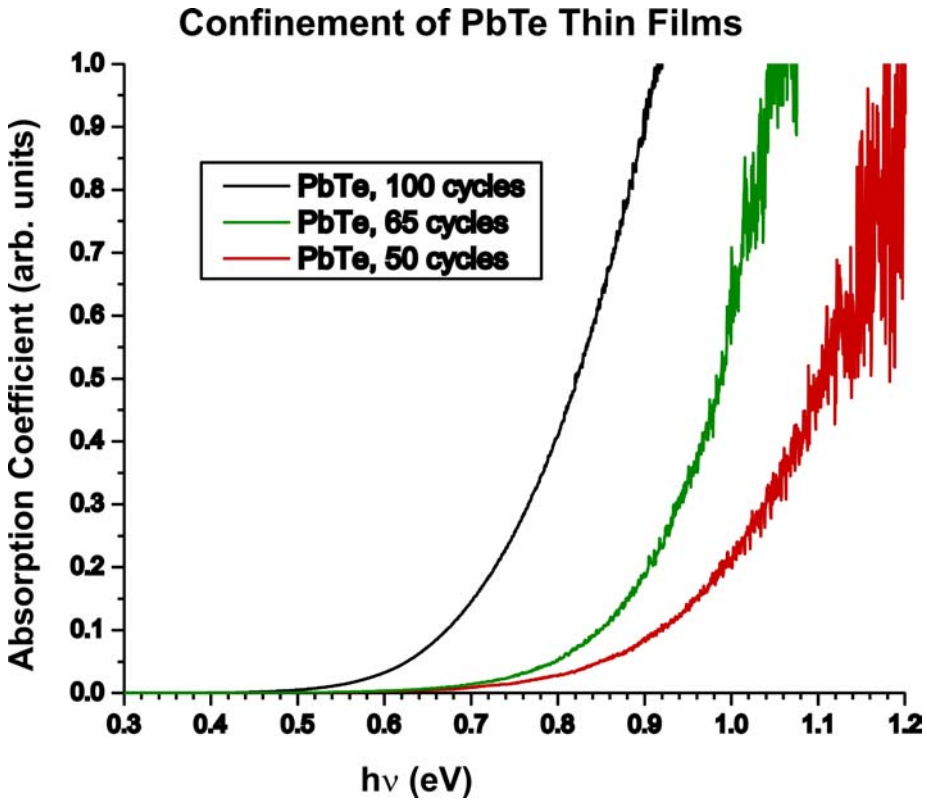

Figure 6.6. Absorption spectrum of a) 50 cycle (red) b) 65 cycle (green) c) 100 cycle (black) electrodeposited PbTe thin film.

Chapter 7

Electrodeposition of PbSe/PbTe superlattice thin films by Electrochemical Atomic Layer Epitaxy (EC-ALE)[6]

[6] Vaidyanathan R, Happek U, Cox S.M, and Stickney J.L, Journal of Applied Physics, submitted (2003).

Abstract

This paper concerns the electrochemical growth of compound semiconductor thin film superlattice structures using electrochemical atomic layer epitaxy (EC-ALE). EC-ALE is the electrochemical analog of atomic layer epitaxy (ALE), a deposition method based on the formation of compounds an atomic layer at a time, using surface limited reactions. Electrochemical surface limited reactions are referred to as underpotential deposits (upd), and EC-ALE is the use of upd in an ALE cycle. PbSe/PbTe thin film superlattices, with modulation wavelengths of 4.23 nm and 7.05 nm, are reported here. The films were characterized using electron probe microanalysis (EPMA), X- ray diffraction (XRD), atomic force microscopy (AFM) and reflection infrared absorption measurements. The 4.23 nm period superlattice was grown on a thin (10 cycle) PbSe pre-layer, and had a composition of $PbSe_{0.52}Te_{0.48}$. The 7.05 nm period superlattice was grown on a thicker (100 cycle) PbTe pre-layer, and had a composition of $PbSe_{0.44}Te_{0.56}$. The primary Bragg diffraction peak for the $PbSe_{0.52}Te_{0.48}$ superlattice corresponded to an average of the (111) diffractions of PbSe and PbTe. First order satellite peaks and a second were observed, indicating a high quality superlattice thin film. When the modulation wavelength of the superlattice was increased to 7.05 nm, on the thicker PbTe pre-layer, Bragg peaks corresponding to both the (200) and (111) plane of the PbSe/PbTe superlattice were observed, with satellite peak shifted 1° closer to the (111). AFM indicates that the superlattice thin films were essentially conformal with the Au substrate. The band gaps of the 4.23 nm and 7.05 nm superlattice thin films were measured to be 0.48 eV and 0.38 eV respectively.

Keywords

PbSe, PbTe, superlattice, IV-VI, Thermoelectric materials, Quantum confinement, UPD, Electrodeposition, EC-ALE, ALE and X-ray diffraction

Introduction

Superlattices are examples of nano-structured materials [1,2], where the unit cell of the material is artificially manipulated in one dimension. By alternately depositing nano films (a few monolayers (ML) thick) of two compounds, a material is created with a new unit cell, defined by the superlattice period, the combined thickness of the two nano films. Changing the number of ML within a period of the superlattice will change its optical properties and XRD. Interfacial sharpness, lattice mismatch between the constituent compounds, and modulation of the stoichiometry throughout the superlattice period profile, all can have substantial effects on the optical and electronic properties of the superlattice.

Superlattices based on IV-VI compound semiconductors are promising in thermoelectric applications[3-5], infrared sensors[6] etc., as well, the current transport properties of IV-VI compound semiconductor superlattices[3-5,7-11] change with periodicity. These IV-VI compound semiconductor materials have large Bohr radii, 50 nm for PbTe and 46 nm for PbSe[12]. When the dimensions of the semiconductor material are less than the Bohr radius, the electron is confined in the superlattice, and optical, electronic and or magnetic properties of the semiconducting material can change due to quantum confinement[12]. IV-VI compound semiconductors like PbSe, PbTe and PbS, have small and relatively equal electron and hole masses, compared to III-V or II-VI compound semiconductors. The result is that they tend to exhibit larger confinement effects when dimensions are less then the Bohr radius, compared to III-V or II-VI superlattice systems[12].

The primary methodologies for forming superlattices with atomic level control are molecular beam epitaxy (MBE) [3,6,13-16], vapor phase epitaxy (VPE) [17], and a number of

derivative vacuum based techniques [4,5,7]. These methods depend on controlling the flux of reactants and the temperature of the substrate and reactants. The growth temperature in MBE and VPE is an important variable, however deposits formed at even moderate temperatures (200-500 °C), result in interdiffusion of component elements. In the formation of a superlattice, individual nanolayers are thin, and a small amount of interdiffusion can have a large effect, blurring of the interfaces and resulting in a material that is more of an alloy then a superlattice. The integrity of a junction frequently determines the quality of a device.

Electrodeposition is a low-temperature technique, minimizing interdiffusion, and is thus appealing for the formation of superlattices [2,11,18,19]. Electrochemical formation of superlattices has been pioneered by Switzer et al [2]. One of the standard methods for compound electrodeposition is co-deposition, where a set reduction potential or current density is applied to a single solution containing precursors for all the elements in a compound. Co-deposition of PbSeTe multilayer periodic structure have been reported by Strelsov et.al.[20-22]

Atomic layer epitaxy (ALE) is a method [23-26] for forming compound thin films one atomic layer at a time. Surface limited reactions are used to deposit each atomic layer. The use of surface limited reactions should improve morphology and facilitates monolayer control of the growth rate. ALE offers greater control over deposit structure than methods based on controlling reactant fluxes for all elements simultaneously. The principle is that by limiting growth to a monolayer at a time, 2D growth, epitaxy will be promoted. Our group has been developing the electrochemical analog of ALE, electrochemical atomic layer epitaxy (EC-ALE) [27-29]. EC-ALE uses electrochemical

surface limited reactions, referred to as underpotential deposits (UPD) to form compound semiconductors one atomic layer at a time. Upd [30-34] is the deposition of an atomic layer of one element on a second, at a potential prior to that needed to form bulk deposits of the first element. An EC-ALE cycle would then be where an atomic layer of the first element is deposited at its upd potential from a solution containing its precursor, the solution would then be exchanged for a solution of a precursor for the second element, and an atomic layer of it would be deposited at its underpotential, resulting in the formation of a monolayer of the desired compound. The number of cycles determines the thickness of the deposit.

II-VI compounds such as CdTe[29,35-38], CdS[29,36,39-41], ZnSe[42], CdS/CdSe superlattices[43] and CdS/HgS junctions[40] have been successfully formed using using EC-ALE, as have some III-V compounds: GaAs[44,45], InAs[46], InSb[47] and superlattices of InAs/InSb[47]. Torimoto et al. reported quantum confinement in thin films of ZnS[48], CdS[49], and PbS[50] and superlattices of ZnS/CdS [51,52] grown by EC-ALE. We have also reported the quantum confinement of PbSe[53] and PbTe [54] thin films grown by EC-ALE.

Ideally, two lattice matched compounds are chosen to form a superlattice[2]. PbSe and PbTe have a significant lattice mismatch, 6%, and are thus considered to form strain layered superlattice structures [55], where dislocations and island growth during superlattice formation with MBE are expected. In this paper we report the formation of PbSe/PbTe strained layer superlattice thin films, electrodeposited using EC-ALE.

Experimental

An automated electrochemical thin-layer flow deposition system was used for the formation of thin films. The system consisted of a series of solution reservoirs, computer

controlled pumps, valves and a potentiostat. Most of the hardware used has been described in previous articles [28,47,56]. The system is contained within a nitrogen purged Plexiglas box, to reduce the influence of oxygen during electrodeposition. A thin-layer electrochemical flow cell, designed to promote laminar flow, was used for the depositions, and consisted of a Au working electrode, Au coated indium tin oxide (ITO) auxiliary electrode and a Ag|AgCl (3M NaCl) reference electrode (Bioanalytical systems, Inc., West Lafayette, IN).

Solutions used include: 0.2 mM $Pb(ClO_4)_2$ (Alfa Aesar, Ward Hill, MA), pH 5.5, buffered with 50.0 mM $CH_3COONa{\cdot}3H_2O$ (J.T.Baker); 0.2 mM TeO_2 (Alfa Aesar, Ward Hill, MA), pH 9.2, buffered with 50.0 mM Sodium borate; and 0.2 mM SeO_2 (Alfa Aesar, Ward Hill, MA), pH 5.5, buffered with 50.0 mM $CH_3COONa{\cdot}3H_2O$ (J.T.Baker) . A pH 7.0 rinse solution was used as well. The pH values of all solutions were adjusted with CH_3COOH and KOH (Fischer Scientific, Pittsburgh, PA). Supporting electrolyte, 0.1 M $NaClO_4$ (Fischer Scientific, Pittsburgh, PA), was added to each solution. Solutions were made with water from a Nanopure water filtration system (Barnstead, Dubuque, IA), fed from the house distilled water system. All chemicals were reagent grade or better.

Substrates were glass microscope slides (Gold Seal products), etched in HF and rinsed with HNO_3 briefly, prior to insertion into the vapor deposition chamber. The substrates were annealed in the turbo pumped deposition chamber at 400 °C for 12 hrs before vapor deposition. Thin, 3 nm, films of Ti were first vapor deposited, followed by 600 nm of Au, while the substrates were held at 400 °C. The substrates, removed from the chamber, were dipped in nitric acid and rinsed with nanopure water. Prior to use, the substrates

were annealed using a H_2 flame (to a dull orange glow in the dark), cleaned again in hot nitric acid and rinsed with nanopure water.

AFM studies were performed using Nanoscope 2000 (Digital Instruments, Santa Barbara, CA) in the tapping mode. Absorption measurements were performed using a variable angle reflection rig in conjunction with a Bruker 66v FTIR spectrometer equipped with a Si detector. Glancing angle X-ray diffraction patterns were acquired on a Scintag PAD V diffractometer, equipped with a 6" long set of Sola slits on the detector to improve resolution in this asymmetric diffraction configuration. Electron probe microanalysis (EPMA) studies were performed using a Joel JXA-8600 super probe.

Results and Discussion

4:4 Superlattice

The starting potentials in the deposition program were determined from cyclic voltammograms for each element on the Au substrates. Experience has shown that optimal potentials, those that result in a ML/cycle, may shift to more negative potentials as the deposit grows, over the first 10 to 30 cycles depending on the compound, before reaching steady state potentials. Steady state potentials of -0.3 V for Pb, -0.3 V for Se and -0.4 V for Te were previously reported [53,54] by this group for the EC-ALE deposition of these elements in preliminary studies of the formation of PbSe and PbTe compound semiconductor thin films.

For the 4:4 superlattice, each period was grown with 4 cycles (ML) of PbSe and 4 of PbTe. The deposit consisted of 81 periods, on a pre-layer of 10 atomic layers of PbSe. The pre-layer allowed attainment of steady state potentials before compound alternation was initiated. The period program worked as follows: the flow cell was first filled with

the Pb^{2+} solution for 2 sec at a potential of -0.3 V. The potential was held without solution flow for 15 sec to allow Pb atomic layer deposition. The cell was then rinsed with the blank for 2 sec and filled with the Te precursor ($HTeO_3^-$) solution, at –0.4 V, at which point flow was stopped, and Te was deposited for 15 secs. Excess $HTeO_3^-$ ions were then rinsed out of the cell using the blank solution, for 2 secs, to complete the cycle. This cycle was intended to form a ML of the IV-VI semiconductor PbTe, and was repeated 4 times to form a PbTe nanofilm. The complimentry PbSe nanofilm was grown in a similar manner: the cell was again filled with the Pb^{2+} solution at a -0.3 V for 2 sec, and Pb was deposited for 15 sec. Excess Pb^{2+} was removed by rinsing with the blank for 2 sec, and then the cell was filled for 2 sec with the Se precursor ($HSeO_3^-$) solution at -0.3 V. Se was deposited for 15 sec, after which the cell was rinsed again with blank for 2 sec. This cycle was intended to form a ML of PbSe and was also repeated 4 times, to form a nanofilm of PbSe. This whole program, 4 cycles of PbTe and 4 cycles of PbSe, formed one period of the superlattice, and was repeated 80 times.

Figure 7.1 shows the X-ray diffraction pattern for the 81 period 4:4 PbSe/PbTe superlattice. The (111) diffraction peak, along with both ± first order satellite peaks, and one second order peak, are evident for the superlattice. The satellites were equidistant from the sides of the (111) diffraction peak.

The superlattice period, H, can be calculated using the following equation[7], from the angular distance $\Delta(2\theta)$ between the satellite and the (111) Bragg peak:

$$H = 57.3\ \lambda / \Delta(2\theta)\ \mathrm{Cos}\theta \qquad \text{----------} \qquad (1).$$

In the present study, the period thickness was found to be 4.23 nm. If we think of a ML of the compound as being one atomic layer of Pb atoms and one of Te or Se, essentially a

monolayer of (111) PbSe or PbTe out of the rock salt structure, the thickness of this period should be 2.1 nm, rather then the 4.23 nm determined from XRD. The assumption that one atomic layer of Pb and one layer of Te would be the natural result of EC-ALE is not necessarily true, it may be that one cycle of deposition naturally results in growth of what would be considered here two ML of the compound, as the natural amount. This results suggests that the optimal deposition conditions for both PbSe and PbTe by EC-ALE should be further investigated. In the 4:4 superlattice, odd 2^{nd} order satellite peaks were observed, indicative of a square wave modulation of the lattice and uniform composition through the superlattice [2].

EPMA of the deposits indicated a composition of $PbSe_{0.52}Te_{0.48}$, slightly rich in Se, as might be expected, as the initial pre-layer was 10 cycles of PbSe. Infrared absorption measurements (Figure 7.2) suggested a band gap for the superlattice of 0.48 eV, blue shifted from the band gaps for either of the component compounds, and thus suggesting the presences of quantum confinement in the deposit.

6:6 Superlattice

Figure 7.3 shows the X-ray diffraction pattern for a 40 period 6:6 PbSe/PbTe superlattice thin film. Each period of the superlattice was made up of 6 cycles of PbSe and 6 cycles of PbTe. The superlattice was deposited on a pre-layer of 100 cycles of PbTe. In Figure 7.3, (111) and (200) Bragg diffraction peaks, along with first order satellite peaks, are evident in a relatively noisy XRD pattern. Satellite peaks were positioned equidistant about the (111) Bragg diffraction peak, similarly to those in Figure 7.1. In addition, minimal satellites can be detected equally spaced about the (200) peak. From the spacing of the

(111) satellite peaks, a superlattice period, H, of 7.05 nm was suggested. This is, again, about twice the anticipated thickness, in this case H = 3.1 nm was expected if we consider each cycle to form a single (111) compound monolayer. Comparing the two superlattices, the relative increase in thickness/period between the 4:4 and 6:6 superlattices was about as expected, given that each cycle appears to result in about two layers instead of one. EPMA suggested a stoichiometry of $PbSe_{0.44}Te_{0.56}$ for the overall deposit, a little heavy in Te. However, given that a 100 cycles of PbTe was used as the pre-layer, this stoichiometry is not surprising. Figure 7.5 shows the infrared absorption data for this 6:6 superlattice deposit, which suggests a band gap of 0.38 eV. Increasing the superlattice period, from 4.23 nm to 7.05 nm, resulted in a red shift of the thin film band gap, from 0.48 to 0.38 eV, as would be expected.

An AFM image (Figure 7.5) of the $PbSe_{0.52}Te_{0.48}$ superlattice displayed some little white dots, apparently growing at grain boundaries. Those dots were probably indications of some initial 3-D growth. The scan size of the image is 5μm X 5μm, and the Z scale was 50 nm. The thin film deposit consisted of crystallites 300 nm in diameter, essentially conformal with the Au substrate. The small amount of 3D growth is consistent with an unoptimized cycle program, and the apparent deposition of two compound ML each cycle, instead of the expected one ML. Studies to optimize the cycles for both PbSe and PbTe are presently underway.

Significant changes in the XRD pattern were evident between the 4:4 and 6:6 superlattices, including the appearance of a more prominent (200) orientation. These changes probably resulted from the fact that PbTe was used instead of PbSe for the pre-layer, and that 100 cycles of PbTe were grown for the 6:6 deposit, where only 10 cycles

of PbSe were grown before the 4:4 deposit. For instance, it may be that the (200) peak in Figure 7.3 may be mostly the result of the 100 cycles of PbTe used as a pre-layer. Why the XRD quality went down between Figure 7.1 and 7.3 is not clear, but part may be due to the fact that only 40 periods of the 6:6 were grown instead of the 81 grown of the 4:4. Other possibilities include variability in the quality of the Au on glass substrates, as some show a much increased roughness, and the glancing incident angle XRD method used is very sensitive to small variations in the sample position. Finally, it may have to do with the lattice match, it may be that the 6:6 period is too long, exceeding the critical thickness for the materials, and a large increase in the defect density resulted. Further studies of the dependence of the XRD of these superlattices on the growth conditions are underway.

It is notable, that while PbSe films grown on Au on glass substrates resulted essentially polycrystalline deposits [53], 100 cycle PbTe deposits showed a single (200) diffraction peak [54]. This may help explain why the (200) peak is present for the 6:6 deposit formed on a 100 cycle PbTe pre-layer. However, what is not yet clear is why both superlattices appear to grow with a prominent (111) orientation, rather then the (200)?

IV-VI compounds PbSe and PbTe have band gaps of 0.26 eV and 0.29 eV respectively. Previous studies of lead chalcogenide superlattices have suggested that they have type II [57-61] band alignment, which usually results in superlattice band gaps less than either of the constituent semiconducting compounds. In the present study the band gaps of the superlattices are blue shifted from the band gaps for the constituent elements. The individual 4 or 6 cycle compound nanolayers in the superlattice should have band gaps greater then 1 eV, but the superlattices evidence band gaps of 0.48 and 0.38 eV respectively, an over all blue shift with respect to the bulk compounds, but a red shift

from that expected for the individual compound nanolayers. To better understand these effects, use of larger period superlattices, thicker nanolayers of the compounds, will be grown, as confinement effects should decrease, and a net red shift may be observed if they are type II superlattices. Alternatively, the extra confinement could be the result of the stress involved in forming the lattices, as noted they should be strained layer superlattices. Defects incorporated as the lattices are grown, related to the lattice mismatch, may result in nanoclustering, the confinement from which may contribute to observed blue shifts. In addition, as noted above, that while the conditions for the EC-ALE cycles are good, they are not yet optimized, and some 3D growth is present. These features may help to account for the observed optical properties. Overall, it is clear that optimal cycle conditions for the deposition of the constituent compounds should be developed, and that more lattices should be formed with larger periods, in order to better understand these results.

Conclusions

PbSe/PbTe superlattices have been successfully formed using EC-ALE with 4:4 cycle and 6:6 cycle periods. From XRD, second order satellite diffraction peaks indicate the formation of a very good quality superlattice, and suggested a square wave modulation of the lattice and uniform composition modulation throughout the thin film. Increasing the superlattice period red shifted the adsorption spectrum for the superlattice deposits, consistent with a decrease in the degree of quantum confinement in the superlattice, as the period increased. The literature suggests these materials should form type II superlattices, however, the band gap was blue shifted from those of the individual compounds, suggesting a type I. On the other hand, the extent of the blue shift was

considerably less then expected. These results are very encouraging, but suggest more studies to investigate the quality of the superlattice deposits, the dependence on thickness and symmetry of the period, and the importance of a pre-layer to the resulting deposit structure. In addition, by studying the dependence of the band gap on period thickness, questions concerning the type of superlattice, type I or type II, may be answered.

Acknowledgements

Support from the National Science Foundation, Materials and Chemistry, and the NSF DMR NER, Nanoscale Experimental Research program, is gratefully acknowledged.

References

[1] J. A. Switzer, M. J. Shane, and R. J. Phillips, Science 247, 444 (1990).

[2] J. A. Switzer, in *Electrochemistry of Nanomaterials*, edited by G. Hodes (Wiley-VCH, 2001), p. 67-101.

[3] T. C. Harman, P. J. Taylor, D. L. Spears, and M. P. Walsh, J. Electron. Mater. 29, L1-L4 (2000).

[4] H. Beyer, J. Nurnus, H. Bottner, A. Lambrecht, T. Roch, and G. Bauer, Appl. Phys. Lett. 80, 1216-1218 (2002).

[5] T. C. Harman, P. J. Taylor, M. P. Walsh, and B. E. LaForge, Science 297, 2229-2232 (2002).

[6] A. Y. Ueta, E. Abramof, C. Boschetti, H. Closs, P. Motisuke, P. H. O. Rappl, I. N. Bandeira, and S. O. Ferreira, Microelectron. J. 33, 331-335 (2002).

[7] S. I. A. Fedorov A.G, Sipatov A.Yu, Kaidalova E.V, Journal of Crystal Growth 198, 1211-1215 (1999).

[8] D. A. Broido and T. L. Reinecke, Appl. Phys. Lett. 77, 705-707 (2000).

[9] D. A. Broido and T. L. Reinecke, Phys. Rev. B 6404, art. no.-045324 (2001).

[10] M. S. Dresselhaus, Y. M. Lin, S. B. Cronin, O. Rabin, M. R. Black, G. Dresselhaus, and T. Koga, in *Recent Trends in Thermoelectric Materials Research Iii*; *Vol. 71* (Academic Press Inc, San Diego, 2001), p. 1-121.

[11] I. Nicic, C. Shannon, M. J. Bozack, M. Braun, S. Link, and M. El-Sayed, in *Electrodeposition and characteriazation of CdTe/PbTe superlattices: A preliminary investigation*, Washington D.C., 2001 (ECS).

[12] F. W. wise, Acc. Chem. Res. 2000, 773-780 (2000).

[13] Y. Guldner, G. Bastard, J. P. Vieren, M. Voos, J. P. Faurie, and A. Million, Phys. Rev. Lett. 51, 907 (1983).

[14] G. C. Osbourn, IEEE J. Quant. Electron. QE-22, 1677 (1986).

[15] Y. Sakuma, O. M., K. K., and O. N., Journal of Crystal Growth 115, 324 (1991).

[16] C. Mailhiot and D. L. Smith, Critical Reviews in Solid State and Materials Sciences 16, 131 (1990).

[17] G. R. Booker, P. V. Klipstein, M. Lakrimi, S. Lyapin, N. Mason, I. J. Murgatroyd, R. Nicholas, T. Y. Seong, S. D.M, and W. P.J., Journal of Crystal Growth 146, 495 (1995).

[18] E. A. Streltsov, N. P. Osipovich, A. S. Lyakhov, and L. S. Ivashkevich, Inorganic Materials 33, 442-446 (1997).

[19] J. A. Switzer, C.-J. Hung, B. E. Breyfogle, M. G. Shumsky, R. V. Leeuwen, and T. D. Golden, Science 264, 1573 (1994).

[20] E. Streltsov, N. P. Osipovich, L. S. Ivashkevich, and A. S. Lyakhov, Doklady Akademii Nauk Belarusi 41, 62-65 (1997).

[21] E. A. Streltsov, N. P. Osipovich, L. S. Ivashkevich, A. S. Lyakhov, and V. V. Sviridov, Russian Journal of Applied Chemistry 70, 1651-1653 (1997).

[22] E. A. Streltsov, N. P. Osipovich, L. S. Ivashkevich, and A. S. Lyakhov, EA 44, 407-413 (1998).

[23] F. Herman, R. L. Kortum, C. D. Kuglin, and J. P. Van Dyke, in *Methods in Computational Physics*; *Vol. 8*, edited by B. Alder, S. Fernbach, and M. Rotenberg (Acamdemic Press, New York, 1968), p. 193.

[24] T. Suntola and J. Antson, in *US Patent* (USA, 1977).

[25] C. H. L. Goodman and M. V. Pessa, JAP 60, R65 (1986).

[26] H. Sitter and F. W., Festkorperprobleme-Advances in Solid State Phyics 30, 219 (1990).

[27] J. L. Stickney, in *Advances in Electrochemical Science and Engineering*; *Vol. 7*, edited by D. M. Kolb and R. Alkire (Wiley-VCH, Weinheim, 2002), p. 1-107.

[28] J. L. Stickney, T. L. Wade, B. H. Flowers Jr., R. Vaidyanathan, and U. Happek, in *Encyclopedia of Electrochemistry*; *Vol. in press*, edited by E. Gileadi and M. Urbakh (Marcel Dekker, New York, 2002).

[29] B. W. Gregory and J. L. Stickney, Journal of Electroanalytical Chemistry 300, 543 (1991).

[30] D. M. Kolb, M. Przasnyski, and H. Gerisher, JEC 54, 25-38 (1974).

[31] R. R. Adzic, D. N. Simic, A. R. Despic, and D. M. Drazic, JEC 65, 587-601 (1975).

[32] D. M. Kolb and H. Gerisher, SS 51, 323 (1975).

[33] D. M. Kolb, in *Advances in Electrochemistry and Electrochemical Engineering*; *Vol. 11*, edited by H. Gerischer and C. W. Tobias (John Wiley, New York, 1978), p. 125.

[34] R. R. Adzic, in *Advances in Electrochemistry and Electrochemical Engineering*; *Vol. 13*, edited by H. Gerishcher and C. W. Tobias (Wiley-Interscience, New York, 1984), p. 159.

[35] F. Forni, M. Innocenti, G. Pezzatini, and M. L. Foresti, Electrochemica Acta 45, 3225-3231 (2000).

[36] E. S. Streltsov, I. I. Labarevich, and D. V. Talapin, Doklady Akademii Nauk Belarusi 38, 64 (1994).

[37] B. H. Flowers Jr., T. L. Wade, M. Lay, J. W. Garvey, U. Happek, and J. L. Stickney, JEC in press (2002).

[38] K. Varazo, M. D. Lay, and J. L. Stickney, JEC in press (2002).

[39] B. E. Boone and C. Shannon, Journal of Physical Chemistry 100, 9480-9484 (1996).

[40] A. Gichuhi, B. E. Boone, and C. Shannon, Langmuir 15, 763-766 (1999).

[41] M. Innocenti, G. Pezzatini, F. Forni, and M. L. Foresti, JECS 148, c357 (2001).

[42] G. Pezzatini, S. Caporali, M. Innocenti, and M. L. Foresti, JEC 475, 164-170 (1999).

[43] S. Zou and M. J. Weaver, Chemical Physics letters 312, 101-107 (1999).

[44] I. Villegas and J. L. Stickney, Journal of Vacuum Science & Technology A 10, 3032 (1992).

[45] I. Villegas and J. L. Stickney, Journal of the Electrochemical Society 139, 686 (1992).

[46] T. L. Wade, L. C. Ward, C. B. Maddox, U. Happek, and J. L. Stickney, Electrochemical and Solid State Letters 2, 616 (1999).

[47] T. L. Wade, R. Vaidyanathan, U. Happek, and J. L. Stickney, JEC 500, 322-332 (2001).

[48] T. Torimoto, A. Obayashi, S. Kuwabata, H. Yasuda, H. Mori, and H. Yoneyama, Langmuir 16, 5820-5824 (2000).

[49] T. Torimoto, S. Nagakubo, M. Nishizawa, and H. Yoneyama, Langmuir 14, 7077 (1998).

[50] T. Torimoto, S. Takabayashi, H. Mori, and S. Kuwabata, JEC 522, 33-39 (2002).

[51] H. Yoneyama, A. Obayashi, S. Nagakubo, and T. Torimoto, Abstracts of the Electrochemical Society Meeting 99-2, 2138 (1999).

[52] T. Torimoto, A. Obayashi, S. Kuwabata, and H. Yoneyama, JECS in press (2000).

[53] R. Vaidyanathan, U. Happek, and J. L. Stickney, Electrochimica Acta submitted (2003).

[54] R. Vaidyanathan, U. Happek, and J. L. Stickney, Journal of Crystal Growth submitted (2003).

[55] G. Springholz and K. Wiesauer, Phys. Rev. Letters 88, 015507-1 (2002).

[56] T. L. Wade, B. H. Flowers Jr., R. Vaidyanathan, K. Mathe, C. B. Maddox, U. Happek, and J. L. Stickney, in *Electrochemical Atomic Layer Eptitaxy: Electrodeposition of III-V and II-VI Compounds,*, 2000 (Materials Research Society), p. 145.

[57] W. Jantsch, G. Bauer, P. Pichler, and H. Clemens, Applied Physics Letters 47, 738-740 (1985).

[58] V. V. Bondarenko, V. V. Zabudskii, and F. F. Sizov, Semiconductors 32, 665-667 (1998).

[59] V. V. Zabudsky, F. F. Sizov, and V. V. Tetyorkin, Modelling and Simulation in Materials Science and Engineering 3, 575-582 (1995).

[60] F. F. Sizov, J. V. Gumenjuksichevskaya, V. V. Tetyorkin, and V. V. Zabudsky, Acta Physica Polonica A 87, 441-444 (1995).

[61] F. F. Sizov and A. Rogalski, Progress in Quantum Electronics 17, 93-164 (1993).

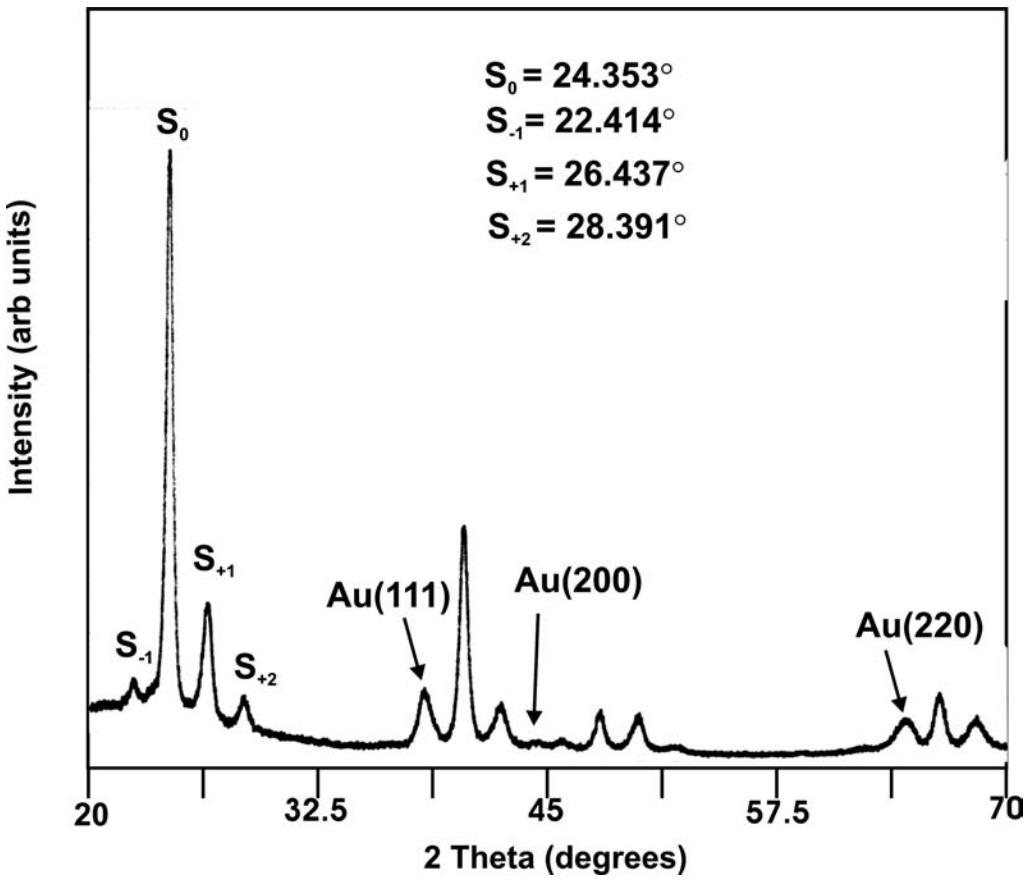

Figure 7.1. X-ray diffraction of 81 period 4PbTe / 4PbSe superlattice.

Buffer layer is 10 cycle PbSe. Angle of incidence is 1°, Cu -Kα source .

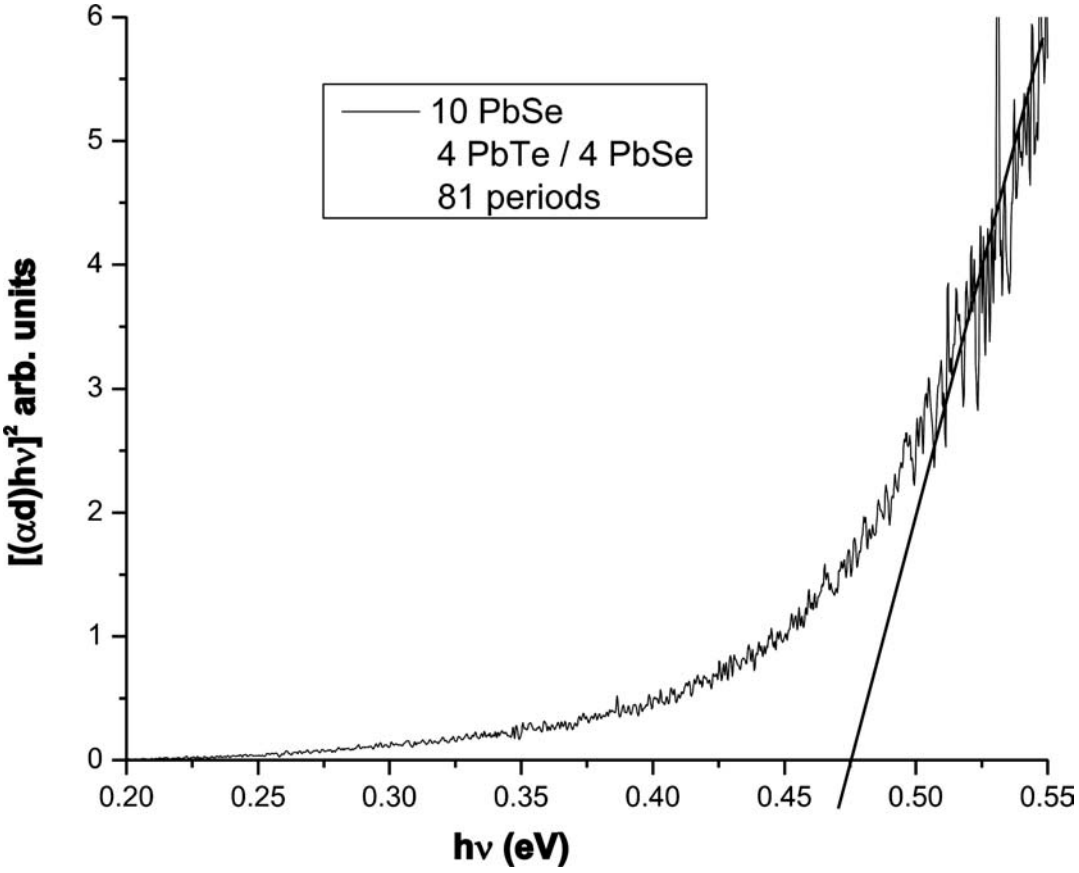

Figure 7.2. Reflection absorption measurements for 81 period 4PbTe / 4PbSe superlattice.

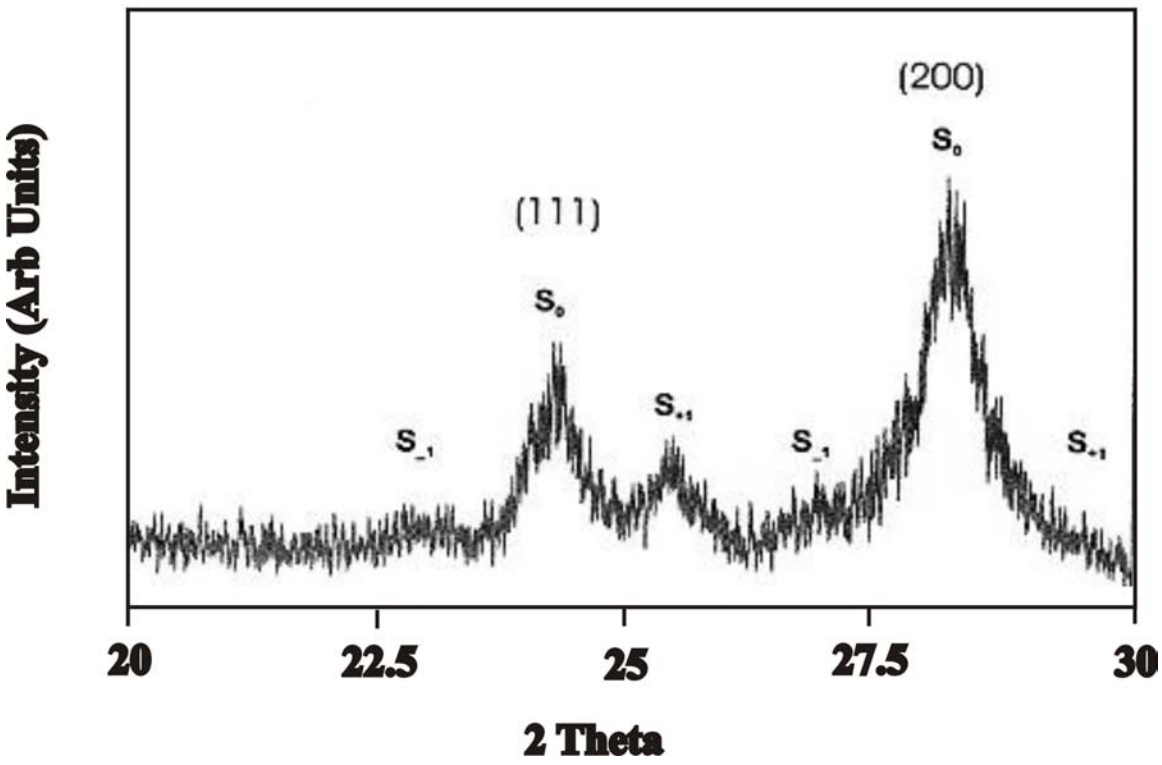

Figure7.3. X-ray diffraction of 40 period 6PbTe / 6PbSe superlattice.

Buffer layer is 100 cycle PbTe. Angle of incidence is 1°, Cu -Kα source.

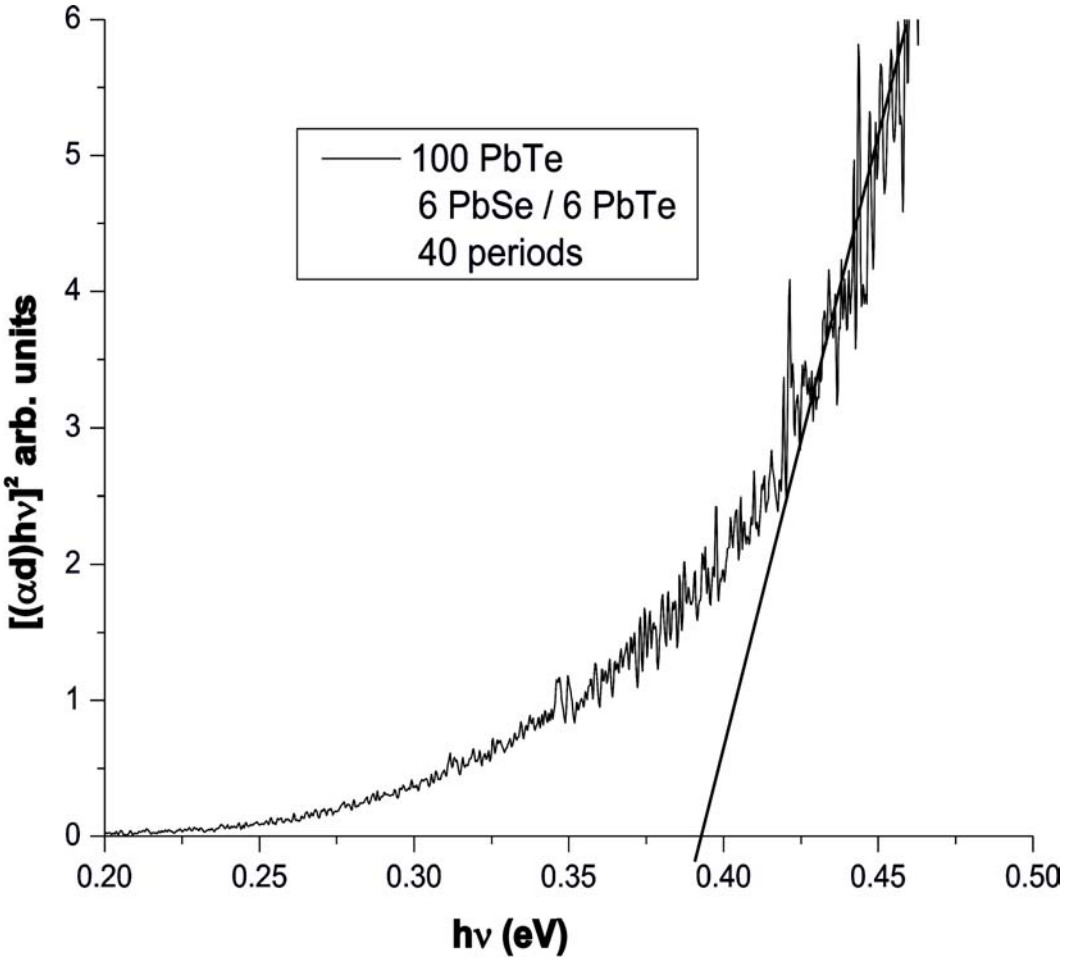

Figure7.4. Reflection absorption measurements for 40 period 6PbTe / 6PbSe superlattice.

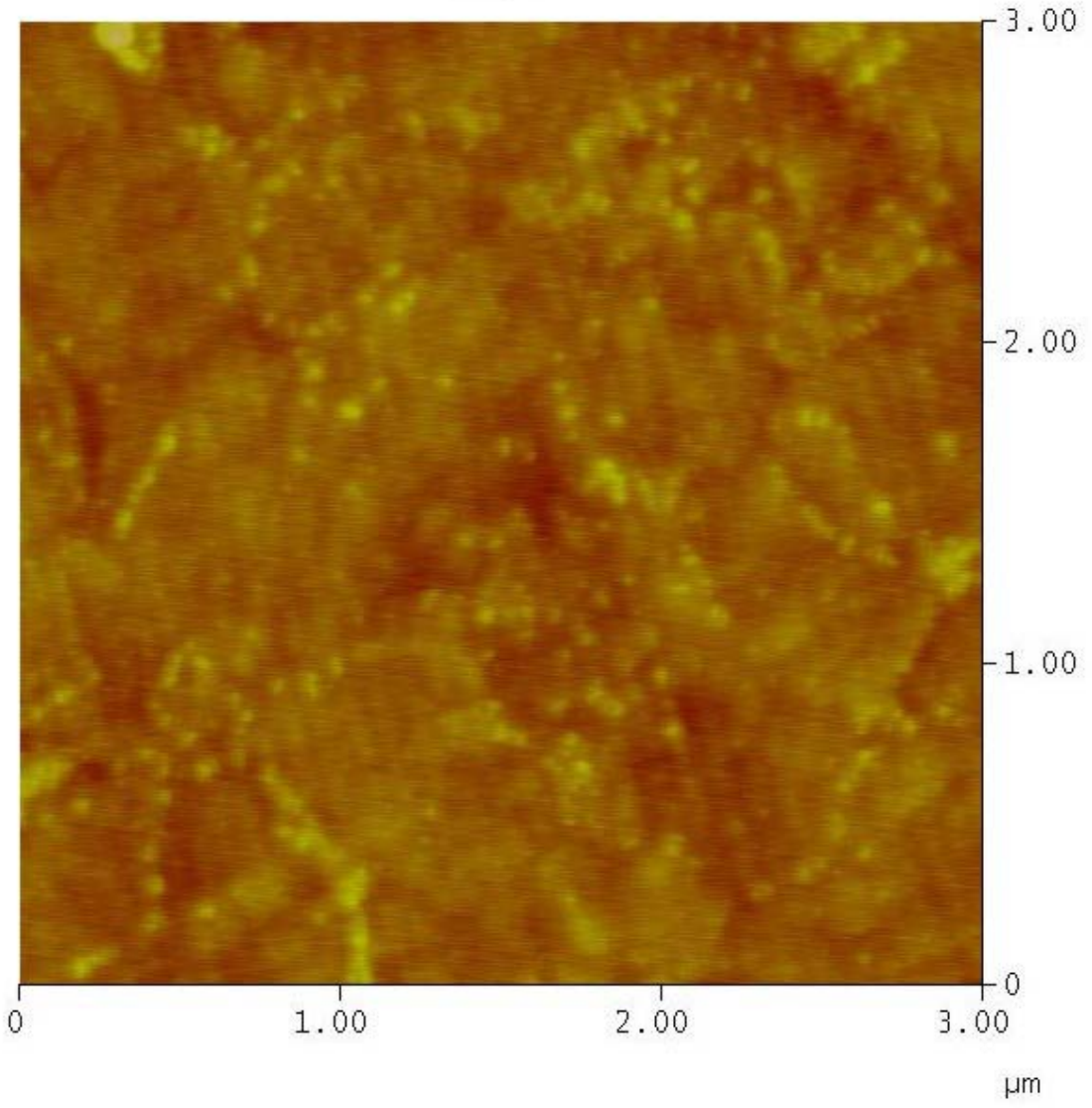

Figure7.5. AFM image of 81 period 4PbTe / 4PbSe superlattice electrodeposited on annealed Au on glass substrate.

Chapter 8

Conclusions and Future Studies

Initial studies in the InAs electrodeposition by EC-ALE, suggested a steady state deposition potential of –0.665 V for In and –0.775 V for As is required to obtain 2-D growth and stoichiometric deposit. The band gap of InAs thin film showed a dependence on the size of Au crystallites in the substrate. Small Au crystallites 50-100 nm, present in un-annealed substrate, blue shifts the band gap of InAs from its bulk value due to quantum confinement.

Deposition programs were developed for the formation of Cu_2Se and In2Se3 thin films. Different phases, Cu_2Se and Cu_3Se_2 were found in thin films that were made 200 cycles or more. Phase transformation of Cu_2Se is energetically favored at room temperature and also presence of excess copper in the deposits may also be a factor in the composition of the thin film. Films that were less than 200 cycles thick, composed mainly of Cu_2Se and the band gap was found to be 1.6 eV. In_2Se_3 thin films were also electrodeposited and Raman measurements showed that the films were composed of amorphous and crystalline materials. Attempts were made towards the formation of CuInSe2 thin films, by alternating atomic layers of Cu_2Se and In_2Se_3 compound semiconductors. EPMA, and x-ray diffraction suggested that thin films were copper rich. (Cu:In:Se 2:1:2). Further studies involving better complexing agent for Cu to shift the deposition potentials to –0.3 V is necessary to prevent indium from stripping during the Cu deposition and facilitate the formation of CIS.

Deposition potentials were identified for the electrodeposition of PbSe, PbTe and PbSe / PbTe thin films. Quantum confinement effects were observed for thin films of PbSe and PbTe electrodeposited by EC-ALE. The band gap of 10 – 25 cycle PbSe (bulk – 0.26 eV) deposit is blue shifted to 1 eV or more. Even a 100-cycle PbTe thin film band gap is blue

shifted due to strong confinement effect. EPMA indicated that the films were stoichiometric and the lead chalcogenide thin films were rock salt structure, observed by x-ray diffraction. PbTe thin films have a preferential orientation in the (200) plane compared to the poly crystalline nature of PbSe thin films. Te and Se seem to deposit in the over potential regime and hence control over the atomic layer Se and Te deposition needs further research.

PbSe / PbTe superlattice thin films indicated good stoichiometry and Bragg diffraction peaks with equidistant 2^{nd} order satellites were observed. Change in the thickness of the period will provide the necessary information to determine the type (I or II) of the PbSe / PbTe superlattice.

Semiconductor nanoclusters have been formed using EC-ALE in the pores of polycarbonate membranes. Technical problems with ingression of Au into the holes in the polycarbonate membrane were responsible for the excessive vertical height of the nanoclusters, and the dips in the centers. The high aspect ratio of these pores may have also caused some problems with ion exchange between steps in the EC-ALE cycle, possibly resulting in a small amount of co-deposition during formation of the nanostructures. The possibility of forming low aspect ratio template materials (30-50 nm diameter holes, but only and 100-500 nm tall) should be pursued.

Formation of quantum confined thin films and superlattices provides a variety of flexibility in the nanometer regime to manipulate the optical, magnetic and transport properties of the semiconductor thin films. Future studies involving the formation of PbSe, PbTe nanowires and nanowire superlattices, and quantum dots in aluminum templates will give rise to very interesting 2-D and 3-D quantum confinement properties

and formation of nanowire superlattice should be pursed to realize the limit of quantum confinement in the lead chalcogenides.